Vol. 27, No. 11 & 12, 2004

ISSN O250-541X

# National Academy

# SCIENCE LETTERS



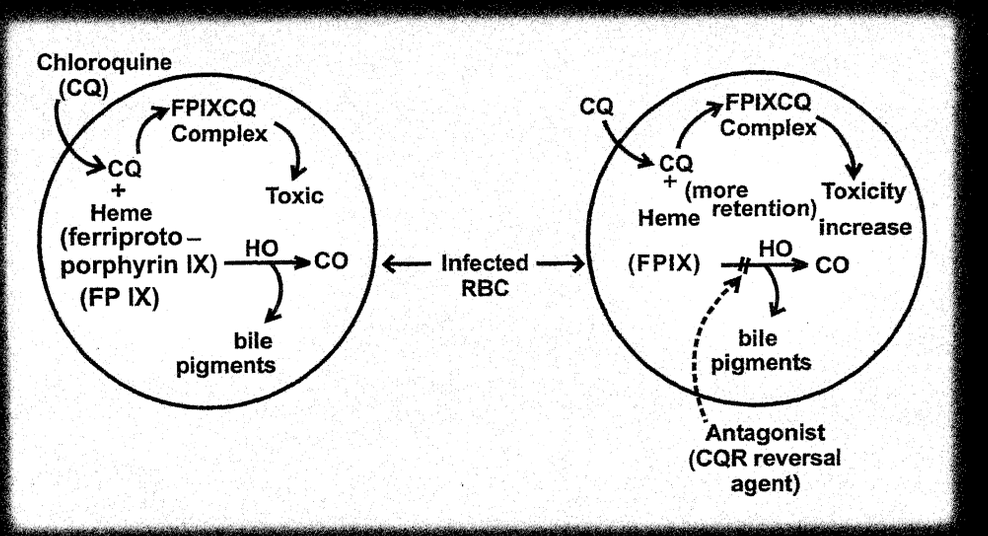


*Published by*

**The National Academy of Sciences, India**

# The National Academy of Sciences, India

**(Registered under Act XXI of 1860)**
**Founded 1930**

## COUNCIL FOR 2004

### President

1. Prof. Jai Pal Mittal, Ph.D.(Notre Dame), F.N.A., F.A.Sc., F.N.A.Sc., F.T.W.A.S., Mumbai.

### Two Past Presidents (including the Immediate Past President)

2. Prof. S.K. Joshi, D.Phil., D.Sc.(h.c.), F.N.A., F.A.Sc., F.N.A.Sc., F.T.W.A.S., New Delhi.
3. Dr. V.P. Sharma, D.Phil.,D.Sc.,F.A.M.S.,F.E.S.I., F.I.S.C.D., F.N.A., F.A.Sc., F.N.A.Sc., F.R.A.S., New Delhi.

### Vice-Presidents

4. Dr. P.K. Seth, Ph.D., F.N.A., F.N.A.Sc., Lucknow.
5. Prof. M. Vijayan, Ph.D., F.N.A., F.A.Sc., F.N.A.Sc., F.T.W.A.S., Bangalore.

### Treasurer

6. Prof. S.L. Srivastava, D.Phil.,F.I.E.T.E., F.N.A.Sc., Allahabad.

### Foreign Secretary

7. Dr. S.E. Hasnain, Ph.D., F.N.A., F.A.Sc., F.N.A.Sc., F.T.W.A.S., Hyderabad.

### General Secretaries

8. Dr. V.P. Kamboj, Ph.D., D.Sc., F.N.A., F.N.A.Sc., Allahabad.
9. Prof. Pramod Tandon, Ph.D., F.N.A.Sc., Shillong.

### Members

10. Dr. Samir Bhattacharya, Ph.D., F.N.A., F.A.Sc., F.N.A.Sc., Kolkata.
11. Prof. Suresh Chandra, D.Phil., Grad.Brit.I.R.E., F.N.A.Sc., Varanasi.
12. Prof. Virander Singh Chauhan, Ph.D., D.Phil.(Oxford), F.N.A., F.N.A.Sc., New Delhi.
13. Prof. Asis Datta, Ph.D., D.Sc., F.N.A., F.A.Sc., F.N.A.Sc., F.T.W.A.S.,New Delhi.
14. Prof. Kasturi Datta, Ph.D., F.N.A., F.A.Sc., F.N.A.Sc., F.T.W.A.S., New Delhi.
15. Prof. Sushanta Dattagupta, Ph.D., F.N.A., F.A.Sc., F.N.A.Sc., F.T.W.A.S., Kolkata.
16. Dr. Amit Ghosh, Ph.D., F.N.A., F.A.Sc., F.N.A.Sc., Chandigarh.
17. Prof. H.S. Mani, Ph.D.(Columbia), F.A.Sc., F.N.A.Sc., Chennai.
18. Prof. G.K. Mehta, Ph.D., F.N.A.Sc., Allahabad.
19. Dr. G.C. Mishra, Ph.D., F.N.A.Sc., Pune.
20. Dr. Ashok Misra, M.S.(Chem.Engg.), M.S.(Polymer Sc.), Ph.D., F.N.A.Sc.,Mumbai.
21. Prof. Kambadur Muralidhar, Ph.D., F.N.A., F.A.Sc., F.N.A.Sc.,Delhi.
22. Dr. Vijayalakshmi Ravindranath, Ph.D.,F.N.A.Sc., F.T.W.A.S., Manesar.
23. Prof. Ajay Kumar Sood, Ph.D., F.N.A., F.A.Sc., F.N.A.Sc., F.T.W.A.S., Bangalore.

### Special Invitees

1. Prof. M.G.K. Menon, Ph.D.(Bristol), D.Sc.(h.c.), F.N.A., F.A.Sc., Hon. F.N.A.Sc., F.T.W.A.S., F.R.S., Mem.Pontifical Acad.Sc., New Delhi.
2. Dr.(Mrs.) Manju Sharma, Ph.D., F.N.A.A.S., F.A.M.I., F.I.S.A.B., F.N.A.Sc., F.T.W.A.S., New Delhi.
3. Prof. P.N. Tandon, M.S., D.Sc(h.c.), F.R.C.S., F.A.M.S., F.N.A., F.A.Sc., F.N.A.Sc., F.T.W.A.S., Delhi.
4. Prof. Girjesh Govil, Ph.D., F.N.A., F.A.Sc., F.T.W.A.S., Mumbai.

CONTENTS

*Cover page photograph :* Possible mode of action of a chloroquine resistance reversal agent. (page no 387)

Published by Dr. V.P. Kamboj, General Secretary for the National Academy of Sciences, India, 5, Lajpatrai Road, Allahabad-211002 and Printed by National Graphics, Allahabad.
Co-sponsored by C.S.T., U.P., Lucknow.

# EDITORS' PAGE

It has been a pleasure for us to be associated with the publication of this journal and to see it completing one more year successfully. Satisfaction has been our "reward". All human scientific endeavours or the past were full of such "small rewards". However, more prevalent these days are the tall talks about "awards" won by scientists. This is more so in Indian scenario because most social/political/technical organizations announce some sort of awards whenever they, in their dream. "stumble" upon the idea that science needs encouragement. The positive impact (or otherwise) of having too many awards need to be carefully analyzed.

Is winning "Award" the final goal of our scientific, investigations or we have also to think of the science which follow out of our efforts? Can we not take "Awards" as the by-product of the rewarding experience of doing good and meaningful science? Does winning one "Prestigious Award" give a license to stop being really scientifically active and start using that "Award" as a step to get another award? We invite comments/views/related policy issues from fellow scientists for publication in this journal to generate a debate because Indian experiences have been widely different in this regard (both ways). Scientists themselves have to earnestly think of the pros and cons, It is accepted and expected that "Awards" would trigger more enthusiasm. particularly in the awardee and generally in his entire sphere of influence.

One of the most prestigious scientific award of India is Bhatnagar Award which Hon. Prime Minister of India has graciously presented recently to the selected scientists below the age of 45 years for their excellent scientific contributions. Through this journal, on behalf of the National Academy of Sciences, we congratulate all the recipients and wish them success in life, We hope that they would continue to be scientifically productive and further enhance the prestige of Indian Science. The readers of this journal, easily accessible to many Indian scientists, would like to have a glimpse of the excellent work done by the recent award-winners through their contributed review/overview papers. We request all the current Bhatnagar awardees to give this small reward to a Indian scientific journal, if they can!

We wish all our readers and fellow scientists a **Happy New Year, 2005!!**

**Girjesh Govil**
**Jai Pal Mittal**
**Suresh Chandra**

---

The views expressed here are solely those of one of the Editors and do not necessarily reflect those of the Academy or the Institute where he works.

# Role of magnetic resonance imaging (MRI), MR spectroscopy (MRS) and other imaging modalities in breast cancer

**Uma Sharma, Virendra Kumar AND N.R. Jagannathan***

*Department of NMR, All India Institute of Medical Sciences, New Delhi - 110029, India.*

**For correspondence :*

*E-mail: nrjgj@yahoo.co.in*

Received June 30, 2004; Accepted June 30, 2004

## Abstract

**Breast cancer is the commonest cancer among women world over and the diagnosis continues to generate fear and turmoil in the life of patients and their families. This article describes the currently available techniques used for screening primary and recurrent breast cancers and the evaluation of therapeutic response of breast cancer with special emphasis on MRI and MRS techniques. MRI, a noninvasive technique, provides anatomic images in multiple planes enabling tissue characterization. Contrast enhanced MR studies have been found to be useful in the diagnosis of small tumors in dense breast and benign diseases from malignant ones. *In vivo* magnetic resonance spectroscopy (MRS) is another useful technique for diagnosis and for assessing the biochemical status of normal and diseased tissues. Being noninvasive, MR techniques can be used repetitively for assessment of response of the tumor to various therapeutic regimens and for evaluating the efficacy of drugs at the both at the structural and molecular level. An overview of the various aspects of different imaging modalities used in breast cancer research including various *in vivo* MR methodologies with clinical examples is presented in this review.**

**(Keywords: Mammography/ultrasound/magnetic resonance imaging (MRI)/contrast enhanced MRI/ *in vivo* $^{1}H$ and $^{31}P$ magnetic resonance spectroscopy (MRS)/ breast cancer)**

## Introduction

Breast cancer is the leading cause of cancer related death among women of 40 and 55 years of age and is the most frequent malignancy in women world-wide[1,2]. In India, one out of every 20 women has the risk of developing breast cancer in Delhi and Mumbai.[3] The early diagnosis of breast cancer is therefore crucial to reduce disease-specific mortality and to improve other clinical outcomes. This has led to exploration of techniques for the diagnosis of breast cancer in high-risk women. Number of research projects is underway to develop/improve detection, diagnosis and characterization of primary and recurrent breast cancers and their

response to various treatment regimens. Mammography is the first line of imaging modality used, which can potentially detect small lesions before they are palpable and clinically apparent[4]. In young women particularly due to dense breast it is difficult to distinguish a mass and fatty tissue and many false negative mammogram are reported[5-7]. Further research into improving mammography image quality with the use of computer-assisted techniques is expected to improve detection.

In recent years, MRI of the breast has gained increasing importance in the field of breast imaging. Large-scale trials have confirmed the technique's high sensitivity for primary and recurrent breast cancers[8-14]. Breast MRI was first reported in the 1980s, but early results were disappointing. Subsequently, intravenous contrast agents were used with MRI in the late 1980s, offering a clear advantage. Contrast enhanced (CE) MRI relies on the enhancement of MR signal intensity after the administration of a contrast agent, and therefore, the issue of breast density is usually not problematic as with mammography. In general, malignant tumors showed fast uptake of contrast and show high intensity while surrounding normal tissues do not enhance. Numerous studies in different patient populations and with different techniques have proved that MR is useful in detecting most invasive cancers[15-17].

Even though MRI has proven to be an indispensable diagnostic tool, it is often found to be nonspecific in defining the underlying pathology at the molecular level. However, *in vivo* MR spectroscopy could be an alternative methodology because it can detect the biochemical alterations accompanying the disease processes. Information on metabolites associated with specific disease process and their relative levels depicting the biochemical status in a particular region of the tissue or organ can be obtained which may help to understand the various metabolic processes of normal and pathological tissues. The technique can also be used repetitively to monitor the response of tumors to various therapeutic modalities and efficacy of drugs[18-21].

In this review several breast cancer imaging modalities such as mammography, ultrasound and CEMRI are discussed in the sections to follow, although because none of these techniques is without drawbacks, the search will continue until an ultimate technique is discovered. In addition, the role of MR in the diagnosis and follow up of chemotherapeutic treatment of breast cancer patients is reviewed.

### (a) Mammography

Mammography is a special type of X-ray imaging which is used to create a detailed image of the breast. Like simple X-ray imaging procedure, a film coated with a special phosphor is placed under the breast and low dose X-rays are transmitted through the compressed breast. As X-rays pass through the breast they are attenuated to different extent depending on the different densities of tissues. The X-ray photons then encounter the phosphor coating of the film, which glows in proportion to the intensity of the photons striking it, thus exposing the film with an image of the internal structures of the breast. Mammography takes advantage of the different X-ray attenuating characteristics of the breast tissues to differentiate between normal and abnormal structures. Fat is very dense and absorbs or attenuates a great deal of the X-rays. The

connective tissue around the breast ducts and fat is less dense and attenuates or absorbs far less X-ray energy. Mammography has a high sensitivity and can visualize 85 to 90% of breast cancers in women older than 50 years of age. It can also reveal a tumor before a lump can be felt[22]. Despite higher sensitivity, its specificity is low to about 30% in some cases and 65%[23,24] to a high of 80%[25] in other studies. In particular, mammography is less sensitive and less specific in younger women, who tend to have dense breast tissue. The technique also has a relatively high false-negative rate[26,27]. Studies indicate that only 1 in every 4 to 6 biopsies reveal breast cancer, which means that as many as 75% of biopsies are performed for benign lesions and are therefore unnecessary[25,26]. There continues to be a need for an imaging technique that is highly sensitive and specific, relatively non-invasive, cost effective and offers a high predictive value of breast cancer.

### (b) Digital Mammography

As discussed earlier with conventional film screen mammography images are recorded on a film using an X-ray. With digital mammography, the breast image is captured using a special X-ray detector, which converts the images into a digital picture for review on a computer. With digital mammography, magnification, orientation, brightness, and contrast of the image can be altered after the exam is completed to help the radiologist to clearly see certain areas[28]. Selective magnification of the region of interest of the image eliminates the need for the supplemental views that may be necessary with conventional mammography sparing the patient's additional exposure to radiation[28,29]. A variety of computer-assisted programs have been developed which identify abnormal areas and help distinguish benign lesions from potentially malignant ones. These are useful in cases that would ordinarily require a second reader because of suspicious findings. Despite the numerous advantages of digital mammography compared with conventional film-screen mammography, there are some disadvantages due to technologic limitations that will be resolved in future. A potential disadvantage of digital mammography is reduced spatial resolution. Current digital systems are limited by the size of pixels technologically available.

### (c) Ultrasound

An adjunct to conventional mammography, ultrasound is particularly useful in the evaluation of dense breasts. The method has demonstrated efficacy in differentiation of cysts from solid masses, abscesses, imaging of women younger than 25 years old with a palpable mass, imaging guidance in core needle biopsy, etc[28]. Ultrasound has several potential disadvantages, for example, it is impossible to consistently image micro-calcifications. Furthermore, there is significant overlap in the morphologic characteristics of benign versus malignant lesions.

### (d) Breast MR Imaging

*Principle of MRI*

Magnetic interaction between nuclei of atoms and radio frequency (RF) field in the presence of an external magnetic field ($\mathbf{B}_o$) is the basic phenomenon to generate an MR image[30]. In addition to positive charge, some nuclei, for example, proton ($^1$H), phosphorus ($^{31}$P), etc. have an inherent property called spin (I) or spin angular

momentum and behave like magnetic dipoles. The nuclear spin generates a magnetic field i.e. magnetic moment. When a sample containing these nuclei (or a patient) is placed in a strong magnetic field, these will tend to orient either parallel or anti-parallel to the field. Spin population is more in parallel orientation, being the lower energy state. A second magnetic field i.e. RF pulse is applied which induces transition and the nuclei are flipped with the absorption of energy from a lower energy state (parallel) to higher energy state (an anti-parallel orientation). After switching off the RF pulse, the nuclei emit energy and return to the lower energy state. This emitted signal is detected by the receiver and is processed to generate either an NMR spectrum or an MR image. Clinical MR imaging of human body relies on the abundant and strong signal of mobile protons primarily from water and fat present in the tissues. The spatial distribution of these mobile protons obtained is represented as an image that provides anatomical as well as pathological information. For further details readers are referred to standard text books and reviews[31-33].

*Relaxation Times*

As discussed earlier when the RF pulse is switched off, the nuclei will begin to realign by loosing its energy and relax back to its original position. There are primarily two mechanisms of relaxation: (a) spin-lattice (longitudinal) relaxation (T1), and (b) spin-spin (transverse) relaxation (T2). As the nuclei return to the lower energy state, energy is lost by interaction with the surrounding lattice or environment. This process is governed by a time constant TI and is called as spin-lattice (longitudinal) relaxation time. T2 denotes the spin-spin (transverse) relaxation time. This refers to the loss of energy due to interaction with other nuclei aligned with the magnetic field. T2 relaxation is actually confounded by $T2^*$ relaxation, which is much shorter and results from inhomogeneity in the magnetic field. T1 and T2 are specific tissue characteristics. Their value varies depending on other factors such as magnetic field strength. Nevertheless, at a given field strength, different tissues have different characteristic T1s and T2s[31,32]. It is important to realize that T1 and T2 relaxation times are occurring simultaneously during any given imaging procedure, and both govern the signal intensity in an MR image. MR images weighted by T1, T2 or PD may be produced by varying the MR acquisition parameters like repetition time (TR) and time for echo (TE).

*Magnetic field gradients*

The basis of MRI is that the Larmor precession frequency is used to mark the position of an object within the scanned volume. The precession frequency is directly proportional to $\mathbf{B_0}$. A magnetic field gradient coil can modify the strength of $\mathbf{B_0}$, and hence the Larmor frequency, depending on the position (x) within the scanner. MRI systems are generally characterized by the strength of the magnetic field.

There are three main steps in generating an image: slice selection; phase encoding and frequency encoding for image formation. Three separate coils one each for the x, y and z - directions that are independently controlled are situated within the bore of the magnet of the MRI scanners. Prior to actual image acquisition, the magnetic field is same at all points throughout the patient's body. The

combination of a field gradient inhomogeneity and excitation by a specific frequency permits slice selection, the first step in image formation. A magnetic field gradient Gs (slice selection gradient) are applied at right angles to the slice that is to be selected. It can be applied in any direction, depending on the orientation of the slice being imaged. Due to gradient field, Larmor frequency will vary along the slice-selection direction. In association with this gradient field, a 90° RF pulse is applied and only the nuclei that match the frequency of the RF pulse will now be rotated through 90° and only these nuclei of this particular slice will precess and yield an NMR signal.

The stronger the gradient field, the thinner will be the slice. Similarly, narrow bandwidth RF pulses, produces thinner slices. Among the three pairs of gradient coils i.e. x-gradient, y-gradient and z-gradient, the z-gradient changes the gradient magnetic field along the z-axis thereby allowing a slice of the patient to be selected for imaging. The x-gradient coils produce a magnetic field gradient across the patient and therefore the horizontal axis across the patient, thus providing spatial localization along the x-axis of the patient. This technique is usually called 'frequency encoding'. The y-gradient coils produce magnetic field gradient through the patient from front to back, and by convention, the y-axis is the vertical axis through the patient used for 'phase encoding' the NMR signal. Together, the y- and x-gradients allow precise determination of where within the imaging plane the contribution to the NMR signal from each voxel or pixel originates. The z-gradient is always used for selection of a transaxial plane to be imaged and is called 'slice selection' gradient. To select the axial, sagittal or coronal plane for imaging, the z-, x-, or y-gradients, respectively, will be energized as magnetic fields add vectorially. When all the three gradients are energized at the same time, an oblique plane is defined. MR images are assigned shades of gray, white, and black to the strength of the MR signal produced by the protons.

The MR signal data for image formation is collected by using a set of instructions, which are defined as pulse sequences through a powerful computer. These pulse sequences accomplish two tasks. Firstly, to collect the data in an orderly fashion so that the position of the signals can be determined - i.e., the pixel position - and this is the function of the gradient magnetic fields as outlined earlier. Secondly, it influences the image contrast - pixel character - by specifying the timing and power of the RF pulses. Many of the parameters that have to be specified in a pulse sequence, such as the timing and magnitude of gradient magnetic fields (normally denoted as $G_x$ or $G_y$ or $G_z$) are included in the computer software.

A number of MRI pulse sequences are in use, they all may be categorized into two main groups built around either the spin-echo (SE) or the gradient recalled echo (GRE) and the images acquired in either a single-echo or a multi-echo approach[31,34]. The most commonly used sequences are: partial saturation, inversion recovery, spin echo, FLASH (fast low angle shot), GRASS (gradient recalled acquisition in steady state), and others. In order to obtain images with good contrast and quality, one needs to specify (i) type of pulse sequence, (ii) time intervals TR, TE, etc. (iii) matrix size, (iv) number of signal averages, (v) plane of image, (vi) spatial separation of

the slice, etc. Multi-slice and multi-echo technique help to decrease total scan time.

## Contrasts in MRI

As mentioned in earlier sections the primary sources of inherent tissue contrast in MRI are three: proton (spin) density (PD) and relaxation times, T1 and T2. The PD within soft tissues vary by only a few percent while there is more wide variation in T1 and T2 sometimes by more than 100% among soft tissues and therefore have important effect on image contrast.

The signal intensity in an MR image is a function of T1, T2 and image acquisition parameters such as TR (time of repetition) and TE (time of echo). The MR images are either PD, T1-weighted or T2-weighted images. They usually do not refer to images that display PD, T1 or T2, instead, the terms refer to the relative weight with which the three parameters affect the tissue contrast in MR images. The tissues with short T1 will appear bright on T1- weighted image while tissues with long T1 will appear dark. In general, tumor tissues have longer T1 and T2 values compared to normal tissues[31-33]. The T1-weighted image acquired on breast cancer patients showed tumor tissue as dark while fat and normal tissue appear as white areas as shown in Fig. 1a. In T2 - weighted image of sagittal section of the breast (Fig. 1b), fat appears as dark while tumor appears white. T1 - weighted images provides better anatomical details (morphology) while T2 images are useful for identifying the tissue pathology.

MRI is highly sensitive to physical, chemical and biological characteristics of tissues and fluids. The ability to visualize, detect and diagnose abnormalities may be affected by several factors such as image contrast, signal-to-noise ratio, spatial resolution, temporal resolution in dynamic contrast-enhanced MRI and the presence of artifacts. In addition to proton density, T1 and T2, several other parameters like the magnetic susceptibility, chemical shift and magnetization transfer also influence contrast in an MR image. Moreover, functional parameters like diffusion, perfusion, flow and uptake of contrast also affect the contrast of MR images. It is important to note that the signal intensity of MR images is usually not directly proportional to a single tissue parameter. In most cases a pulse sequences are optimized to produce an image weighted to a particular tissue parameter.

There have been numerous technological advances in MR imaging of breast, including introduction of intravenous gadolinium-based contrast agents; the development of dedicated breast surface coil; and the introduction of standard imaging sequences. Today, MR imaging of breast generally is performed with a dedicated coil that permits simultaneous imaging of both breasts using gadolinium-based intravenous contrast agents.

## (e) Contrast Enhanced MRI of Breast

Breast lesions usually show high signal intensity on MR images compared to normal surrounding tissues following the administration of intravenous (IV) contrast agents. This phenomenon occurs due to the hyper-vascularity of growing tumors and increased uptake of contrast media by tumors.

The difference in faster uptake of contrast agent by malignant compared to benign or normal tissues helps distinguish-

ing these using MRI. Numerous studies have shown that malignant tumors frequently reveal faster and higher levels of enhancement when compared to normal surrounding tissues. Tumors in a number of anatomic sites including breast, bladder, bone and prostate[35-38] have been evaluated using contrast CEMRI. The contrast agents are freely diffusible, that is, they readily pass from the intravascular space into the interstitium and give rise to parenchymal enhancement. The use of fast imaging sequences and the development and application of tracer kinetic modeling techniques now provides a complete understanding of the physiological basis of contrast enhancement in breast cancer. With optimal data collection, sequences can be designed to be sensitive to tissue perfusion and blood volume (so-called T2* methods) and/or permeability and extra cellular leakage space (so-called T1 methods)[39].

Perfusion-weighted images can be obtained by analyzing the passage of the contrast medium through the tissues. When a bolus of paramagnetic contrast agent passes through blood capillaries, it generates $\mathbf{B_0}$ inhomogeneities that result in a decrease in the signal intensity of surrounding tissues. This effect can be observed with susceptibility-weighted T1 or T2*- weighted sequences, the latter providing greater sensitivity and contrast to perfusion effects. MR systems capable of fast image acquisition are required to characterize adequately these effects. Tracer kinetic principles are used to quantify T2* phenomena and estimates of tissue perfusion characteristics are derived. These include relative blood volume (rBV), relative blood flow (rBF) and mean transit time (MTT). Quantifying T2* effects is currently restricted to the brain because the intact blood-brain barrier retains the contrast agent within the intravascular space. Quantification cannot readily be applied to areas with very leaky capillaries e.g. breast cancer. The usefulness of perfusion imaging for characterizing breast lesions has been reported[40,41]. These studies have shown that T2*-weighted perfusion imaging is feasible in breast and that the technique shows promise in differentiating benign from malignant lesions. Kuhl *et al.*[40] and Kvistad *et al.*[41] compared T2* images with T1 imaging and showed that malignant tissues showed stronger decrease in signal intensity whereas perfusion effects in fibroadenomas were minor. This was explained on the basis of perfusion characteristics alone, despite significant overlap in T1 enhancement patterns. The pathophysiolgical explanation for this observation probably relates to differences in microvessel arrangements, density and size in tumors and fibroadenomas.

Gadolinium chelates readily pass from the blood into extra-cellular space of tissues, at a rate determined by the permeability of the capillaries and their surface area. The degree of enhancement seen on T1-weighted images is dependent on a number of physiological and physical factors. These include tissue perfusion, capillary permeability to contrast agent, volume of the extra-cellular leakage space, native T1 relaxation time of the tissue, contrast agent dose, imaging sequence used and parameters utilized and machine scaling factors. Key histological features that correlate with tissue enhancement on T1-weighted images are difficult to find. Vascular density in malignant tissue is higher than normal parenchyma, but there is an overlap with benign lesions including inflammatory and proliferative processes[42,43]. Various studies on breast MR

have shown that malignant tissues enhance earlier and to a greater extent than benign breast disease. This difference is most marked in the early period (1-3 min) after bolus contrast medium administration[35,44]. However, other investigators[10,45] have demonstrated that while cancers tend to enhance faster than benign lesions, there is a clear overlap in the enhancement rates of benign and malignant lesions.

A dose of 0.2 mmol/kg body weight of contrast medium was used in early breast MRI studies using spin-echo sequences. Now-a-days breast MR examinations are performed with gradient-echo techniques due to their higher T1 sensitivity with a contrast medium dose of 0.1 mmol/kg body weight. However, in general there is ambiguity with regard to the effective dose of contrast agents for breast examinations. One report claimed a higher sensitivity with 0.16 mmol/kg of gadopentetate dimeglumine compared with the standard dose (0.1 mmol/kg)[46]. This study was performed on a 1 T magnet, used 3-D gradient echo sequences with 3-mm section thickness. These investigators found that the ability to detect small lesions and to discriminate benign and malignant lesions was improved in relation to contrast medium dose.

A dynamic CEMRI is recommended to maximize specificity. But higher temporal resolution imposes limitation of reduced spatial resolution or decreased coverage. Higher temporal resolution techniques appear to improve the specificity of examinations because of better characterization of the signal intensity time curve. Study by Boetes *et at.*[35] suggested that characterization of breast lesions is optimal at 1-2 s image acquisitions. The highest specificity demonstrated to date with breast MRI has been with fast 2D-dynamic contrast-enhanced techniques (with imaging times from 1 to 12 s per study).

High-resolution 3D techniques with voxel sizes less than 1 mm provide high sensitivity imaging. This is performed with fat suppression in approximately 3-4 min and differential enhancement between malignant and benign lesions is greatest. Image interpretation is based on morphological characteristics. Several investigators[45,47] have reported the architectural features identified on high spatial resolution contrast-enhanced MR imaging studies that are used for lesion diagnosis.

### (f) *In vivo* MR Spectroscopy

*31 P MR Spectroscopy:*

Over the past decade *in vivo* MRS has increasingly been applied in evaluating breast carcinoma using the nucleus $^{31}P$. Several review articles discusses the results obtained using $^{31}P$ MRS on breast cancer patients[48]. $^{31}P$ MR spectra are simple to comprehend since the MR signals are observed only from the relatively mobile compounds, which are in mM concentration. Thus, monitoring the relative concentration of various $^{31}P$ metabolites noninvasively helps to study the biochemistry of diseased and normal states of tissues and can also be used to monitor the efficacy of several therapeutic interventions. The $^{31}P$ MR spectrum of the normal breast tissue (Fig. 2) include information on resonances from phosphate groups of nucleotide-tri-phosphate, in general, β-adenosine-tri-phosphate (ATP), at -16 ppm, signal at -2.5 ppm is characteristic of γ-ATP while the signal at -7.5 ppm contains contributions from the α-phosphate groups of both ATP and

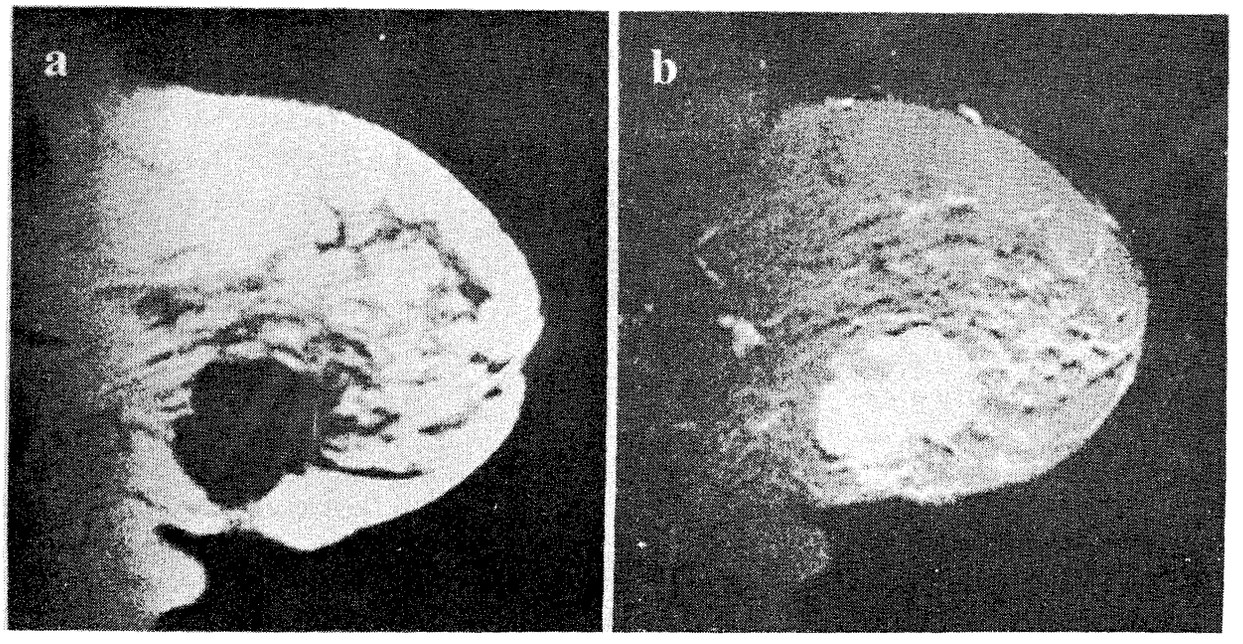


Fig. 1– (a) Tl - weighted sagittal MR image of a patient suffering from infiltrating duct carcinoma of the breast showing the tumor area as hypo-intense, while in T2 – weighted sagittal image (b) the tumor tissue appears as hyper-intense area.

adenosine – di – phosphate (ADP). The resonance at 5 ppm is observed due to inorganic phosphate (Pi) and in some cases resonance due to phosphocreatine (PCr) may also be observed which could be due to chest wall.

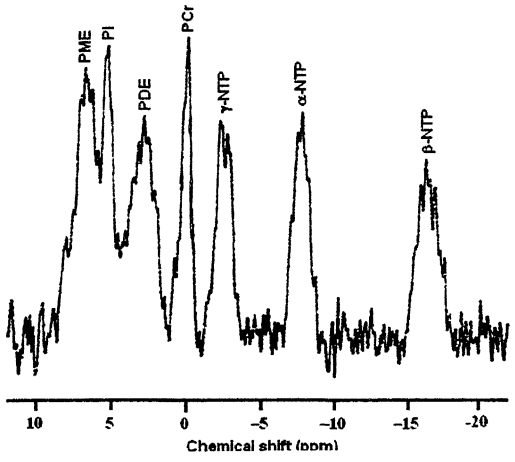


Fig. 2– $^{31}$P MR spectrum from the normal breast tissue of a volunteer.

Signals from metabolites involved in phospholipids metabolism are also observed. Primarily the signals arise from phosphomonoesters (PME; 6 – 8 ppm) and phosphodiesters (PDE; 2 – 4 ppm). The PME peak contains several compounds such as sugar phosphates and phospho choline (PC). The metabolic state of cells can thus be monitored using PME peak. Increase in PME in malignant cells suggests alterations in lipid metabolism[49,50]. Glycerophosphocholine (GPC) and phosphoethanol amine (PE) are major PDE components observed in $^{31}$P spectra and the importance of these metabolites has been discussed elsewhere[51]. $^{31}$P MR spectroscopy demonstrated the presence of high PME content in human breast cancers[52,53] and was found to be lower in the normal breast tissue while during the second week PDE/PME ratio was higher than at the other stages of the menstrual cycle[54]. PME was also seen to be increased in lactating breast by a factor of two compared to the non-lactating premenstrual breast[48]. In general, the phosphate metabolites were lower in the post-menopausal women compared to the pre-menopausal women. Using ISIS localization, Payne *et al.*[55] studied the normal breast tissues and observed higher level of PME at the late follicular (LF) phase of the menstrual cycle compared to the early luteal (EL) phase while PDE was maximum at the early follicular (EF) phase compared to the LF phase. Significant changes in PME were noticed compared to that observed in PDE. Higher PME in human breast tumors has been demonstrated by a number of investigators using *in vivo* methods[52,53,56]. In excised breast carcinoma in culture medium, the content of PME and NTP was three times higher than in benign breast lesions[57]. Ng. *et al.*[58] reported higher total phosphate level in breast carcinomas compared to the normal breast from non-menstruating women. In untreated human breast tumors PME was found to be higher than in the spectra of normal breast of post-menopausal women.

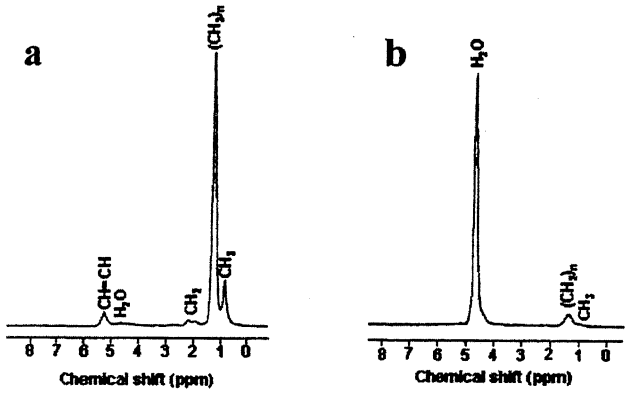


Fig. 3– (a) $^{1}$H MR spectrum acquired from an 8 ml voxel localized in the normal breast tissue of a healthy volunteer. (b) $^{1}$H MR spectrum from an 8 ml voxel positioned from the tumor region of a patient suffering from infiltrating duct carcinoma of the breast.

*$^1H$ MR Spectroscopy:*

Recently, considerable interest has also been shown in the use of proton MRS methods for noninvasive detection of biochemical differences between malignant and normal breast tissues in breast cancer patients. Fig. 3a shows the $^1H$ MR spectrum (without water suppression) from the normal breast tissue of a volunteer. The intense peaks in the spectra observed at 1.33 ppm are due to methylene [-$(CH_2)_n$-] protons of the lipid while the water peak is at 4.7 ppm. Fig. 3b shows the spectrum obtained from a tumor tissue (infiltrating duct carcinoma) which is dominated by water with little contribution from lipid. The water suppressed proton spectrum from the tumor[59] of a patient suffering from infiltrating duct carcinoma is shown in Fig. 4b while the corresponding voxel location in Fig. 4a. It is observed that the spectrum from the tumor tissue is different from the normal and the unaffected breast tissue. In tumor spectrum, water peak dominates with low contribution from the protons of the fatty acid chains in comparison to the control and the unaffected breast. Comparison of water- to-fat (W/F) ratio among the above three groups showed that the tumors are characterized by high W/F values[60,61] which varied from 1 to 30, while in controls the value is 0.34 ± 0.25 and in the unaffected contralateral breast tissue of the breast cancer patients it is 0.35 ± 0.42. Observation of elevated W/F ratio in breast cancer patients is in agreement with the generally established trend that tumors have considerably higher water content[62,63]. Mackinnon *et al.*[63] also reported changes in lipid content with tumor development and progression. The W/F ratio can also be used to monitor the efficacy of the treatment procedures in breast cancer patients[60,61]. A statistically significant reduction in the W/F ratio was observed in patients who have undergone the complete course of chemotherapy regimen (1.2 ± 1.5) compared to the pre-therapy value of 7.2 ± 7.4.

In the proton MR spectra acquired with water suppression of tumor tissue in addition to the residual water and lipid peak, a peak at 3.2 ppm due to choline containing compounds was also observed as shown in Fig. 4b. The intensity of the Cho peak was monitored prior to and one week after the completion of the 3rd or 6th cycle of neoadjuvant chemotherapy for assessment of the effect of the therapy[59]. The Cho resonance was found to be either reduced or absent in patients receiving complete course of chemotherapy indicating response to chemotherapy[59]. The sensitivity of *in vivo* MRS in detecting Cho was 78% and the specificity was 86%. Similar findings have also been reported by others[64,65].

Absolute concentration of Cho in breast lesions from *in vivo* proton MRS has also been documented[66,67]. Mackinnon *et al.*[67] reported elevation of Cho levels in malignant breast tumors compared to benign cases from *in vitro* NMR of FNAB samples. Of the various choline-containing compounds (Cho, GPC, and PC) that contribute to the peak at 3.2 ppm in *in vivo* MRS, an increase in phosphocholine appears to be highly probable[66,68]. The studies show the rate of transport and metabolism of Cho in primary cultures of human mammary epithelial cells and MCF7 human breast cancer cells. The rate of Cho transport under physiological Cho concentration was found to be two fold higher in cancer cells.

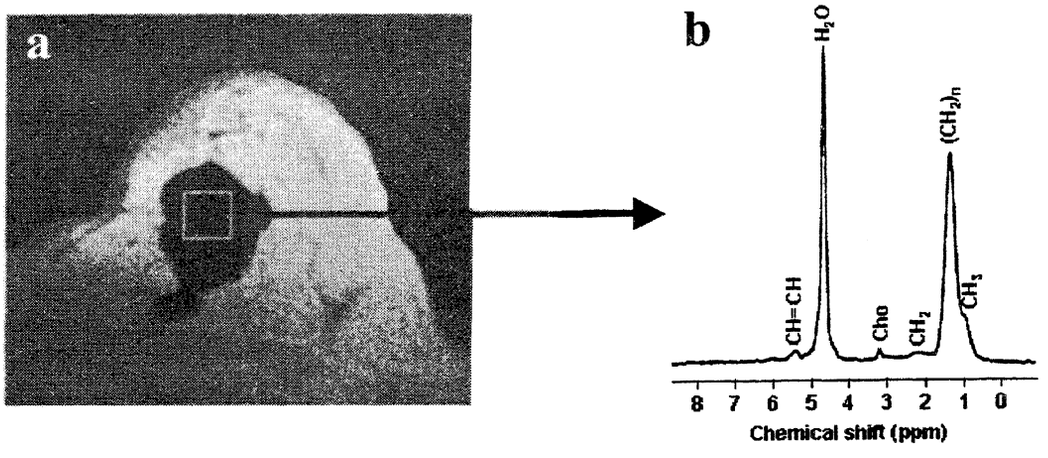


Fig. 4– (b) $^1H$ MR spectrum obtained from an 8 ml voxel with water suppression from a patient suffering from infiltrating duct carcinoma showing the choline metabolite. The corresponding voxel location is shown in (a).

## Conclusion

More research focusing on the early diagnosis with improved sensitivity and specificity and evaluation of response to chemotherapeutic agents in breast cancer patients would be useful for improved survival. Screening procedures like clinical breast examination, ultrasound, and mammography are often limited in sensitivity and specificity. The area of biomedical MR is experiencing a rapid expansion due to its noninvasive nature, avoidance of ionizing radiation and its ability to generate high-resolution images. Presently, MRS and MRI are acting as a complementary tool to histology, mammogram and other accepted techniques. Increasing use of these methods is expected for basic research, clinical investigations and ultimately for patient diagnosis. *In vivo* MRS can now be used as a unique means to probe the biochemistry of living systems with diagnostic importance. MRS is currently employed for clinical investigation in many sites around the world, including India. The sensitivity and specificity of *in vivo* MRS for several disease patterns particularly for small lesions need to be improved before MRS can be incorporated into clinical practice. The increased availability of 3 T and 4 T magnets would further enhance the spectral quality, particularly for proton MRS studies.

## Acknowledgements

The Department of Science and Technology, Government of India, is acknowledged for financial support (SP/SO/B27/95 and SP/SO/B21/2001) in carrying out this project.

## References

1. Greenlee, R.T., Hill-Harmon, M.B., Murray, T., Thun, M. *et al.* (2001) *CA Cancer J. Clin.* **51** : 15.
2. National Cancer for Health Statistics. SEER cancer statistics review, 1973-1995. Bethesda, MD: US National Cancer Institute, 1998.
3. NCRP (National Cancer Registry Programme) 2001: Consolidated report 1990-1996, an incidence and distribution of cancer, Indian Council of Medical Research, New Delhi, 2001.
4. Baker, L.H. (1982) *CA Cancer J. Clin.* **32** : 194.
5. Huo, Z., Giger, A.L., Olopade O.I., Wolverton, D.E., Weber, B.L., Metz, C.E., Zhong, W. & Cummings, S.A.(2002) *Radiology* **225** : 519.
6. Kolb, T.M., Lichy, J. & Newhouse, J.H. (2002) *Radiology* **225** : 165.
7. Tilanus-Linthorst, M., Verhoog, L., Obdejin, I.M. Bartels, K., Menke-Pluymers, M., Eggermont, A., Klijn, J., Meijers-Heijboer, H., van der Kwast, T. & Brekelmans, C. (2002) *Int. J. Cancer* **102** : 91.
8. Heywang-Kobrunner, S.H. (1994) *Invest. Radiol.* **29**: 94.
9. Heywang-Kobrunner, S.H., Viehweg, P., Heinig, A. & Kuchler, C. (1997) *Eur. J. Radiol.* **24** : 94.
10. Gilles, R, Guinbretiere, J.M., Lucidarme, O., Cluzel, P., Janaud, G., Finet, J.F., Tardivon, A., Masselot, J. & Vanel, D. (1994) *Radiology* **191** : 625.
11. Boetes, C., Mus, R.D., Holland, R., Barentsz, J.O., Strijk, S.P., Wobbes, T., Hendriks, J.H. & Ruys, S.H. (1995) *Radiology* **197**: 743.
12. Kuhl, C.K. (2000) *Eur. Radiol.* **10**: 46.
13. Morris, E.A. (2002) *Radiol. Clin. N. Am.* **40**: 443.
14. Morris, E.A. (2003) *Seminars in Ultrasound, CT, and MRI* **24** : 45.
15. Kaiser, W.A. & Zeitler, E. (1989) *Radiology* **170** : 681.
16. Orel, S.G., Schnall, M.D., Powell, C.M., Hochman, M.G., Solin, L.J., Fowble, B.L., Torosian, M.H. & Rosato, E.F. (1995) *Radiology* **196** : 115.
17. Fischer, U., Kopka, L. & Grabbe, E. (1999) *Radiology* **213** : 881.
18. Danielsen E. R. & Ross B. D. (1999) *Magnetic Resonance Spectroscopy Diagnosis of Neurological Diseases* (New York: Marcel Dekker).

19. Gadian D. G., Connelly A., Duncan J. S., Cross J. H., Kirknam F. L., Johnson C. L., Vargha-Khadem F., Nevile B. G. & Jackson, G. D. (1994) *Acta Neurol. Scand.* **152** : 116.

20. Mukherji, S. K. (1998) *Clinical Applications of Magnetic Resonance Spectroscopy* (New York: John Willey & Sons).

21. Young. I. R. & Charles. H. C. M.R. (1996) *Spectroscopy Clinical Applications and Techniques* (Cambridge: Martin Dunitz).

22. Abdel-Dayem, H.M., Scott, A.M., Macapinlac, H. A. *et al.* (1994) in *Nuclear Med Annual* Freeman LM., ed. Lippincott-Raven, New York, 181.

23. Fenlon, H.M., Phelan, N., Tierney, S., Gorey, T. & Ennis, J.T. (1998) *Clin. Radiol.* **53** : 17.

24. Kopans, D.B. (1992) *Am.J. Radiol.* **158** : 521.

25. Flanagan, D.A., Gladding, S.B. & Lovell, F.R (1998) *Am. Surg.* **64** : 670.

26. Khalkhali, I., Cutrone, J., Mena, I.G., Diggles, LE., Venegas, R.J., Vargas, H.I., Jackson, B.L, Khalkhali, S., Moss, I.F. & Klein, S.R. (1995) *Radiology* **196** : 421.

27. Pollei, R., Mettler, F., Barstow, S. Moradian, G. & Moskowitz, M. (1987) *Radiology* **163** : 459.

28. Reynolds, H.E. (1999) *Hematol. Oncol. Clin. North Am.* **13** : 333.

29. Hogge, J.P., Freedman, M.T. (1997) *Semin. Roentgenol.* **32** : 50.

30. Raghunathan, P. & Jagannathan, N. R. (1996) *Curr. Sci.* **70** : 695.

31. Stark, D.D. & Bradley, W.G. (1998) *Magnetic Resonance Imaging* (New York : Mosby).

32. Jagannathan, N.R. (2003) *Proc. Indian Natl. Sci. Acad.* **B69** : 423 and (2004) *Curr. Sci.* **86** : 42.

33. Jagannathan, N. R. (2001) *MR Imaging and Spectroscopy in Pharmaceutical and Clinical Research* (New Delhi: Jaypee Brothers).

34. Edelman, R R Hesselink, J. R. & Zlatkin M. B. (1995) *Clinical Magnetic Resonance Imaging* (2nd edn.) (Philadelphia: W B Saunders).

35. Boetes, C., Barentsz, J. O., Mus, R.D., van der Sluis, R.F., van Erning, L.J., Hendriks, J.H., Holland, R. & Ruys, S.H. (1994) *Radiology* **193** : 777.

36. Barentsz, J.O., Jager, G.J., van Vierzen, P.B. Witjes, J.A, Strijk, S.P., Peters, H., Karssemeijer, N. & Ruijs, S.H. (1996) *Radiology* **201** : 185.

37. Verstraete, K.L., De Deene, Y., Roels, H., Dierick, A., Uyttendaele, D. & Kunnen, M. (1994) *Radiology* **192**: 835.

38. Padhani, A.R, Gapinski, C.J., Macvicar, D.A., Parker, G.J., Suckling, J., Revell, P.B., Leach, M.O., Deamaley, D.P. & Husband, J.E. (2000) *Clin. Radiol.* **55** : 99.

39. Padhani, A.R. (1999) *Br. J. Radiol.* **72** : 427.

40. Kuhl, C.K., Bieling, H., Gieseke, J. Ebel, T., Mielcarek, P., Far, F., Folkers, P., Elevelt, A. & Schild, H.H. (1997) *Radiology* **202** : 87.

41. Kvistad, K.A., Lundgren, S., Fjosne, H.E. Smenes, E., Smethurst, H.B., Haraldseth, O. (1999) *Acta Radiol.* **40** : 45.

42. Weind, K.L, Maier, C.F., Rutt, B.K., Moussa, M. (1998) *Radiology* **208** : 477.

43. Stamper, P.C., Winston, J.S., Herman, S., Klippenstein, D.L., Arredondo, M.A., & Blumenson, L.E. (1997) *Breast Cancer. Res. Treat.* **45** : 39.

44. Gilles, R., Guinebretiere, J.M., Shapeero, L.G., Lesnik, A., Contesso, G., Sarrazin, D., Masselot, J. & Vanel, D. (1993) *Radiology* **188** : 473.

45. Stamper, P.C., Herman, S., Klippenstein, D.L., Winston, J.S., Edge, S.B., Arredondo, M.A., Mazurchuk, R.V. & Blumenson, L.E. (1995) *Radiology* **197** : 387.

46. Heywang-Kobrunner, S.H., Haustein, J., Pohl, C., Beck, R, Lommatzsch, B., Untch, M., Nathrath, W.B. (1994) *Radiology* **191** : 639.

47. Orel, S.G., Mendonca, M.H., Reynolds, C. Schnall, M.D., Solin, L.J., Sullivan, D.C. (1997) *Radiology* **202** : 413.

48. Podo, F. (1999) *NMR Biomed.* **12** : 413.

49. Segebarth, C. M., Baleriaux, D., Arnold, D. A., Luyten, P. R. & Hollander, J. A. den. (1987) *Radiology* **165** : 215.

50. Maris, J., Evans, A., Mclaughlin, A., Angio, G. J. D., Bolinger, L., Manos, H., & Chance, B. (1985) *N. Engl. J. Med.* **312** : 1500.

51. Williams, S.R., Crockard, H. A. & Gadian, D.G. (1989) *Cerebrovasc. Brain. Metab. Rev.* **1** : 91.

52. Sijens, P.E., Wijrdeman, H. K., Moerland, M. A., Bakker, C. J., Vermeulen, J. W. & Luyten, P. R. (1988) *Radiology* **169** : 615.

53. Glaholm, J., Leach, M. O., Collins, D. J., Mansil, J., Sharp, J. C., Madden, A., Smith, I. E. & Mc Cready, V. R (1989) *Lancet* **1** : 1326.

54. Twelves, C.J., Porter, D. A., Lowry, M., Dobbs, N. A., Graves, P. E. Smith, M. A., Rubens, R D. & Richards, M. A. (1994) *Br. J. Cancer* **69**:1151.

55. Payne, G. S., Dowsett, M. & Leach, M. O. (1994) *Breast* **3** : 20.

56. Park, J. M. & Park, J. H. (2001) *Korean J. Radiol.* **2** : 80.

57. Degani, H., Horowitz, R. & Itzchak, Y. (1986) *Radiology* **161** : 53.

58. Ng, T. C., Graundfest, S., Vijaykumar, S., Baldwin, N. J., Majors, A. W., Karalis, I., Meaney, T. F., Shin, K. H., Thomas, F. J. & Tubbs, R. (1989) *Magn. Reson. Med.* **10** : 125.

59. Jagannathan, N. R., Seenu, V., Coshic, O., Dwivedi, S. N., Julka, P. K., Srivastava, A. & Rath, G. K. (2001) *Br. J. Cancer* **84** : 1016.

60. Jagannathan, N. R., Singh, M., Govindaraju, V., Raghunathan, P., Coshic, O., Julka, P. K. & Rath, G. K. (1998) *NMR Biomed.* **11** : 414.

61. Jagannathan, N.R., Kumar, M., Raghunathan, P., Coshic, O., Julka, P. K. & Rath, G. K. (1999) *Curr. Sci.* **76** : 777.

62. Bakker, C. J. G. & Vriend, J. (1983) *Phys. Med. Biol.* **28** : 331.

63. Mackinnon, W. B., Huschtscha, L., Dent, K., Hancock, R., Paraskeva, C. & Mountford, C. E. (1994) *Int. J. Cancer* **59** : 248.

64. Yeung, D. K., Chung, H. S. & Tse, G. M. (2001) *Radiology* **220** : 40.

65. Kvistad, K. A., Bakken, I. J. & Gribbested, I. S. (1999) *J. Magn. Reson. Imaging* **10** : 159.

66. Roebuck, J. R., Cecil, K. M., Schnall, M. D. & Lenkinski, R. F. (1998) *Radiology* **209** : 269.

67. Mackinnon, W. B., Barry, P. A., Malycha, P. L., Gillett, D. J., Russel, P., Lean, C. L., Doran, S. T., Clough, B. H., Barra Bilous, M. & Mountford, C. E. (1997) *Radiology* **204** : 661.

68. Katz-Brull, R., Margalit, R., Bendel, P. & Degani, H. (1998) *MAGMA* **6** : 44.

# Heme metabolism: An innovative approach to harness resistance malaria*

**Pratima Srivastava**

*Pharmacokinetics and Metabolism Division, Central Drug Research Institute, Chattar Manzil Palace, P.O. Box 173, Lucknow-226001, India.*

email: *pratimacdri@yahoo.com*

Received July 17, 2004

## Abstract

The complex pathophysiology and the increasing severity of malaria infection as well as fast emergence of relapse cases in malaria and parasite strains (plasmodia) resistant to chloroquine and other new generations of antimalarials (ROLLING BACK OF MALARIA) necessitate the integrated work in the field of malariology. The work considered for Prof. B.K. Bacchawat Memorial Young Scientist Award Lecture is maiden report for the presence of heme oxygenase and biliverdin reductase in different species and strains viz. *Plasmodium knowlesi* (simian) P. *berghei/P. yoelii* (rodent) and *P. falciparum/P. vivax* (human) of malarial parasites. Initial studies revealed that Heme oxygenase of the parasite has 67% and 85% nucleic- and amino acid sequences homology with the heme oxygenase gene of *Corynebacterium diphtheriae.* Also, heme biosynthetic enyzmes viz. 5-aminolevulinic acid synthase, 5-aminolevulinic acid dehydrase, ferrochelatase and tryptophan pyrrolase were studied in rodent, primate and human malaria parasites. Detailed study of different enzymatic properties, show dissimilarities between the parasite and corresponding hepatic host enzymes. The activities of heme biosynthetic enzymes were elevated in the resistant strains of *P.berghei* and *P.falciparum*, thus responsible for increased hemoprotein cytochrome P-450 in some resistant strains. Heme oxygenase, biliverdin reductase activites were found to be in accordance with the degree of resistance experienced/acquired by the parasite, (*P. falciparum /P.berghei /P.yoelii*) ie. in case of resistant parasites (acquired or field isolates) the activity of the enzymes were higher , which can be taken as resistance marker. Resistant modulators synthesized by CDRI as well as others were found to be selective inhibitors of Heme oxygenase of the parasites *in vitro* and *in vivo*, resulting in increased retention of heme and thus chloroquine required for reversal of resistance of the malarial parasites. Therapeutic dose of Chloroquine was able to kill the chloroquine resistant *Plasmodium berghei* as well as multidrug resistant *Plasmodium yoelii nigeriensis* infection in *Mastomys coucha* and Swiss albino mice respectively, in conjunction with the resistant reversal agents (inhibitors of parasitic heme oxygenase).

(Key words : heme oxygenase / malaria / resistance / heme / bilirubin / hemozoin / resistant reversal agents)

*Prof. B.K. Bachhawat Memorial Young Scientist Award Lecture, delivered on July 19, 2004 at Allahabad.

## Introduction

Malaria is a major cause of morbidity and mortality in many areas of the world, particularly in sub-Saharan Africa and southeast Asia. The number of malaria infections reach 200 million annually, resulting in 1 to 3 million deaths per year. Children are the most frequent victims, comprising 85% of all malaria related mortality[1] . Even worse, widespread drug resistance and the lack of novel antimalarials present major challenges in our future fight against malaria. The causative agent of human malaria is the protozoan parasite *Plasmodium* of which *Plasmodium falciparum* is the most virulent. The lifecycle of *Plasmodium* includes its insect vector, the female *Anopheles* mosquito, and the human host. Malarial parasites or plasmodia spends a portion of its life cycle inside the host's erythrocytes. During the intraerythrocytic cycle, *Plasmodia* ingest 25 - 75% of the host cell hemoglobin. The hemoglobin is degraded inside the parasite's food vacuole (pH 4.5-5.5) by specific proteases, and the amino acids from the degraded globin are used as the building blocks for the parasite's own intermediary metabolism. Upon hemoglobin cleavage, free heme is released. Free heme is cytotoxic, it destabilizes and lyses the membranes and releases hydrolases into the parasite's cytoplasm resulting in the killing of the parasites. Therefore, detoxification of the liberated heme is critical for plasmodia survival.

In mammals, free heme is degraded via the heme oxygenase / biliverdin reductase pathway. A report exist regarding the absence of heme oxygenase in malarial parasites[2]. In *P. falciparum*, heme detoxification is achieved by polymerizing free heme into insoluble crystalline material called hemozoin (also termed malaria pigment)[3,4]. Hemozoin is believed to be structurally identical to that of beta-hematin in which ferric iron of one heme is coordinated to the propionate carboxylate group of the next heme[5] . However, hemozoin too is supposed to be harmful to the parasites . Important functions like oxidative burst, phagocytosis and the expression of MHC class II are severely impaired in hemozoin-fed phagocytes. It seems therefore likely that hemozoin loading may play an important role in the impairment of the immune response seen in *P.falciparum* malaria.

## Heme Oxygenase

Heme oxygenase is a microsomal origin enzyme which cleaves the tetrapyrrole ring structure of heme at the alpha methene bridge to form an open tetrapyrrole, biliverdin. Biliverdin is subsequently converted to bilirubin by biliverdin reductase. Heme oxygenase is present from unicellular organism (*Cornebacterium diptheriae*) to mammals. Heme oxygenase was discovered in 1974 as a molecular wrecking ball, it has now found prevalence in all kinds of human pathophysiology ranging from stroke, cancer, multiple sclerosis and malaria to transplantation and in immune response. The physiological significance of heme oxygenase is

1. In the formation of bile pigments which are excellent antioxidants.

2. Maintaining the levels of proxidant heme to nontoxic state.

3. Iron liberated from heme by the action of Heme oxygenase can be utilized in the hemoproteins formation.

4. carbonmonoxide can be used as a second messenger (Fig. 1).

$$Heme+3NADPH_2+O_2 \longrightarrow$$

$$biliverdin+Fe^{2+}+CO+3NADP+3H_2O.$$

In mammals, the activity of heme oxygenase is highest in the spleen, where senescent erythrocytes are sequestrated and destroyed.

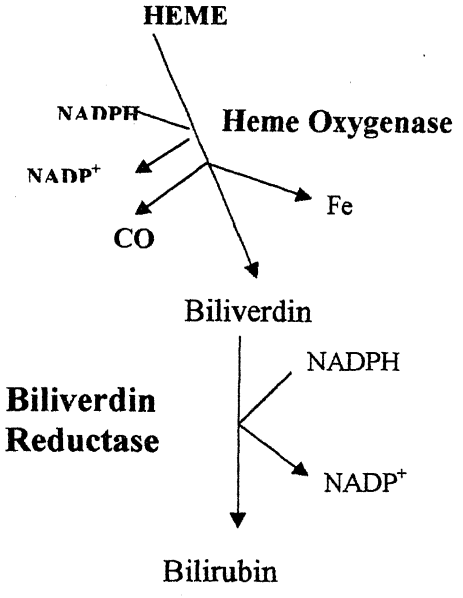


Fig. 1– Heme Degrading Pathway

Keeping all the above information into account, it seems necessary that the malarial parasites living in the viscinity of free heme pool, should have the possession of heme detoxifying/degrading pathway which can help in scouraging the harmful effects of heme on the parasites.

## 1. Biochemical and molecular characterization of Heme Oxygenase in Malarial parasites:

Heme, when in its free form (generally formed by the tear and wear of the important hemoproteins) is a toxic biomolecule. It can retard or inhibit the functions of the nucleic acids as well as proteins. In the biosystem the toxicity of heme is countermanded or harnessed by the presence of heme degrading system comprising of heme oxygenase and biliverdin reductase. The intraerythrocytic stages of the malarial parasites dwell in the red blood cells, utilising its hemoglobin for survival and propagation.

In this process hemoglobin is being degraded by the parasite proteases into heme and globin, globin is further acted upon by the parasite proteases to be converted into amino- acid, which are utilized by the parasite as protein building blocks. Heme can be polymerized into hemozoin, the malarial pigment, which is supposed to be less toxic than heme, but only 30% of the heme undergoes polymerization and nothing was known about the fate of the remaining 70% of the heme moiety (Fig. 2).

For the first time presence of **heme oxygenase** and **biliverdin reductase** have been shown in different intraerythrocytic stages (schizonts, rings and trophozoite) as well as different species and strains of *Plasmodium knowlesi* (simian)[6], *P. berghei/P. yoelii* (rodent)[7] and *P. falciparum/P. vivax* (human) cell free malarial parasites. Initial studies revealed that Heme oxygenase of the parasite has 67% and 85% nucleic acid and amino acid sequences homology respectively with the heme oxygenase gene of *Corynebacterium diphtheriae* (the protozoan pathogen responsible for causing diphtheria).

The pathway has been recently for the first time, included by Prof. Hagai Ginsburg in the **Malaria Parasite Metabolic Pathways** –Hemoglobin digestion and Ferriprotoporphyrin IX Polymerization (*http://sites.huji.ac.il/malaria/redox/html*).

It has also secured its place in the "**Innovative India**" edited by Prof. L.K. Sharma and Seema Sharma in the chapter entitled, "The challenge of malaria control" –2000.

limiting heme biosynthetic enyzmes viz. 5-aminolevulinic acid synthase, 5-aminolevulinic acid dehydrase, ferrochelatase and tryptophan pyrrolase were studied in rodent, primate and human malaria para-

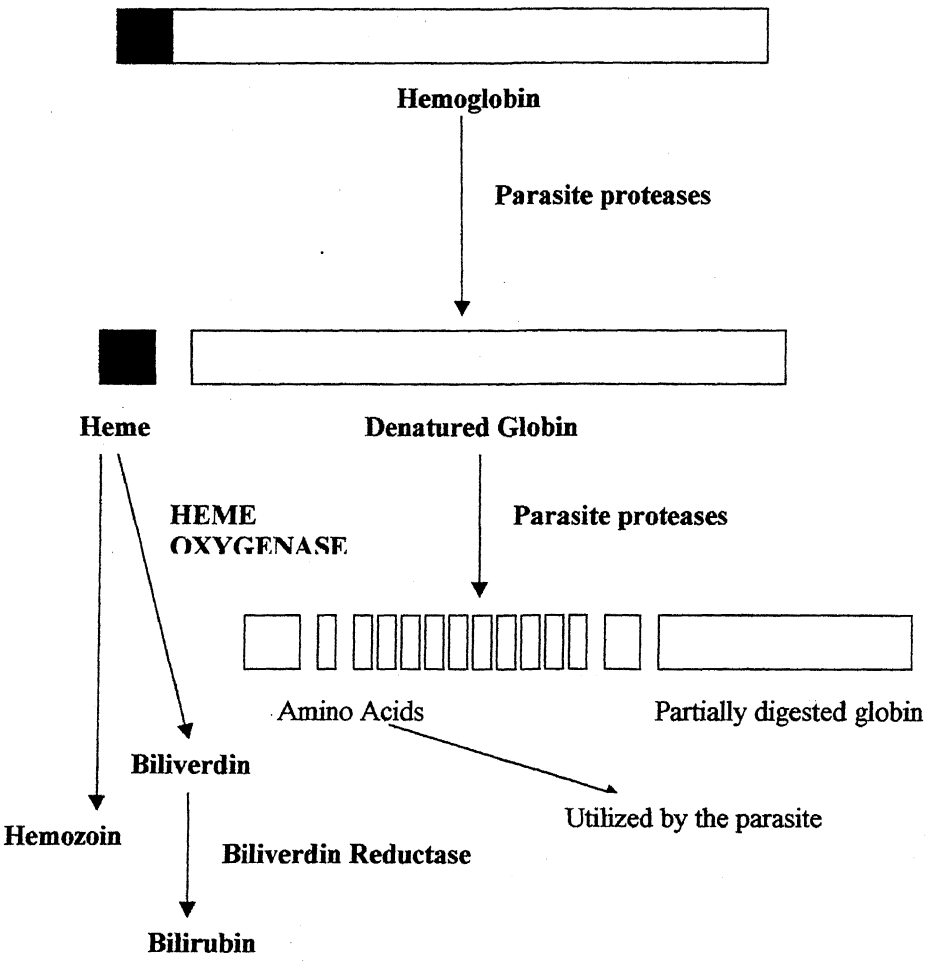


Fig. 2– Heme detoxification system in malarial parasites—What is the need?

## 2. Heme Biosynthesis in Plasmodia:

A well-organised heme biosynthetic pathway was found to be present in the cell free malarial parasites. Important and rate sites. Detailed study of different enzymatic properties show dissimilarities between the parasite and corresponding hepatic host enzymes[8].

### 3. Heme Metabolism in Resistance strains of Plasmodia:

The activities of Heme biosynthetic enzymes were elevated in the resistant strains of *P.berghei* and *P.falciparum*, thus responsible for the cause of increased hemoprotein cytochrome P-450 in some resistant strains, resulting in enhanced drug metabolism.

Heme oxygenase, biliverdin reductase activites were found to be elevated in accordance with the degree of resistance experienced/acquired by the parasite, (*P. falciparum / P.berghei / P.yoelii*) i.e. in case of resistant parasites (acquired or field isolates) the activity of the enzymes were higher, which can be taken as resistance marker. High activity of heme oxygenase can be the result of the enhanced hemoprotein formation as well as its breakdown in case of the resistant parasites and this may also contribute towards the acquisition of the drug resistance by the parasites. Enhanced heme oxygenase is also responsible for appreciable less heme content in case of the resistant parasites as compared to the sensitives ones. The alteration in the levels of the nonenzymatic entities as well as in the activities of the enzymatic entities were found to be dependent on the degree/ titre of resistance being experienced by the resistant malarial parasites[9].

### 4. Resistance modulators:

Pharmacophore, which can alter the resistance property of the resistant malarial parasites, are considered as resistant reversal agents or resistant modulators. There are several mechanisms by which they impart their action, however, the basic point in all is the harnessing of the property, which is different in the resistant (those parasite strains, which are not eradicated by the therapeutic dose of the antimalarial drugs) and the sensitive (those parasite strains, which are eradicated by the therapeutic dose of the antimalarial drugs) malarial parasites. Based upon the findings that the resistant malarial parasites have enhanced activity of the enzyme heme oxygenase than the sensitive parasites, attempts were made to synthesize the pharmacophore which are inhibitors of heme oxygenase. Pharmacophores designed as Resistant modulators synthesized by CDRI as well as other places were found to be selective inhibitors of Heme oxygenase of the parasites *in vitro* and *in vivo*, resulting in increased retention of heme and thus providing more opportunity for the therapeutic dose of chloroquine to be in the vicinity of the resistant parasites. Resistant reversal agents along with the therapeutic dose of chloroquine were able to kill the resistant parasites, which alone either of the one was unable to perform, thus it is evident that resistant reversal agents are not antimalarials but they potentiate the action of chloroquine, by selective inhibition of heme oxygenase, leading to enhanced heme level and thus more amount of the toxic heme-chloroquine complex formation in the resistant parasites, eradicating them completely[10-13].

### Conclusion

Malaria globally being the top-priored disease has become unmanageable due to its resurgence by the acquisition of resistance against the commonly used antimalarials. Understanding the cause for the acquisition of resistance is extremely essential for designing the strategy to combat malaria. Molecular and biochemical studies on heme oxygenase in malarial parasites have added another step in the existing ladder to explain the mechanism

responsible for the acquisition of resistance by the parasites, as well as useful as a **marker of resistance.** The above findings **future resistance modulators. Arresting** of any step of the same may be a **suitable chemotherapeutic target.**

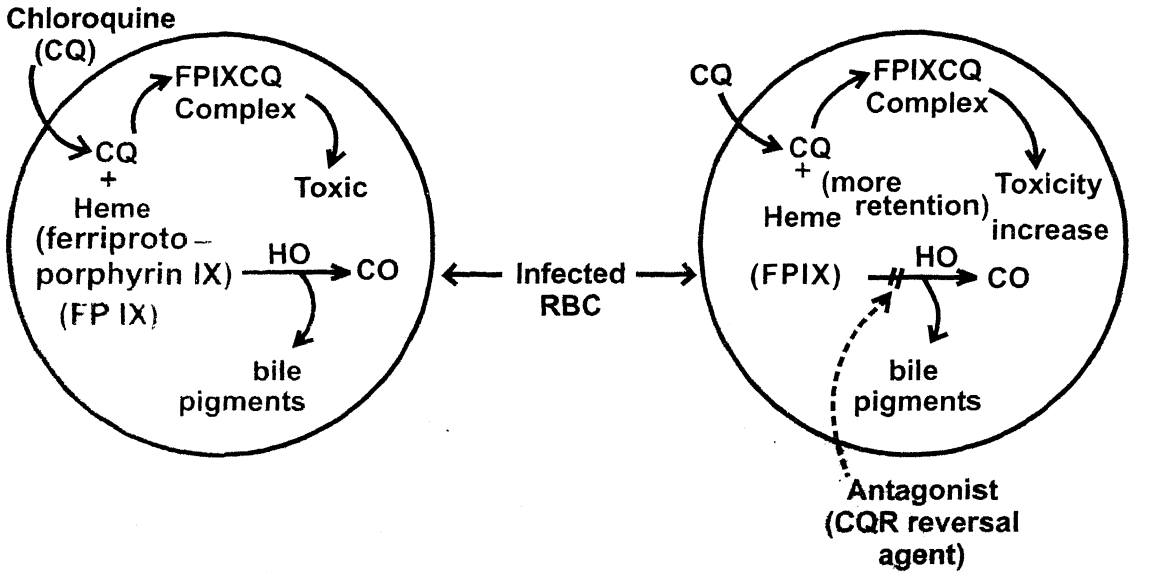


Fig. 3- Possible mode of action of a chloroquine resistance reversal agent

are of immense importance, as interference in the heme degradation will lead to accumulation of toxic heme which in conjunction with chloroquine become potential suicidal agent to the malarial parasites. Based on the above strategy compounds were designed by CDRI as potential, selective inhibitors of heme oxygenase which may result as a possible **approach for the design of future resistance modulators**

Heme is an essential, integrated, prosthetic group of important hemoproteins of the biosystem. Molecular and biochemical studies on plasmodial heme oxygenase explain the mechanism for the acquisition of resistance, as well as its usefulness as resistance **marker** besides providing **approach for the design of**

## Acknowledgements

The author is thankful to Director General, CSIR, for nomitation, Director, CDRI and Dr. V.C. Pandey, Ex Dy Director, Biochemistry division, CDRI, Lucknow.

## References

1. Bradley, T. (1996) www-micro.msb.le.ac.uk/ Bradley/ Bradley.html
2. Meshnick, S. R. (1996) *Annals of Tropical Medicine and Parsitology* **90**(4): 367.
3. Rosenthal, P. J. a. M., S.R. (1996) *Molecular and Biochemical Parasitology* **83**: 131.
4. Slater, A.F.G. et al. (1991) *Proc. Natl. Acad. Sci. U.S.A.* **88**: 325.
5. Sullivan, D., Gluzman, I.Y., & Goldberg, D.E. (1996) *Science* **271**: 219.

6. Srivastava, Pratima, Puri, S.K., Dutta, G.P. & Pandey, V.C. (1992) *Medical Science Research* **20**: 321.

7. Srivastava, Pratima & Pandey, V.C. (1995) *International Journal of Parasitology* **25**: 1061.

8. Srivastava, Pratima & Pandey, V.C. (1998) Experimental Parasitology **88**: 60.

9. Srivastava, Pratima, Pandey, V.C., Misra, A.P., Gupta,P., Raj, K. & Bhaduri, A.P.(1998) *Bio-organic Medicinal Chemistry* **6**: 181.

10. Srivastava, Pratima, Pandey, V.C. & Bhaduri, A.P. (1995) *Tropical Medicine and Parasitology* **46**: 83.

11. Srivastava, Pratima & Pandey, V.C. (1995) *Malaria Weekly* **Nov 6**: 16.

12. Batra, S., Srivastava, P., Raj, K., Pandey, V.C. & Bhaduri, A.P. (2000) *Journal of Medicinal Chemistry* **43**:3428.

13. Sharma, V.L., Bhadari, K., Shankar, G., Singh, H.K., Srivastava, P. & Pandey, V.C. (2004) *Indian J of Chemistry* **43** :207.

# Investigations on natural stain, allophycocyanin for staining of human genomic DNA and their diagnostic applications

***M. Kuddus AND P. W. Ramteke**

*Department of Biotechnology, Allahabad Agricultural Institute - Deemed University, Allahabad – 211007, India.*

*E-mail: kuddus_biotech@yahoo.com*

Received June 7, 2004; Accepted June 28, 2004

## Abstract

**Allophycocyanin (APC) belongs to a family of phycobiliproteins, extracted from *Anacystis nidulans*, was examined for its binding affinity towards humans genomic DNA. The genomic DNA was isolated from human's blood, stained with allophycocyanin and examined under UV trans-illuminator after electrophoresis.**

**Allophycocyanin dye showed high affinity towards genomic DNA. It reacted with the human genomic DNA at high dilution of $>2\times10^5$. The allophycocyanin was seen to have no affinity towards RNA and proteins (BSA, papain). The result suggest that APC is a valuable natural dye without any biohazards and may have wide application in diagnostic studies such as fluorescent microscopy, fluorescence immunoassay, flow cytometry and fluorescence activated cell sorting and analysis.**

**(Keywords: allophycocyanin/ fluorescent dye/ phycobiliproteins/ DNA staining)**

Allophycocyanin (APC) belongs to a family of phycobiliproteins that are well suited as a fluorescent reagent for immunological analysis since they have a broad excitation spectrum and fluoresce with high quantum yield[1].

Phycobiliproteins are stable and highly soluble proteins derived from cyanobacteria and eukaryotic algae that possess a monodisperse population of prosthetic fluorophores. This is used by some classes of plants to increase the efficiency of photosynthesis by collecting light energy at wavelengths over which chlorophyll absorbs poorly.

Phycobiliproteins are well suited as fluorescent dyes since they possess many fluorescent groups (bilin chromophores) of several distinct types per protein[1]. They also have high quantum yields that are constant over a broad pH range. The isoelectric point of phycobiliproteins[2] ranges from 4.7 to 5.3. The biliproteins are highly water-soluble and show no change in spectroscopic or physical properties on storage in aqueous solution for long periods of time[3].

Oi and coworkers introduced the phycobiliproteins as a novel class of fluorescent tags in 1982[4]. These naturally

occurring fluorescent macromolecules immediately comes wide spread use in many diagnostic and clinical assay, in histochemistry and in diverse research applications[5]. Therefore the objective of present study was to investigate the staining properties of allophycocyanin, extracted from *Anacystis nidulans,* for genomic DNA.

**1. Extraction of Genomic DNA :** DNA was isolated by applying protocol developed by Bangalore Genie, Bangalore as described below. After isolation of genomic DNA its concentration was determined through spectrophotometer then it is diluted to maintain the concentration of 1mg/ml.

Blood was collected in EDTA coated collection tube and stored at 4°C. In 1.5 ml test tube 300µl of blood pipette out and centrifuged at 5000rpm for 5 min at room temperature, removed the serum by discarding supernatant and resuspended the pellet in 1 ml of solution A (solution A, B and C were provided by Bangalore Genie Kit). The solution was mixed by inversion, lefts at room temperature till see a clear lysed RBC solution and centrifuged at 5000rpm for 2 min at room temperature. Removed the supernatant and repeat the process once again, keeping the small white nucleated cell pellet. To the whit pellet 600µl of solution B was added, mixed well at room temperature for 5 min and centrifuged at 10,000rpm.

Supernatant was collected in fresh tube; 0.9 ml of ethanol was added to this to precipitate the DNA and spin at 10,000rpm for 5 min. Washed the DNA twice with 95% ethanol and finally with 75% ethanol. Air-dries the DNA pellet for 2 min at room temperature then 150-200µl of solution C was added and incubates at 55°C for 10 min to improve solubility. Centrifuged at 10,000rpm for 2 min to remove any insoluble materials and supernatant was collected. This DNA was used immediately for staining.

**2. Dilution of allophycocyanin (APC) :** The allophycocyanin (1mg/ml) was serially diluted upto 1:2,00,000 with 0.01mM phosphate buffer saline (PBS) solution as mentioned below:

| S. No. | PBS (ml) | APC (ml) | Dilution Ratio of APC |
|---|---|---|---|
| 1 | 9 | 1 | 1:10 |
| 2 | 9 | 1 | 1:100 |
| 3 | 9 | 1 | 1:1000 |
| 4 | 9 | 1 | 1:10000 |
| 5 | 9 | 1 | 1:100000 |
| 6 | 5 | 5 | 1:200000 |

**3. Staining of genomic DNA :** The isolated DNA was analyzed by gel electrophoresis. The DNA was stained and detected by allophycocyanin dye instead of the generally used fluorescent dye ethidium bromide[6]. Along with the test sample the standard DNA molecular weight marker was run as positive control and different proteins like RNA, bovine serum albumin (BSA) and papain were also run as negative controls.

For gel electrophoresis 0.8% agarose was used and 5µl of genomic DNA (1µl/mg), 5µl of standard DNA molecular weight marker (1.25µg/l) and 10µl of RNA, BSA and papain solution were incubated with 5µl of allophycocyanin dye in an Eppendorf tube for 10 minutes at 25±2 °C. These were loaded in the wells with the loading dye. Electrophoresis was carried out at 50 volts. After electrophoresis the gel

was observed for the presence of DNA stained with the fluorescent dye, on trans-illuminator.

*Results and Discussion* : The binding capacity of allophycocyanin to the Human genomic DNA was determined by employing electrophoretic technique. The bands of standard DNA molecular weight marker were seen to fluoresce but no fluorescence was seen along the path of the other proteins such as RNA, BSA and papain (Fig. 1). The dye stained the genomic DNA even at high dilution i.e. $2\times10^5$. It was also shown that there is no effect of dilution of allophycocyanin on the sharpness of the DNA bands if the concentration of DNA is constant. The genomic DNA could thus be stained and detected by the allophycocyanin.

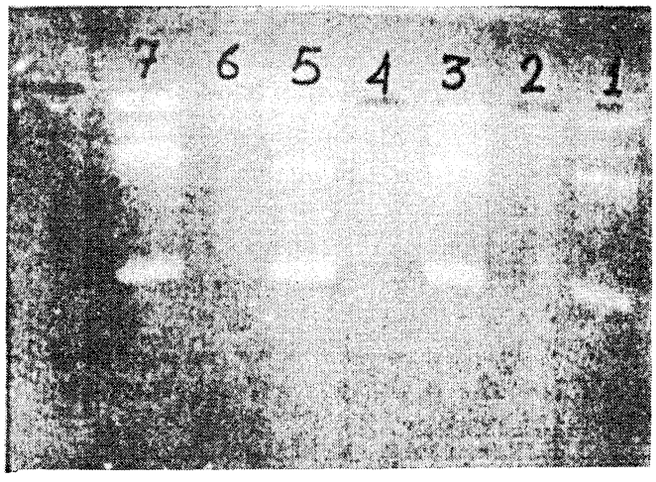


Fig. 1– Fluorescent staining of genomic DNA and different protein with APC using 0.8% agarose gel electrophoresis

Lane 1, 3, 5 and 7: Genomic DNA with APC; Lane 2: BSA with APC; Lane 4: Papain with APC; Lane 6: RNA with APC

Allophycocyanin is not species specific because it can bind to different human genomic DNA and hence can be used as non-specific DNA stain. From the present study, it can be detected that the purified allophycocyanin has great affinity towards the human genomic DNA. The dye migrates very well on gel electrophoresis without dissociation even at 1:200000 dilutions. The allophycocyanin has no specificity for any other proteins as it can not stain them and thus can be suitably employing in genomic DNA analysis.

The allophycocyanin is natural in origin and has been found to be without any toxic effects, unlike the conventional synthetic fluorochromes, it can act as a substitute for the generally used ethidium bromide, which is a carcinogenic compound[7]. Ethidium bromide is much cheaper than the allophycocyanin but due to its carcinogenic nature it may be substituted by natural stain such as allophycocyanin.

By using APC as a marker various cell may be detected by adapting avidin/biotin as a non-conventional coupling agent. It can be employed in the diagnostic and in the prognosis of the disease such as chronic lymphatic leukemia. It can be applied in measuring the ploidy and proliferative activity of the tissue or cell in case of malignancy[8].

The other potential use of allophycocyanin as a marker is in the immunofluorescent techniques, as in case of newborn infants suffering from hemolytic disease and in case of autoimmune hemolytic anemia or blood transfusion reaction due to blood group incompatibility. It can be detected by coating of antibody molecule on red cell *in vivo*[8].

It may be concluded from present study that allophycocyanin is a valuable natural

dye without any biohazards and may have wide application in diagnostic studies. Phycobiliproteins like phycocyanin and phycoerythrin has been extensively used in diagnostic studies[4,9,10], so similarly the dye, allophycocyanin was investigated for its potential use in the immunodiagnosis. From the present study, it can be deducted that purified allophycocyanin has great affinity towards genomic DNA. Phycobiliproteins can be utilized as valuable fluorescent probes for analysis of cells and molecule[8]. It can be applied to DNA staining, fluorescence microscopy, fluorescence immunoassay, flow cytometry and fluorescence activated cell sorting and analysis. However the wide use of allophycocyanin may be limited by availability of raw materials i.e. blue green algae and high cost of purified allophycocyanin.

## References


1. Hardy, R.R. (1986) *Handbook of Experimental Immunology* 4th Ed., ed. Weir, D.M.
2. Glazer, A.N. (1981) *The Biochemistry of Plant.* Academic Press, p. 51.
3. Karuna-Karan, A. & Schick, B. (1990) *Cosmetics and Tolletries* **105** : 78.
4. Oi, V.T., Glazer, A.N. & Stryer, L. (1982) *J. Cell Biol.* **93** : 981.
5. Glazer, A.N. & Stryer, L. (1990) *Methods in Enzymology,* ed. Wilchek, M. and Bayer, E.A., p. 88
6. Maniatis, T., Fritsch, F.F. & Sambrook, J. (1982) *Molecular Cloning: A Laboratory Manual.* Cold Spring Harbor Press, USA.
7. Arad, S. & Yaron, A. (1992) *Trends Food Sci. Technol.* **3**: 92.
8. Kulkarni, S.U., Badakere, S.S., Oswald, J. & Kamat, M.Y. (1996) *Biotech Lab International Sept-Oct 1996* : 14.
9. Good, M.J., Hage, W.J., Mummery, C.L. & Boonstra (1992) *J. Histo. Chem. Cytochem.* **40** : 1353.
10. Kronick, M.N. & Grossman, P.D. (1983) *Clin. Chem.* **29** : 1582.

# Giemsa C-banding and karyological studies in species of *Rhinopetalum* (*Liliaceae*)

**Gholamreza Bakhshi Khaniki**

*Department of Biology, Payame Noor University, P.O.Box 19395-4697, Tehran, Iran.*

*E-mail: bakhshi@pnu.ac.ir*

Received June 24, 2002; Revised February 23, 2004; Accepted August 24, 2004

**Abstract**

**C-band patterns and karyology are described for three Old World *Rhinopetalum* species. All species have a similar basic karyotype (n=12), consisting of large symmetric (m, sm) and smaller asymmetric (t, st) chromosomes, but C-bands differ between them. The bands are rather few, located at intercalary, telomeric, centromeric and rarely secondary constriction regions. The genus *Rhinopetalum*, is comparatively richer in heterochromatin. The patterns are characterized by the occurrence of thick telomeric/subtelomeric heteromorphic bands in the second pair of m-chromosomes. Presence of a distinct centromeric band in the short arms of these m-chromosomes in *Rh. bucharicum* discriminate it from the two allied species. A certain level of banding heteromorphy was observed mostly in term of bands size. It is obvious from this study that diversity exists between individual species studied both in the dispersion and quantity of detectable heterochromatin and chromosome morphology. Further aspects of banding patterns, band heteromorphy, chromocenters, equilocal position of bands and the role of C-banding in taxonomy are discussed.**

**(Keywords : *Rhinopetalum/Liliaceae*/karyotype/ Giemsa C-banding/heterochromatin/Iran)**

*Introduction* : The development of Giemsa C-banding in plants[1] has introduced a new era in plant chromosome identification. With the aid of C-banding procedures, more detailed karyotypes have been produced for several plant species[2-12]. Giemsa C-banding often facilitates both identification of individual chromosomes and the recognition of specific rearrangements. Moreover, C-banded karyotypes can lead to species identification or at least the assignment of a particular specimen to a group of species with similar banding patterns. By examining the inter and intra specific variation in heterochromatin content, some insights may be gained into the species relationships within and between plant genera[10].

The genus *Fritillaria* s. lat. includes c. 100 species growing in temperate regions of the northern hemisphere of the globe[13], with the exception of eastern North America. Baker[14] in his review of the genus, disposed the species in ten subgenera, of which three, *Rhinopetalum*, *Korolkowia* and *Notholirion*, are now mostly accepted as distinct genera under the same name[15,16]. According to Losina-Losinskaya[15], the genus *Rhinopetalum* contains five species, *Rhinopetalum gibbosum* (Boiss.) Losinsk. & Vved., *Rh.*

*karelinii* Fisch. ex D. Don, *Rh. arianum* Losinsk. & Vved., *Rh. bucharicum* (Regel) Losinsk., and *Rh. stenantherum* Regel, three of which are studied here.

There is a high degree of uniformity in chromosome morphology. The karyotype of the genus group is bimodal, always consisting of large, ± symmetric (m, sm), and smaller asymmetric (st, t) chromosome pairs. Further, the close morphological similarity of the asymmetric chromosome pairs usually prohibits the identification of homologous pairs. In this genus, the basic chromosome number is x=12, as in related genera of *Liliaceae*, such as *Tulipa*[10-11,13] and *Lilium* [12].

The constitutive heterochromatin in chromosomes of some species of *Rhinopetalum* has also been examined by Giemsa C-banding techniques[9], but so far detailed C-band patterns and karyomorphological studies on a large number of populations have never been made.

The aim of the present investigation is to give a general overview of the variation of C-banding patterns between and among species with the aid of the Giemsa C-banding method, and to provide data useful for phylogenetic and cytotaxonomic works.

*Materials and Methods* : The specimens for this study were collected by the author from different localities which span parts of the distribution areas of the genus *Rhinopetalum* in Iran (Table 1), except *Rh. bucharicum* which was received from other sources. The bulbs collected were cultivated under uniform conditions in Göteborg Botanical Garden, Sweden, in clay pots sunk in indoor beds, in order to check the morphological characters and also for root tips preparations for chromosomal studies. Vouchers are deposited in the Herbarium of the Göteborg University (GB). Each population in the following is assigned a collection number preceded by the abbreviation GBK which stands for the author's name. For chromosome studies, I used root tip meristem. The roots were pretreated with a mixture of 0.2% colchicine and 0.002 M 8-hydroxyquinoline (1 vol. each) for 2–3 hours at room temperature, fixed in Carnoy fixative (ethanol/acetic acid 3:1) for 24 hours, transferred to 70% alcohol and stored in -20° C until used. Fixed material was washed in distilled water and hydrolysed in 1 M HCL for 15 min. at room temperature. After another rinse, they were softened in a mixture of 10–20% pectinase (Sigma, from *Aspergillus niger*, dissolved in 40% glycerol) and 1% cellulase (Calbiochem) (1 vol. each) at 37° C for 1 hour (for acetic orcein staining, only 5% powdered pectinase for 2–3 hours at room temperature was used).

The meristematic tip of the roots was separated and squashed in 45% acetic acid on a clean glass slide. Coverslips were removed after freezing in liquid nitrogen and slides immersed in 95% ethanol, dried in compressed air and stored in an exsiccator for a week. Dried slides were treated in freshly prepared 5% hot Barium hydroxide [$Ba(OH)_2$] at 50–52° C for 7 min., washed in running tap water for 1 hour and immersed in 2 x SSC (pH=7.0) at 60° C for 60 min. After a rinse in Sørensen's phosphate buffer (pH 6.81), cells were stained in 1.5% Giemsa (buffered to pH 6.81) for 5–8 min., rinsed, dried, and permanented in D.P.X mountant. Differences in concentration of the $Ba(OH)_2$ solution and treatment time turned out to influence the later staining quality and also slightly the number of bands

revealed. Also the time of staining in the Giemsa bath was critical. The preparations were observed with a Carl Zeiss photo-microscope. The best meta-phasic plates were drawn by using a Camera Lucida, and photographed by an Olympus microscope using an Agfa-Ortho film (15 Din/25 Asa).

Karyograms were prepared from drawings of metaphase chromosomes. Generally, the following features were used to characterise the karyotypes, based on the recommendations of Bentzer et al[4]: pair (figure indicating the pairs of homologous chromosomes in decreasing order of the length), type, i.e. kind of chromosome, according to centromere position and arms ratio, real and relative length of the individual chromosomes, short (S) and long (L) arms of the chromosomes and r-index (L:S[18]). With regard to SAT-chromosomes, care was taken in recording the satellites as they may often be very variable in appearance[19], simply due to the cell 's physiological stages, chromatin condensation or even from the method of squashing. Different degrees of contraction of chromosomes may cause slight differences in relative length and band position. In the idiograms, constructed as the mean of 10 measured metaphase plates per population, each chromosome is given with the maximal number of C-bands observed. All measurements and percentage values given in the tables are mean values from 10 plates from a representative population.

*Results and Discussion* : Holmquist[20], Vosa[21] and Sumner[22] assumed that C-banding involves differential DNA extraction and linear differentiation from the fixed material. This is achieved by the following three sequential treatments all of which are essential: acid treatment (e.g. 1 N HCL) depurinates DNA, whereas a mild base causes DNA denaturation, and hot salt (e.g. 2 x SSC at 60° C) induces chain breakage and preferential solubilization of fragmented DNA from euchromatin. The pectinase plus cellulase treatment which I have applied prior to the essential three stages (acid, mild base, hot salt) resulted in much sharper and more persistent banding. With the methods previously[9,22] used for *Fritillaria* s. lat., my material did not respond with staining of bands. Of 21 modifications tried, the present method gave the best results, although it does not reveal as many bands as that of La Cour[9]. We should keep it in mind that Giemsa C-banding method is a very sensitive method and that results obviously differ from chemical to chemical, from material to material, and laboratory to laboratory. Clearly, the chromosomes of different species may have an entirely characteristic chemical architecture, but differences in band numbers for the same material from one laboratory to another is also to be suspected.

The somatic chromosome number was 2n=2x=24 for all material investigated. All populations studied were found to have C-bands in their chromosome complements, some more than the others. The size of the C-bands varies from dot-like or small (thin and pale) to relatively large. They occur within intercalary, telomeric, centromeric and secondary constriction regions, of which the latter location is less common. It is clear from this study that differences exist between the species studied in the distribution and amount of detectable heterochromatin their chromosomes carry (Figs 1-4). Details of the karyotypes are summarised in Tables 2–8.

Table 1– Localities of the populations studied of *Rhinopetalum*.

| Pop. no. | Species | Locality |
|---|---|---|
| VACRATOT s.n. | *Rh. bucharicum* | Tadjikistan: Hissar mountains, 1400 m. |
| GBK 1 | *Rh. gibbosum* | Tehran: Park-e Chitgar, clay loam, associated with *Allium*, *Fraxinus* and *Pinus* (park trees), 1450 m. |
| GBK 2 | | Tehran: Lavasanat, Afjah, Naroon mountain (central Elborz), rocky slopes, among grasses, 1800–2200 m. |
| GBK 3 | | Tehran: Karaj, Mardabad, very frequent in gypsum soils (saline situation), usually among *Alhagi, Haloxylon Tribulus*, *Euphorbia*, and *Lactuca*, 1350 m. |
| GBK 4 | | Khorasan: Bojnord to Gorgan, Rabatcharbil village, steppic areas mainly covered by *Artemisia*, 1100–1300 m. |
| GBK 17 | | Mazendaran: Gorgan, Golestan forest, near the road, among *Populus* and shrubs, 1600 m. |
| GBK 32 | | Tehran: Qom to Arak, steppic areas, among xerophytes and halophytes, 1400 m. |
| GBK 43 | | Khorasan: Torbat-e Haydariyeh to Mashhad, steppic areas, among *Artemisia, Lactuca, Peganum harmala, Alhagi, Tribulus, Haloxylon, Atriplex* and short grasses, 1700 m. |
| GBK 45 | | Khorasan: Kashmar to Sabzevar, steppic places, among halophytes and xerophytes, 1800 m. |
| GBK 46 | | Khorasan: Nishabour, Akhlamad, Abshar valley, rocky slopes, 1700 m. |
| GBK 42 | *Rh. arianum* | Khorasan: Torbat-e Jam, Hari Rud (close to the border of Afghanistan), desert and sandy places, 1700 m. |

Table 2– Karyotype of *Rh. bucharicum* (Tadjikistan: Hissar mtns.). Karyotype formula: 2n=2x=24= 4m + 14st + 6t.

| Pair | L + S (μm) | L (μm) | S (μm) | L+S% | L% | S% | L:S | Type |
|---|---|---|---|---|---|---|---|---|
| 1 | 22.1 | 12.9 | 9.2 | 11.82 | 6.90 | 4.92 | 1.40 | m |
| 2 | 19.2 | 12.2 | 6.1 | 10.70 | 6.75 | 3.95 | 1.70 | m |
| 3 | 17.5 | 15.6 | 1.1 | 9.38 | 8.32 | 1.06 | 7.85 | t |
| 4 | 16.5 | 14.5 | 1.1 | 8.84 | 7.80 | 1.04 | 7.5 | t |
| 5 | 15.7 | 13.0 | 2.7 | 8.41 | 6.97 | 1.44 | 4.84 | st |
| 6 | 15.5 | 12.9 | 2.6 | 8.27 | 6.88 | 1.39 | 4.95 | st |
| 7 | 14.5 | 11.1 | 2.6 | 7.79 | 6.40 | 1.39 | 4.60 | st |
| 8 | 14.2 | 13.0 | 1.1 | 7.58 | 6.97 | 0.61 | 11.42 | t |
| 9 | 13.6 | 10.1 | 2.6 | 6.84 | 5.87 | 0.97 | 6.05 | st |
| 10 | 12.1 | 11.2 | 1.7 | 6.95 | 6.01 | 0.94 | 6.40 | st |
| 11 | 12.6 | 10.9 | 1.7 | 6.75 | 5.84 | 0.91 | 6.41 | st |
| 12 | 12.5 | 10.4 | 2.1 | 6.67 | 5.55 | 1.12 | 4.95 | st |

Table 3– Karyotype of *Rh. gibbosum* (GBK 3). Karyotype formula: 2n=2x=24=4m + 10st + 10t.

| Pair | L + S (μm) | L (μm) | S (μm) | L+S% | L% | S% | L:S | Type |
|---|---|---|---|---|---|---|---|---|
| 1 | 20.5 | 12.3 | 8.2 | 11.35 | 6.81 | 4.54 | 1.50 | m |
| 2 | 18.7 | 11.0 | 7.7 | 10.35 | 5.65 | 4.70 | 1.20 | m |
| 3 | 16.4 | 14.5 | 1.8 | 9.18 | 8.10 | 1.08 | 7.50 | t |
| 4 | 16.3 | 13.4 | 2.9 | 8.90 | 7.20 | 1.70 | 4.24 | st |
| 5 | 15.6 | 13.2 | 2.5 | 8.67 | 7.30 | 1.37 | 5.33 | st |
| 6 | 14.8 | 12.8 | 1.9 | 8.20 | 7.12 | 1.08 | 6.60 | st |
| 7 | 14.7 | 12.9 | 1.7 | 8.11 | 7.16 | 0.95 | 7.53 | t |
| 8 | 13.9 | 12.3 | 1.6 | 7.69 | 6.79 | 0.90 | 7.51 | t |
| 9 | 13.6 | 11.7 | 1.8 | 7.46 | 6.47 | 0.99 | 6.53 | st |
| 10 | 12.7 | 11.4 | 1.4 | 7.04 | 6.30 | 0.74 | 8.51 | t |
| 11 | 11.9 | 10.3 | 1.6 | 6.58 | 5.72 | 0.86 | 6.65 | st |
| 12 | 11.7 | 10.3 | 1.4 | 6.47 | 5.70 | 0.77 | 7.40 | t |

Table 4– Karyotype of *Rh. arianum* (GBK 42). Karyotype formula: 2n=2x=24=2m + 2sm + 16st + 4t.

| Pair | L + S (μm) | L (μm) | S (μm) | L+S% | L% | S% | L:S | Type |
|---|---|---|---|---|---|---|---|---|
| 1 | 17.7 | 11.1 | 6.7 | 11.25 | 7.03 | 4.22 | 1.66 | m |
| 2 | 16.1 | 10.4 | 5.7 | 10.22 | 6.60 | 3.62 | 1.82 | sm |
| 3 | 14.9 | 12.5 | 2.3 | 9.43 | 7.95 | 1.48 | 5.37 | st |
| 4 | 14.0 | 11.1 | 2.0 | 8.90 | 7.58 | 1.32 | 5.74 | st |
| 5 | 13.8 | 11.9 | 1.8 | 8.74 | 7.58 | 1.16 | 6.53 | st |
| 6 | 13.2 | 11.7 | 1.6 | 8.41 | 7.42 | 0.99 | 7.50 | t |
| 7 | 12.5 | 10.7 | 1.8 | 7.80 | 6.77 | 1.03 | 6.57 | st |
| 8 | 11.1 | 10.3 | 1.6 | 7.78 | 6.55 | 1.23 | 5.32 | st |
| 9 | 11.7 | 10.4 | 1.3 | 7.41 | 6.62 | 0.79 | 8.38 | t |
| 10 | 11.4 | 9.9 | 1.6 | 7.25 | 6.26 | 0.99 | 6.32 | st |
| 11 | 10.7 | 9.2 | 1.5 | 6.77 | 5.82 | 0.95 | 6.12 | st |
| 12 | 9.7 | 8.3 | 1.4 | 6.04 | 5.22 | 0.82 | 6.36 | st |

Table 5– Summary of karyotype characters of the material studied.

| Species | 2n | Range of chromosome length (μm) | Total haploid karyotype length (μm) |
|---|---|---|---|
| *Rh. bucharicum* | 24 | 12.5–22.1 | 186.8 |
| *Rh. gibbosum* | 24 | 11.7–20.5 | 180.6 |
| *Rh. arianum* | 24 | 9.7–17.7 | 157.7 |

Table 6– Frequency and distribution of C-bands and heteromorphic bands in the chromosomes of all material studied of *Fritillaria* and *Rhinopetalum*.

Numerator: number of positions with heteromorphic bands; denominator: total number of positions with bands.

Note: dot-like and thin pale bands (presented by double dots and broken lines in idiograms) are not considered in this table.

| Species | Band position | Chromosome no. | | | | | | | | | | | |
|---|---|---|---|---|---|---|---|---|---|---|---|---|---|
| | | 1 | 2 | 3 | 4 | 5 | 6 | 7 | 8 | 9 | 10 | 11 | 12 |
| *Rh. bucharicum* | Intercalary | 0/2 | 0/3 | 0/1 | 0/2 | 0/0 | 0/3 | 0/4 | 0/0 | 0/3 | 0/1 | 0/2 | 0/1 |
| | Centromeric | 0/0 | 0/1 | 0/0 | 0/1 | 0/0 | 0/1 | 0/0 | 0/0 | 0/1 | 0/0 | 0/0 | 0/0 |
| | Telomeric & subtelomeric | 0/0 | 1/1 | 0/0 | 0/1 | 0/1 | 0/0 | 0/0 | 0/1 | 0/0 | 0/1 | 0/0 | 0/0 |
| | Sec. constriction (intercalary) | 0/0 | 0/0 | 0/0 | 0/0 | 0/0 | 0/0 | 0/0 | 0/0 | 0/0 | 0/0 | 0/0 | 0/0 |
| *Rh. gibbosum* | Intercalary | 1/6 | 1/4 | 1/4 | 1/1 | 0/4 | 0/2 | 2/4 | 0/1 | 0/3 | 1/3 | 0/3 | 0/3 |
| | Centromeric | 0/0 | 0/0 | 0/0 | 0/1 | 0/0 | 0/0 | 0/0 | 0/0 | 0/0 | 0/0 | 0/0 | 0/0 |
| | Telomeric & subtelomeric | 0/0 | 1/1 | 0/0 | 0/0 | 1/2 | 0/1 | 0/1 | 0/1 | 0/0 | 0/1 | 0/0 | 0/0 |
| | Sec. constriction (intercalary) | 0/0 | 0/0 | 0/0 | 0/0 | 0/0 | 0/0 | 0/0 | 0/0 | 0/0 | 0/0 | 0/0 | 0/0 |
| *Rh. arianum* | Intercalary | 1/6 | 1/4 | 0/1 | 0/3 | 0/5 | 0/3 | 0/1 | 0/1 | 0/2 | 0/3 | 0/3 | 0/1 |
| | Centromeric | 0/0 | 0/0 | 0/1 | 0/0 | 0/0 | 0/0 | 0/0 | 0/0 | 0/0 | 0/0 | 0/0 | 0/0 |
| | Telomeric | 0/0 | 1/1 | 0/0 | 0/0 | 0/1 | 0/1 | 0/1 | 0/1 | 0/0 | 0/0 | 0/0 | 0/0 |
| | Sec. constriction | 0/0 | 0/0 | 0/0 | 0/0 | 0/0 | 0/0 | 0/0 | 0/0 | 0/0 | 0/0 | 0/0 | 0/0 |

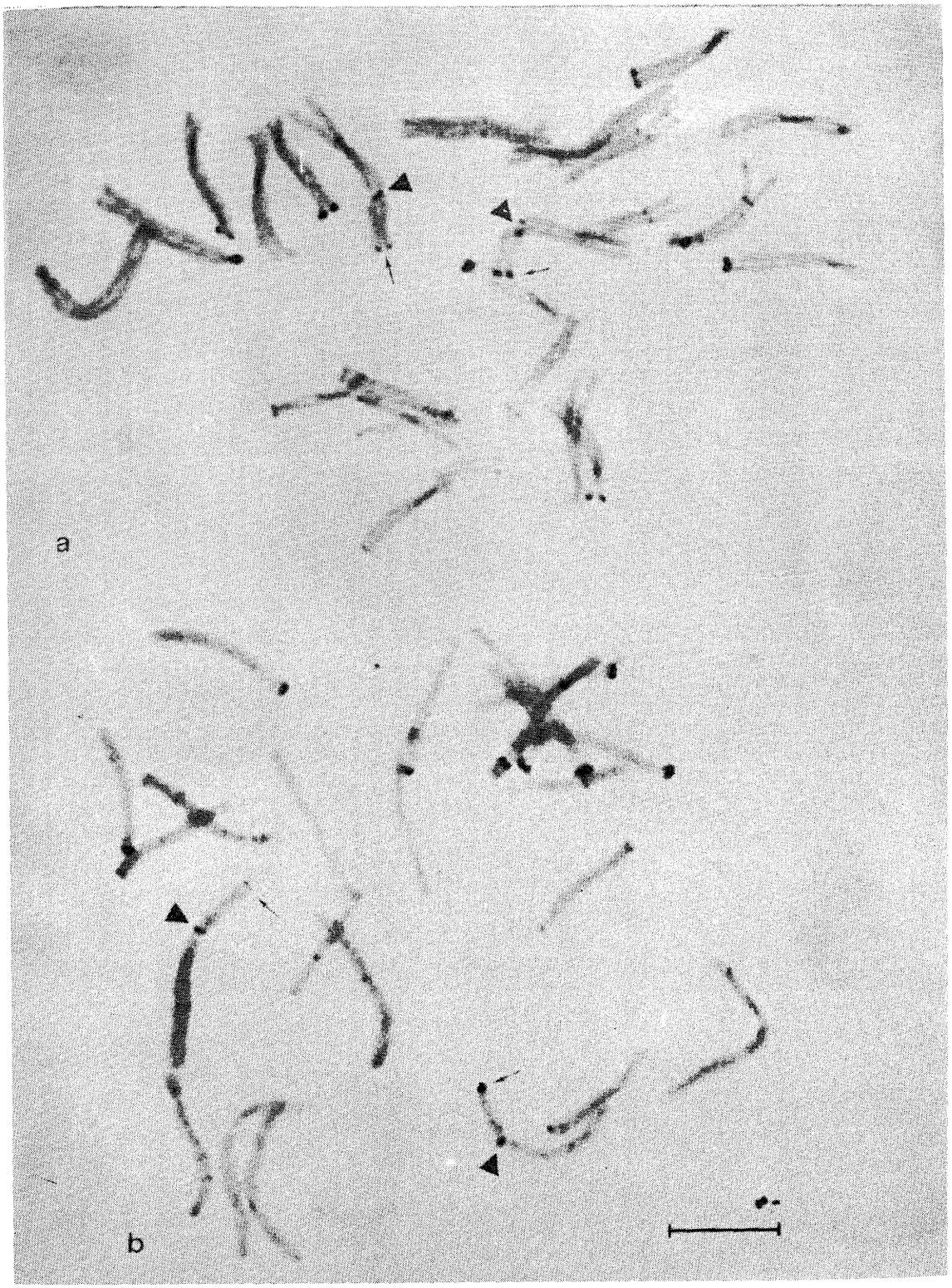


Fig. 1– Giemsa C-banded mitotic metaphase of *Rh. bucharicum* (2n=24). Arrows: heteromorphy in SAT-metacentric chromosomes. Triangles: centromeric band in the short arms of the second pair of metacentric chromosomes. Population from Tadjikistan: Hissar mountains. *a* showing equilocal position of C-bands in both chromatids of each chromosome. Scale bar: 10 μm.

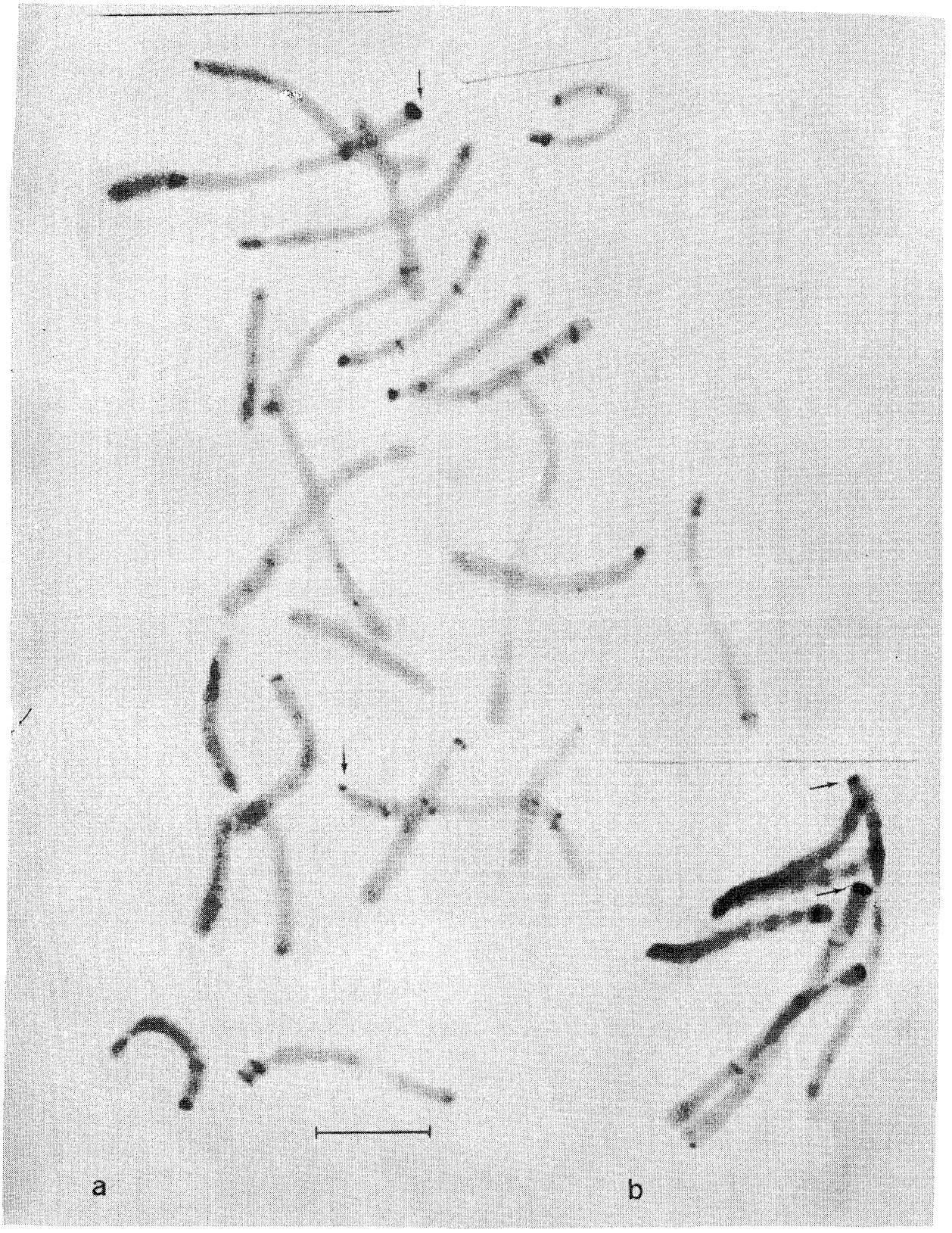


Fig. 2– Giemsa C-banded mitotic metaphase of *Rh. gibbosum* (2n=24). Heteromorphy in width of telomeric bands in the short arms of the second pair of m-chromosomes (arrows). *a* population GBK 3; *b* population GBK 45 (detail of plate). Scale bar: 10 μm.

Table 7– Summary of karyotype characters of the material studied.

| Species | 2n | Range of chromosome length (μm) | Total haploid karyotype length (μm) |
|---|---|---|---|
| *F. imperialis* | 24 | 9.4–19.8 | 157.7 |
| *F. raddeana* | 24 | 9.1–17.9 | 150.9 |
| *F. persica* | 24 | 8.7–17.1 | 141.7 |
| *Rh. bucharicum* | 24 | 12.5–22.1 | 186.8 |
| *Rh. gibbosum* | 24 | 11.7–20.5 | 180.6 |
| *Rh. arianum* | 24 | 9.7–17.7 | 157.7 |

Table 8– Proportion (in %) of Giemsa C-bands to chromosome length.

Note: dot-like and thin pale bands (presented by double dots and broken lines in idiograms) are not considered in this calculation.

| Species | Pop. no. | Chromosome no. | | | | | | % of heterochromatin | | | | | | |
|---|---|---|---|---|---|---|---|---|---|---|---|---|---|---|
| | | 1 | 2 | 3 | 4 | 5 | 6 | 7 | 8 | 9 | 10 | 11 | 12 | in haploid complement |
| *F. imperialis* | GBK 5 | 2.0 | 3.3 | 1.2 | 0.0 | 3.8 | 0.0 | 2.6 | 3.3 | 3.9 | 6.3 | 7.6 | 5.5 | 6.5 |
| *F. raddeana* | GBK 48 | 0.0 | 1.6 | 10.5 | 1.9 | 4.4 | 0.0 | 4.9 | 1.8 | 4.5 | 1.7 | 0.0 | 2.6 | 5.8 |
| *F. persica* | GBK 18 | 0.0 | 0.0 | 0.0 | 5.7 | 0.0 | 0.0 | 4.2 | 7.9 | 0.0 | 6.4 | 0.0 | 0.0 | 4.5 |
| *Rh. bucharicum* | VACRATOT | 1.0 | 7.0 | 1.6 | 0.0 | 4.5 | 3.8 | 1.9 | 3.7 | 4.1 | 2.6 | 6.2 | 2.7 | 5.4 |
| *Rh. gibbosum* | GBK 45 | 1.1 | 8.6 | 1.3 | 1.6 | 8.8 | 9.6 | 12.1 | 3.7 | 3.6 | 5.7 | 0.0 | 0.0 | 8.1 |
| *Rh. arianum* | GBK 42 | 1.0 | 7.8 | 3.0 | 0 | 7.2 | 6.9 | 1.3 | 3.5 | 4.4 | 3.6 | 0.0 | 0.0 | 6.4 |

The genus *Rhinopetalum* is characterised by its deeply depressed nectaries which appear on the outside of the tepals as dark hump- or sac-like projections. These projections are equal in some species, unequal in others. In the latter case, the flowers are zygomorphic. It includes five species, three of them, *Rh. bucharicum, Rh. gibbosum*, and *Rh. arianum*, are karyologicaly studied here.

**(1) *Rh. bucharicum* (Regel) Losinskaya.** Two C-banded plates are shown in Fig. 1. The karyotype contains two metacentric, seven subtelocentric, and three telocentric chromosome pairs (Fig. 4a, Table 2 ). The characteristics of the Giemsa C-banding of *Rh. bucharicum* are the presence of thin pale and dot-like bands mainly in the long arms. Among the two m-chromosomes, pair no. 1 revealed an

intercalary band in each arm, while the second pair presented a heteromorphic band at the subtelomeric end of the short arm, a centromeric band in the short arm and intercalary bands in both arms (Fig. 1). There was usually one satellite on the short arm of this pair. Moreover, intercalary bands are evident in the long arms of pairs nos. 3–4, 6–7, 9–10 and 12, and in the short arms of pairs nos. 6–7 and 11. Telomeric bands are present on the short arms of pairs nos. 5, 8 and 10. Such bands are generally absent in the long arms, but pair no. 4 shows one dot-like band in the telomeric end of the long arm. In addition, there are some centromeric bands in the short arms of pairs nos. 2, 4, 6 and 9. The total karyotype length of the haploid complement in this species is the longest among *Rhinopetalum* species, 186.8 μm, as compared to 157.7 μm and 180.7 μm in *Rh. arianum* and *Rh. gibbosum* (Table 7). The presence of a centromeric band (Fig. 1, arrowheads) in the second pair of m-chromosome distinguishes *Rh. bucharicum* from *Rh. gibbosum* and *Rh. arianum*.

**(2) *Rh. gibbosum* (Boiss.) Losinsk. & Vvedensky.** A banded metaphase plate is presented in Fig. 2. The karyotype of this species comprises two metacentric, five subtelocentric and five telocentric chromosome pairs (Fig. 4b, Table 3). There are frequent thin pale or dot-like bands on the C-banded karyotype, although this is not a constant feature, possibly due to the narrowness of the bands. In m-chromosomes, the first pair contains dot-like bands in three intercalary sites, one thin intercalary and one intercalary heteromorph band in the short arm, and one dot-like band in the long arm. The second pair presents one thick heteromorphic band at the subtelomeric position (adjacent to a small satellite) and one band at an intercalary situation in the short arm, and two dot-like and one heteromorphic band in an intercalary position in the long arm. A satellite is also present in pair no. 8. In addition, intercalary bands are evident in the short arms of pairs nos. 3, 5, 7 and 9 and in the long arms of pairs nos. 3–12. Telomeric bands are present in the short arms of pairs nos. 5–7 and in the long arms of pairs nos. 5 and 10, a subtelomeric band in the short arm of pair no. 8, while a centromeric band is only revealed in the short arm of pair no. 4. Heteromorphy was evident in aspect of band size on pairs nos. 1–3, 5, 7, and 10, being very distinct in pair no. 2. One of its homologues always shows a thick band at the satellite position in the short arm while in the other homologue the band is smaller and less distinct (Fig. 2, arrows). As opposed to *Rh. bucharicum*, a centromeric band is absent from the short arm of the second pair of SAT-metacentric chromosomes in *Rh. gibbosum*. The number and size of chromocentres in interphase nuclei in *Rh. gibbosum* varied according to the amount of constitutive heterochromatin observed in metaphase chromosomes. Large chromocentres may correlate to distinct, deeply stained and thick telomeric and intercalary bands, while the small and pale ones may be correlated to dot-like and thin pale intercalary bands.

**(3) *Rh. arianum* Losinsk. & Vvedensky.** A mitotic plate of this species is presented in Fig. 3. The karyotype consists of one metacentric, one submetacentric, eight subtelocentric and two telocentric chromosome pairs (Fig. 4c, Table 4). All chromosomes have bands either in both arms or in one arm. Of the m-chromosomes, the first pair has five thin pale intercalary bands and one relatively small heteromorphic band. In the second pair not only thin bands are present but also distinct

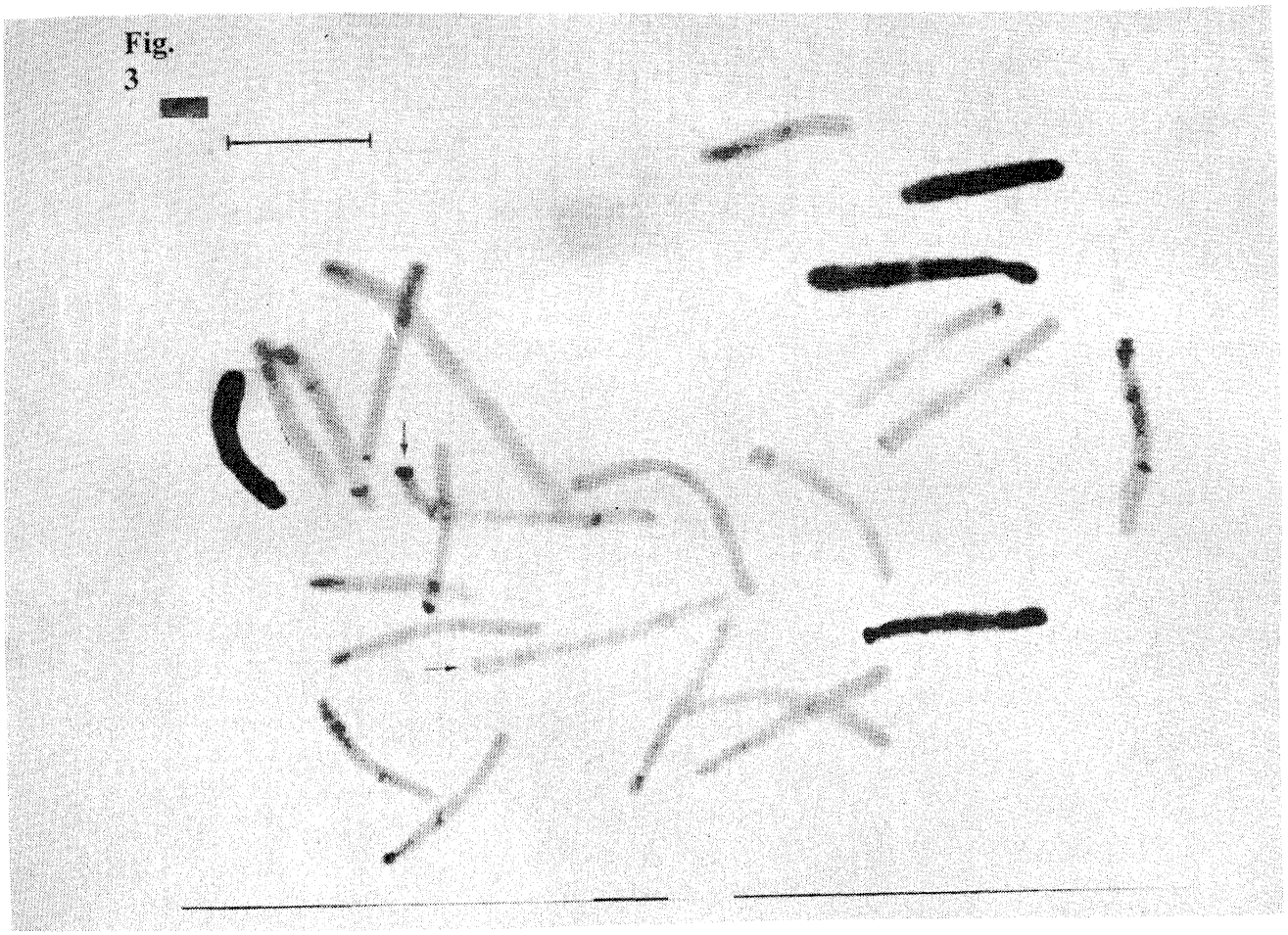


Fig. 3– Giemsa C-banded mitotic metaphase of *Rh. arianum* (2n=24). Heteromorphy in the second pair of m-chromosomes (arrows). Population GBK42. Scale bar: 10 μm.

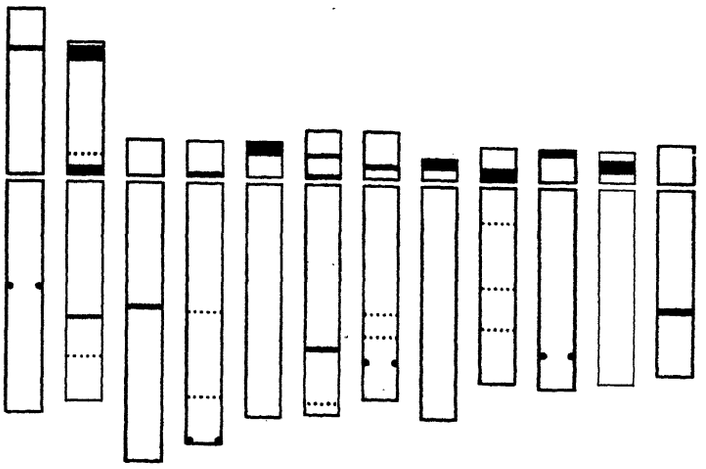


Fig. 4a.


Fig. 4b.


Fig. 4c.

Fig. 4– Haploid idiograms of *Rhinopetalum*, showing interspecific variation in karyotype, band size and numbers. *a Rh bucharicum, b Rh. gibbosum, c Rh. arianum* Stippled areas: heteromorphic bands; dots: dot-like "bands"; broken lines: thin pale bands, not seen in all preparations.

intercalary bands in both arms and a thick heteromorphic band in the telomeric position in the short arm (Fig. 3). Among subtelo- to telocentric pairs, intercalary bands occur of the short arms of pairs nos. 4–6 and 9 and in the long arms of pairs nos. 3–12, but telomeric bands are revealed only in the short arms of pairs nos. 5–8. Absence of telomeric bands in the long arms of the complement is notable in this species. A centromeric band is only revealed in the short arm of pair no. 3. Similar to *Rh. gibbosum*, heteromorphy is remarkable with respect to band size, particularly in pair no. 2. The telomeric heteromorphic band is thick and more clear in one of its homologues while it is much smaller and less distinct in the other one (Fig. 3, arrows). As opposed to *Rh. bucharicum* and similar to *Rh. gibbosum*, a centromeric band is absent from the second pair of m-chromosomes in *Rh. arianum*.

The present observations show that three Old World species of *Rhinopetalum* present C-bands. The chromosomes of *Rhinopetalum* are among the largest found in the plant kingdom. Their total volume and length in relation to mitotic cell boundaries makes it difficult to find a suitable technique of spreading complements into a single plane within the intact cell wall. Because of the uniformity of chromosome size and arm ratio which is a general feature of most *Rhinopetalum*, the grouping of chromosomes in pairs of presumptive homologues, and the identification of homologous pairs in the different species without using C-banding methods was earlier usually difficult, except for metacentric and submetacentric pairs which were very easy to distinguish and group. The chromosome number determinations of 2n=24 for *Rh. bucharicum* is new reports for the geographic zones in which these plants were collected. However, they agree with determinations based on material of these taxa from other areas[23]. So far, the somatic chromosome number of 2n=24 for *Rh. arianum* and *Rh. gibbosum* is reported here for the first time.

In general, the amount of constitutive heterochromatin is relatively low in the species examined (Table 8). According to La Cour[9], Old World species of *Rhinopetalum* usually reveal less banding than those of New World Origin (American species). This is also very clear from the present investigation. It is interesting that the opposite situation applies for heterochromatin revealed by Giemsa banding in *Anemone*, for in that genus much more heterochromatin is detectable in Old World species than in the New World[24]. It may be suggested that differences in C-band content will mean some kind of evolution between species. This evolution may possibly lie in the evolution of DNA with highly repetitive sequences of nucleotides which the constitutive heterochromatin seems most likely to contain.

***The C-banding pattern***. The C-banding pattern is the existence of one common, and ± similar model of banding in a group or groups of plants. This definition matches the "C-banding style"[6,12,25]. Banding patterns can be used to study chromosomal changes that have occurred between related species. In many cases differences in banding patterns between related species are very small, although complete identity is comparatively rare. More often, some differences can be found, even between closely related species. Changes in the amount of heterochromatin, demonstrated by C-banding, are quite common[22]. In the

present investigation C-bands were generally found at intercalary and telomeric positions. C-bands also occur in centromeric regions, but only on either side of the centromere. C-bands at intercalary secondary constrictions were not only apparent in chromosome pairs.

The C-banding pattern in species of the genus *Rhinopetalum* species were generally characterised by some conspicuous telomeric bands mainly in the short arms. The heteromorphic bands in the second pair of m-chromosomes are also remarkable. The many intercalary bands are often inconspicuous (Fig. 4a-c; Figs. 1-3). My observations on *Rhinopetalum* species are partly in agreement with that of La Cour[9]. Presence of a centromeric band in the short arm of the second pair of m-chromosomes (Fig. 1, arrowheads) in *Rh. bucharicum* and its absence in *Rh. gibbosum* and *Rh. arianum* distinguish these species, which otherwise have ± similar banding patterns. The proportion of heterochromatin in the haploid complement of *Rh. bucharicum* is 5.4% but 8.1% and 6.4% for *Rh. gibbosum* and *Rh. arianum* (Table 6).

***Band polymorphism (heteromorphy).*** It is obvious from the present study that heteromorphy is common in the species studied. Thus, the various banding patterns observed may be explained by various rearrangements without subsequent recombination. If recombination is not evolved, e.g. as a consequence of inhibition of chiasma formation in rearranged regions, one would expect a number of individuals with the same banding pattern within a population. In agreement with conditions in other species, two types of band heteromorphy in *Rhinopetalum* were encountered. Firstly, a heteromorphy occurs in size of a particular band. This was mostly common and very distinct among the telomeric and subtelomeric bands (pair no. 2 in *Rh. bucharicum*, *Rh. gibbosum* and *Rh. arianum*). Secondly, heteromorphy may manifest itself in the presence or apparent absence of a particular band. This is prevalent among intercalary and centromeric bands (pairs nos. 1–3, 7, 10 in *Rh. gibbosum*, and nos. 1, 2 *in Rh. arianum*). The heteromorphy for band size was by far the most common, particularly in m-chromosomes of *Rhinopetalum* species (Fig. 4a-c). Distribution of heteromorphic bands in the chromosomes of all material studied are presented in Table 6. Generally, heteromorphy was observed in one site in *Rh. bucharicum*, eight in *Rh. gibbosum*, and three in *Rh. arianum*.

Polymorphism for C-banding patterns seems to be a common phenomenon in almost any plant material investigated. It therefore seems plausible that particular C-bands in themselves do not affect the immediate fitness of a plant. It is, however, somewhat more puzzling that chromosomes must be heteromorphic for non-stained regions[26].

Smith[27] put forward the hypothesis that some bands and some heteromorphy could be produced by unequal crossing-over. A connection like this between distal band variability and distally localised chiasmata was suggested for species of the genus *Anacyclus* and other *Anthemideae* (*Asteraceae*)[6]. Polymorphism of C-bands is inherited in a strictly Mendelian fashion, and has some value in paternity testing, although banding techniques have been superseded by the much more powerful DNA fingerprinting methods[22]. The set of bands revealed by C-banding procedures usually consists of different forms of

heterochromatin, and intraspecific variation in C-banding heteromorphy must be largely due to differences of amounts and kinds of constitutive heterochromatin coupled with variation of chromosome contraction.

### Chromosome banding and taxonomy

Several C-banding studies have attempted to recognise ancestral genomes by heterochromatin markers, especially in allopolyploids.

In the genus *Rhinopetalum*, *Rh. gibbosum* and *Rh. arianum* present almost identical banding patterns. Presence of a centromeric band in the short arm of the second pair of m-chromosomes (Fig. 1, arrowheads) in *Rh. bucharicum* distinguish it from these two allied species. These C-banding results confirm the morphological grouping of these species into two subgroups, based on e.g. nectary morphology[16]. The first subgroup contains the species *Rh. arianum* and *Rh. gibbosum* with zygomorphic flowers and the nectary of the upper segment or segments larger than the rest and much more deeply impressed, produced as broad rounded spurs or horns. Furthermore, the nectary orifice is bordered by two broad, distally fringed lobes, the lower parts of which are densely and shortly hairy. The second group includes *Rh. bucharicum* and *Rh. stenantherum* (not investigated here) with actinomorphic flowers, nectaries all equally deep, and nectary orifice surrounded by two narrow lobes, not fringed but in their lower parts hairy.

In conclusion, this investigation has shown that C-band patterns can be useful in deducing relationships between *Rhinopetalum* species, and that they are also useful for species separation.

I would like to express my deepest gratitude to Dr Karin Persson for helpful discussions, valuable instruction and for critically reading the manuscript. I am also very grateful to Professor Lennart Andersson for reading the manuscript, constructive criticism and suggested improvements.

## References

1. Vosa, C. G. & Marchi, R. (1972) *Nature* **237** : 191.
2. Vosa, C. G. (1973) *Chromosoma* **43** : 269.
3. Vosa, C. G. (1976) *Heredity* **36** : 383.
4. Vosa, C. G. (1976) *Chromosoma* (Berl.) **57** : 119.
5. Filion, W. G. (1974) *Chromosoma* **49** : 51.
6. Schweizer, D. & Ehrendorfer, F. (1976) *Pl. Syst. Evol.* **126** : 107.
7. La Cour, L. F. (1978) *Chromosoma* **67** : 67.
8. La Cour, L. F. (1978) *Heredity* **41** : 101.
9. La Cour, L. F. (1978) *Philos. Trans. Roy. Soc. London, ser.* **285(B)** : 61.
10. Blakey, D. H. & Vosa, C. G. (1981) *Pl. Syst. Evol.* **139** : 47.
11. Blakey, D. H. & Vosa, C. G. (1982) *Pl. Syst. Evol.* **139** : 163.
12. Smyth, D. R., Kongsuwan, K. & Wisudharomn, S. (1989) *Pl. Syst. Evol.* **163** : 53.
13. Bakhshi Khaniki, G. (1998) *Ph.D. thesis*, Gothenburg University, Sweden.
14. Baker, J. G. (1874) *J. Linn. Soc.* (Bot.). p. **14**.
15. Losina-Losinskaya, A. S. (1935) in *Rhinopetalum Fisch.* ed. Komarov V.L., Fl. U.R.S.S. **4** : 228.
16. Bakhshi Khaniki, G. & Persson, K. (1997) *Nord. J. Bot.* **17** : 579.
17. Bentzer, B., Bothmer, R. von, Engstrand, L., Gustafsson, M. & Snogerup, S. (1971) *Bot. Not.* **124** : 65.
18. Levan, A., Fredga, K. & Sandberg, A. (1965) *Hereditas* **52** : 201.
19. Stace, C. A. (1989) *Plant taxonomy and biosystematics*. 2nd Ed. Edwarld Arnold Ltd. – London.

20. Holmquist, G. (1979) *Chromosoma* **72** : 203.

21. Marchant, C. J. & Macfarlane, R. M. (1980) *Bot. J. Linn. Soc.* **81** : 135.

22. Vosa, C. G. (1985) in *Advances in chromosome and cell genetics*, eds. Sharma, A. K. & Sharma, A. p. 79, Oxford, IBH Publ. Co.

23. Sumner, A. T. (1990) *Chromosome banding*. Unwin Hyman, London.

24. Moore, D. M. (1982) Flora Europaea check-list and chromosome index, p. 296. Cambridge University Press.

25. Marks, G. E. & Schweizer, D. (1974) *Chromosoma* **44** : 405.

26. Greilhuber, J. & Speta, F. (1976) *Pl. Syst. Evol.* **126** : 149.

27. Bentzer, B. & Landström, T. (1975) *Hereditas* **80** : 219.

28. Smith, G. P. (1976) *Science* **191** : 528.

# Determination of some sulpha drugs and diuretics with pyridinium chlorochromate (PCC) reagent

**B. K. Dubey, A. K. Tiwari AND I. C. Shukla***

*Department of Chemistry, University of Allahabad, Allahabad-211002, India.*

Received June 19, 2003; Revised October, 30, 2003; Accepted December 2, 2003

## Abstract

**A simple titrimetric method has been developed for milligram determination of some sulpha drugs and diuretics e.g. Sulphacetamide sodium, Sulphamethoxazole, Sulphadiazine, Sulphaguanidine, Acetazolamide, Frusemide and Spironolactone in pure form and in their pharmaceutical preparation. Aliquots containing 1-5 mg of the sample were allowed to react with excess of 3 × $10^{-2}$ N pyridinium chlorochromate (PCC) in the presence of 5 N $H_2SO_4$ for required reaction time at room temperature (25-30°C). After the reaction is over, the unconsumed reagent was back determined iodometrically. The values of % error, SD and CV prove the method to be precise and reproducible.**

**(Keywords: Sulpha drugs/diuretics/ PCC/ iodometry)**

## Introduction

Sulphonamides have been used in the treatment of urinary-tract infections, gastro-intestinal infection nocardiosis and in some other bacterial infections. Diuretics are used in the treatment of oedema, various forms of epilepsy etc. Because of their great medicinal value, their estimation has widely been studied[1-9]. Most of the methods involve sophisticated instrumentation and complicated techniques. The nitrite titration method described in IP[10] also involves platinum electrodes, potentiometer and galvanometer for getting end points. Rigid reaction conditions are to be maintained for achieving accurate and reproducible results. As compared to this method we describe a simple and convenient method for the determination of some sulpha drugs and diuretics with PCC reagent.

## Materials and Method

*Pyridinium chlorochromate (PCC) solution ($3x10^{-2}N$)*

The reagent was synthesised in laboratory[11] and purity checked. 540 mg of PCC was dissolved first in 150 ml glacial acetic acid (Merck) and then made up to the volume with distilled water in 250 ml volumetric flask. The solution was standardised iodometrically. Aqueous solutions of sodium thiosulphate (0.01 N, Merck), Potassium dichromate (0.01 N, Qualigens), Potassium iodide (10%, Baker), Starch (10%, Merck) were also prepared.

*Sample solution (1 mg/ml)* : Accurately weighed 100mg of the pure Sulphacetamide sodium and Aceta-

zolamide were dissolved in distilled water in a 100 ml volumetric flask. Sulphamethoxazole, Sulphadiazine, Sulphaguanidine and Spironolactone were first dissolved in minimum amount of ethyl alcohol while frusemide was dissolved in minimum amount of acetone and then diluted to 100 ml with distilled water.

*Tablet :* Twenty tablets of a particular sample were crushed to a fine powder and the powder equivalent to 100 mg of the sample was taken in 100 ml volumetric flask and dissolved accordingly.

*Drops :* Amounts equivalent to 100 mg of the pure sample were taken and dissolved, in distilled water, in a 100 ml volumetric flask.

*Procedure :* An aliquot containing 1-5 mg of the samples was taken in 100 ml stoppered conical flask followed by the addition of 5 ml of PCC reagent and 10 ml of 5 N sulphuric acid. The reaction mixture was shaken thoroughly and allowed to react at room temp. (25-30° C) for prescribed reaction time. After the reaction is over, 5 ml of 10% potassium iodide was added to it and titrated against standardised sodium thiosulphate solution (0.01 N) to starch end point. A blank experiment was also run under identical conditions using all the reagents except the sample. The amount of the sample was calculated by the following expression. On the basis of percentage error the value of SD and CV were also calculated (Table 1)

$$\text{mg of the sample} = \frac{M \times N\,(B-S)}{n}$$

where, $m$ is mol. wt. of the sample, $N$ is Normality of sodium thiosulphate solution, $B$ is volume of sodium thiosulphate solution for blank, $S$ is volume of sodium thiosulphate solution for sample, $n$ is number of moles of PCC consumed per mole of the sample.

## Results and Discussion

The reaction conditions were established after studying the effect of variables such as reaction time, concentration and amount of PCC reagent and sulphuric acid and reaction temperature. Variation in reaction time was found to influence the reaction. The determination of Sulphacetamide sodium, Sulphamethoxazole, Sulphadiazine and Sulphaguanidine was completed in 5 min. reaction time. Acetazolamide, Frusemide and Spironolactone need 60 min. reaction time. A much more reaction time does not improve the results. The percentage recovery was very low at a lesser reaction time due to incomplete reaction. It was also established that the prescribed concentration of the reagent ($3\times10^{-2}$N) was suitable for accurate results. Similarly the effect of concentration of sulphuric acid was also studied. It was found that the recommended concentration of both the reagents is suitable for the reaction. While studying the effect of temperature, it was observed that the reaction is completed at room temperature (25-30°C). On heating the reaction mixture directly on flame or on water bath, inaccurate results are obtained, perhaps because of the decomposition of the regent. On the basis of the results (Table 1) it is established that the suggested method is reproducible and precise. It can easily be adopted in a pharmaceutical laboratory.

Table 1– Determination of some Sulpha drugs and diuretics in the pure form and in their pharmaceutical preparations with ($3 \times 10^{-2}$N) PCC reagent.

| Sl. No. | Sample | Aliquots taken (ml) | Amount present (mg) | Reaction time (min) | Molecularity | Amount obtained by calculation* (mg) | Error (%) | SD (mg) | CV (%) |
|---|---|---|---|---|---|---|---|---|---|
| 1. | Sulphacetamide sodium (pure) | 1 | 0.999 | | | 0.989 | -0.99 | 0.0028 | 0.2831 |
| | | 3 | 2.997 | 5 | 3 | 2.976 | -0.74 | 0.0028 | 0.0941 |
| | | 5 | 4.995 | | | 4.972 | -0.49 | 0.0030 | 0.0603 |
| (a). | Opthosulf (D) | 1 | 0.963 | | | 0.953 | -1.00 | 0.0020 | 0.2099 |
| | | 3 | 2.889 | 5 | 3 | 2.867 | -0.75 | 0.0022 | 0.0767 |
| | | 5 | 4.815 | | | 4.791 | -0.50 | 0.0026 | 0.0543 |
| (b). | Locula (D) | 1 | 0.968 | | | 0.958 | -1.02 | 0.0028 | 0.2923 |
| | | 3 | 2.904 | 5 | 3 | 2.882 | -0.75 | 0.0017 | 0.0590 |
| | | 5 | 4.840 | | | 4.818 | -0.46 | 0.0030 | 0.0623 |
| (c) | Albucid (D) | 1 | 0.961 | | | 0.951 | -1.00 | 0.0022 | 0.2313 |
| | | 3 | 2.883 | 5 | 3 | 2.862 | -0.74 | 0.0026 | 0.0908 |
| | | 5 | 4.805 | | | 4.782 | -0.48 | 0.0032 | 0.0669 |
| (d) | Opthocid (D) | 1 | 0.966 | | | 0.957 | -0.96 | 0.0030 | 0.3135 |
| | | 3 | 2.898 | 5 | 3 | 2.877 | -0.73 | 0.0033 | 0.1147 |
| | | 5 | 4.830 | | | 4.805 | -0.52 | 0.0018 | 0.0375 |
| 2. | Sulphamethoxazole (pure) | 1 | 0.997 | | | 0.988 | -0.95 | 0.0017 | 0.1721 |
| | | 3 | 2.991 | 5 | 3 | 2.969 | -0.75 | 0.0023 | 0.0775 |
| | | 5 | 4.985 | | | 4.958 | -0.54 | 0.0028 | 0.0565 |
| (a) | Oriprim (T) | 1 | 0.960 | | | 0.950 | -1.04 | 0.0029 | 0.3053 |
| | | 3 | 2.880 | 5 | 3 | 2.855 | -0.82 | 0.0020 | 0.0701 |
| | | 5 | 4.800 | | | 4.770 | -0.59 | 0.0024 | 0.0503 |
| (b) | Antrima (T) | 1 | 0.952 | | | 0.944 | -0.89 | 0.0015 | 0.1589 |
| | | 3 | 2.856 | 5 | 3 | 2.837 | -0.71 | 0.0017 | 0.0599 |
| | | 5 | 4.760 | | | 4.737 | -0.53 | 0.003 | 0.0633 |
| (c) | Sepmax | 1 | 0.956 | | | 0.946 | -1.02 | 0.0026 | 0.2748 |
| | | 3 | 2.868 | 5 | 3 | 2.846 | -0.77 | 0.0030 | 0.1054 |
| | | 5 | 4.780 | | | 4.756 | -0.51 | 0.0028 | 0.0589 |
| (d) | Ciplin (T) | 1 | 0.958 | | | 0.948 | -1.01 | 0.0035 | 0.3692 |
| | | 3 | 2.874 | 5 | 3 | 2.852 | -0.75 | 0.0028 | 0.0982 |
| | | 5 | 4.789 | | | 4.766 | -0.48 | 0.0030 | 0.0629 |

Table 1 Contd..

Table 1 Contd...

| Sl. No. | Sample | Aliquots taken (ml) | Amount present (mg) | Reaction time (min) | Mole-cularity | Amount obtained by calculation* (mg) | Error (%) | SD (mg) | CV (%) |
|---|---|---|---|---|---|---|---|---|---|
| 3. | Sulphadiazine | 1 | 0.995 | | | 0.985 | -1.01 | 0.0022 | 0.2234 |
| | (pure) | 3 | 2.985 | 5 | 3 | 2.962 | -0.78 | 0.0017 | 0.0574 |
| | | 5 | 4.975 | | | 4.949 | -0.53 | 0.0020 | 0.0404 |
| (a) | Sulphadiazine | 1 | 0.984 | | | 0.975 | -0.94 | 0.0014 | 0.1436 |
| | (T) | 3 | 2.953 | 5 | 3 | 2.931 | -0.76 | 0.0015 | 0.0512 |
| | | 5 | 4.921 | | | 4.892 | -0.59 | 0.0022 | 0.0450 |
| 4. | Sulphaguanidine | 1 | 0.996 | | | 0.987 | -0.93 | 0.0021 | 0.2128 |
| | (pure) | 3 | 2.988 | 5 | 3 | 2.967 | -0.71 | 0.0018 | 0.0607 |
| | | 5 | 4.980 | | | 4.955 | -0.50 | 0.0035 | 0.0706 |
| (a) | Sulphaguanidine | 1 | 0.988 | | | 0.978 | -1.05 | 0.0033 | 0.3374 |
| | (T) | 3 | 2.964 | 5 | 3 | 2.941 | -0.78 | 0.0025 | 0.0850 |
| | | 5 | 4.941 | | | 4.917 | -0.49 | 0.0031 | 0.0630 |
| 5. | Acetazolamide | 1 | 0.991 | | | 0.981 | -1.03 | 0.0014 | 0.1427 |
| | (pure) | 3 | 2.973 | 60 | 1 | 2.951 | -0.75 | 0.0011 | 0.0373 |
| | | 5 | 4.955 | | | 4.932 | -0.47 | 0.0011 | 0.0223 |
| (a) | Amide (D) | 1 | 0.964 | | | 0.954 | -1.05 | 0.0024 | 0.2516 |
| | | 3 | 2.892 | 60 | 1 | 2.869 | -0.80 | 0.0015 | 0.0523 |
| | | 5 | 4.820 | | | 4.793 | -0.55 | 0.0030 | 0.0626 |
| (b) | Diamox(T) | 1 | 0.970 | | | 0.961 | -0.90 | 0.0035 | 0.3642 |
| | | 3 | 2.910 | 60 | 1 | 2.889 | -0.73 | 0.0030 | 0.1038 |
| | | 5 | 4.850 | | | 4.822 | -0.57 | 0.0024 | 0.0498 |
| 6 | Frusemide | 1 | 0.993 | | | 0.983 | -1.04 | 0.0022 | 0.2238 |
| | (pure) | 3 | 2.979 | 60 | 2 | 2.957 | -0.75 | 0.0021 | 0.0710 |
| | | 5 | 4.965 | | | 4.943 | -0.45 | 0.0025 | 0.0506 |
| (a) | Lasix (T) | 1 | 0.988 | | | 0.979 | -0.90 | 0.0012 | 0.1226 |
| | | 3 | 2.964 | 60 | 2 | 2.942 | -0.73 | 0.0015 | 0.0510 |
| | | 5 | 4.941 | | | 4.913 | -0.56 | 0.0017 | 0.0346 |
| 7. | Spironolactone | 1 | 0.992 | | | 0.982 | -1.05 | 0.0020 | 0.2037 |
| | (pure) | 3 | 2.976 | 60 | 2 | 2.951 | -0.83 | 0.0023 | 0.0779 |
| | | 5 | 4.960 | | | 4.931 | -0.58 | 0.0028 | 0.0568 |
| (a) | Aldactone (T) | 1 | 0.984 | | | 0.974 | -1.01 | 0.0015 | 0.1540 |
| | | 3 | 2.953 | 60 | 2 | 2.930 | -0.77 | 0.0025 | 0.0853 |
| | | 5 | 4.921 | | | 4.895 | -0.52 | 0.0030 | 0.0715 |

D= Drop, T=Tablet, * = Average of nine determinations

The number of moles of the PCC consumed for the sample depends upon the structure of the compounds. On the basis of molecularity and available literature a possible course of reaction may be suggested for each compound. All the sulpha drugs under study contain amino group, which is easily oxidised to $-NO_2$ group[4]. Thus all the sulpha drugs get oxidised to corresponding nitro derivative. Taking Sulphacetamide sodium as an example, it can be represented in the following way.

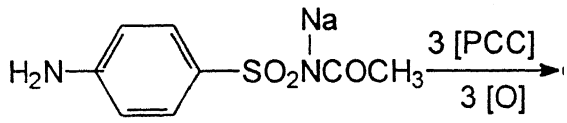


SULPHACETAMIDE SODIUM

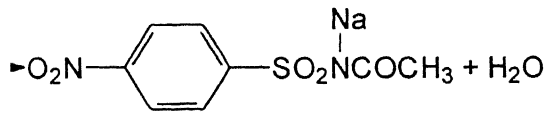


A general reaction for all other sulphonamides may be given as below.

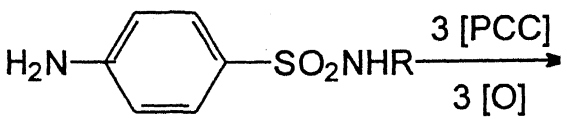


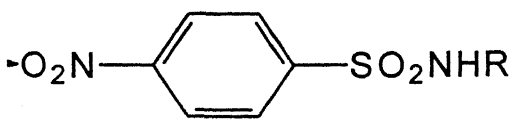


R = 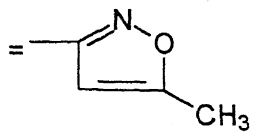 (Sulphamethoxazole)

R = 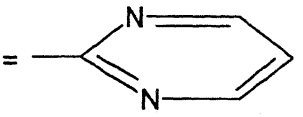 (Sulphadiazine)

R = 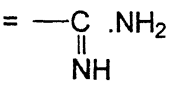 (Sulphaguanidine)

In case of diuretics the structure of the compounds is complicated and needs a reaction time of 60 min. for constant results. In Acetazolamide, since the sulphur atom is present in the ring, it is not easily oxidised. Keeping in view the structure of the compound and the molecularity of PCC reagent following reaction may be proposed.

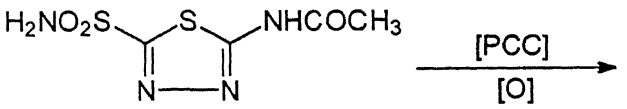


ACETAZOLAMIDE

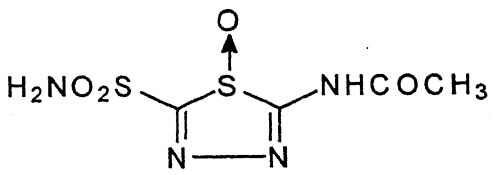


The other compounds which were studied are Frusemide and Spironolactone. Both of them consume two moles of PCC reagent and they may also get converted to corresponding oxidised products.

## Acknowledgements

The authors thank Optho remedies (P) Ltd (Allahabad) and Vibgyor (P) Ltd (Allahabad) for providing pure samples of sulpha drugs and diuretics free of cost.

## References

1. Wahbi, A.M., Abdine, H., Korany, M.A. & El-Yazbi, F.A. (1978) *Pharmazic* **33** : 721
2. Raghuveer, S., Raju, I.R.K., Vatsa, D.K. & Srivastawa, C.M.R. (1993) *The Eastern Pharmacist* **36** : 107.
3. Metz, R., Muth, P., Ferger, M., Bolten, W.W. & Vergin, H. (1996) *J. Chromatogr. A.* **729** (1) : 243
4. Shukla, I.C., Singh, A.L. & Usmani, Q.S. (1980) *Indian Journal of Pharmaceutical Science* **42**(4) : 118
5. Kalashikov, V.P., Dolotova, T.M. & Minka, A.F. (1999) *Farm. Zh.* **5** : 69
6. Shukla, I.C., Shrivastawa, M.K., Singh, D. & Ahmed, S. (1983) *Indian Journal of Pharmaceutical Science* **45**(6) : 249
7. Gomaa, Z.S. (1993) *Biomed. Chromatog.* **7** : 134
8. Rao, G.R. & Raghuveer, S. (1985) *Indian Drugs* **22**(4): 217
9. Dyade, G.K. & Sharma, A.K. (2001) *Indian Drugs* **38** : 75
10. *Pharmacopoeia of India,* 3rd Edition (1985) II: A-64
11. Corey, E.J. & Suggs, J.W. (1975) *Tetrahedron Letter.* 2647.

# Mathematical model of controlled release of solute drugs from biodegradable implants

**Pooja Arora and P. N. Tandon***

*Department of Mathematics, Invertis Institute of Management Studies, Bareilly, India.*

**Formerly in Mathematics Department, H.B.T.I., Kanpur. Present address: 191-193, Karmchari Nagar, Bareilly, India.*

*e-mail: <gopall960@yahoo.co.uk>*

Received April 04, 2004; Accepted June, 28, 2004

## Abstract

**In medical sciences, chronical diseases and pathological states require long term doses of tablets, pills, capsules or ointments, creams, aerosols and injectables. These drugs release promptly but with significant fluctuations within various regions of the body. In this communication, we present a simple model for an alternative method of drug release through erodible polymeric/ ceramic implants of desired geometry which can release the drug at a pre-assigned rate assuring effectiveness at lower end and minimizing adverse effect at the higher end. Such implants need not be removed after drug supply to the site by operating again because the implants are erodible. The model presents a control problem for design parameters for a pre-assigned drug release rate. The effects of various geometric and design parameters have been discussed.**

**(Keywords: Mathematical Model/ biodegradable implants/ solute drug)**

## Introduction

Mathematical and computer modelling play an important role in improving and optimizing the performance characteristics of an idealized system for self regulating release of therapeutic drugs in specific regions in the body. The diffusional release of drugs from an erodible implanted matrix with initial drug loading $c_0 > c_s$ (the solubility limit) releases the drug at the rate of $(c_s - c_0)\frac{du}{dt}$, where $\frac{du}{dt}$ is the velocity of the moving diffusion front. The inward motion of the diffusion front separates the reservoir of unextracted solute from partially extracted region. After releasing drug the polymer also erodes and thus maintains zero concentration at the moving erosion front $x = s(t)$. Thus, both the moving surfaces (diffusion and erosion fronts) constitute moving boundary problem. Moving boundary problems have been applied in several practical situations: heat transfer involving melting phase transition[1], diffusion controlled growth of particles[2] and diffusion release[3]. Very few moving boundary problems related to the diffusional release of dispersed solute from polymer matrices are found in literature[4,5,6]. In a series of papers, Cohen and Emeux[7,8,9] have developed controlled release models as free boundary problems in pharmaceuticals[10] under swelling controlled release and per-

fect sink condition. For variety of medical applications such as in regulating the depth of anesthesia, blood pressure control, optimal cancer therapy, cardiac arrest devices and insulin delivery in diabetic patients, the controlled drug release models can be developed. A controlled implanted drug delivery system may be designed to release drugs at a near constant or other pre-assigned therapeutic dose time rate into the surrounding tissues and eventually into the blood stream where it may be convected to the target site(s). Thus, effective dosage levels can be maintained in the blood and the frequency of drug is reduced for the patient's convenience. The desired properties to be achieved depend with the device design parameters and not on the physiology. Higuchi[4] obtained approximate solution based on pseudo-steady state assumptions which is not applicable to lower solute limiting concentrations. Integral method has been applied to the moving boundary problems encountered in the diffusional release of a solute from polymeric matrix by Lee[5]. In the present communication, we present a preliminary development of an analytical model for controlled release of drug from within monolithic eroding matrix. We formulate a simple analysis to observe the effects of geometry on release rate for various shapes of the devices such as slab of finite thickness and compare with the results available.

## Mathematical Model

Fig. 1 represents the geometrical counterpart of the situation. At any time $t$, the $u(t)$ and $s(t)$ denote moving diffusion and loading to the slab of thickness $s_0$ at $t = 0$, $C_s$ is the limiting solubility concentration of the drug at the diffusion front. One dimensional mass flux across the diffusion front is given by

$$D\frac{\partial c}{\partial x}\bigg|_{x=u(t)} = (c_s - c_0)\frac{du}{dt} \tag{1}$$

where $D$ is the diffusion coefficient assumed to be a constant. Introducing the following non-dimensional quantities:

$$T = \frac{Dt}{s_0^2}, \quad X = \frac{x}{s_0}, \quad U = \frac{u}{s_0}, \quad C = \frac{c}{c_s},$$

$$S = \frac{s}{s_0}, \quad C_0 = \frac{c_0}{c_s}, \text{ and } M = \frac{M}{c_0 s_0},$$

the equation (1) now transforms to

$$\frac{dU}{dT} = \frac{\alpha}{(U-1)+\beta T}, \tag{2}$$

where $\alpha = \frac{c_s}{c_0 - s_s}$, and $\beta = \frac{Bs_0}{D}$,

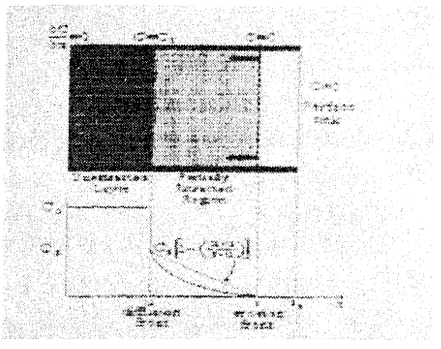

Fig. 1– Released profile of a dispersed solute from an polymer matrix

The corresponding equation for the erosion

$$S(T) = 1 - \beta T \tag{3}$$

Again, using a simple transformatin of variables:

$$V = (U - 1) + \beta T, \tag{4}$$

we transform equation (2) as

$$\frac{dV}{dT}=\beta+\frac{\alpha}{V} \qquad (5)$$

Integration of equation (5) and using (4) with $U(0) = 1$ and $= 0$, these expressions are given below:

$$\beta V-\alpha \ln\left(1+\frac{\beta V}{\alpha}\right)=\beta^2 T \qquad (6)$$

Introducing the following

$$U=V+1-\beta T \qquad (7)$$

and following the approach set out by Shergel and Yu[11], we apply Fick's law to the partially extracted region $u(t)< x<s(t)$ we approximate the concentration distribution as

$$c(x,t)=c_0\left[1-\frac{x-u}{s-u}\right] \qquad (8)$$

Further, the amount of the drug released per unit exposed area of the matrix is equal to the difference of the original mass per unit area of the drug in the region and the amount remaining i.e.

$$m=c_0(S_0-u)-\int_u^s c(x,t)dx, \qquad (9)$$

And finally, we obtain

$$m=c_0(S_0-u)-c_s(s-u)/2 \qquad (10)$$

In non-dimensional form, this can be written as

$$M=(1-U)-\frac{S-U}{2C_0}, \qquad (11)$$

In order to discuss the results in reference to the results obtained by Lee[5], the parameters of this communication are equivalent to those of Lee as given below:

$a=\dfrac{1}{\left(\dfrac{A}{c_s}-A\right)}$, where $c_0 = A$, $c_s$ is same in both and $U(T)= 1-\delta(\tau)$ and $T = \tau$, Results of this communication have been discussed with these considerations in mind.

## Results and Discussions

1. Fig. 2(a) and Fig. 2(b) represent the variation of velocity of the diffusion front $\frac{dU}{dT}$ for different sets of variations of α, β. For a fixed value of β i.e. for constant erosion front velocity, the diffusion front moves faster towards origin with time for increasing values of α. Similar results were observed for increasing values of β. For a fixed value of α, but the movement in the later case is much slower than the previous case.

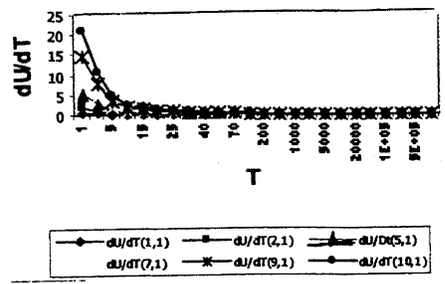


Fig. 2a– *dU/dT vs. T* for different α and fixed β.

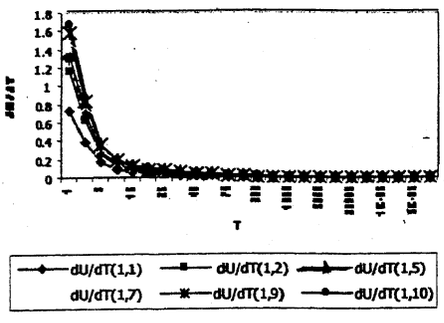


Fig. 2b– *dU/dT vs. T* for different β and fixed α

This may be due to the fact that the erosion front moving towards the diffusion front forces more material into the partially extracted region with faster releases. These results are consistent with those obtained by Lee[5] depicting the variation of $\delta(t) = \frac{s_0 - u(t)}{s_0} = 1 - U(T)$.

2. Fig. 3(a) and Fig. 3(b) present the variations of drug release rate $\frac{dM}{dT}$ with time for different sets of variations of α, β. For a fixed value of α, release rate increases with time for increasing values of β.

Similar results were observed for fixed value of β and for increasing values of α but release rates in the previous case are much larger than those of later case.

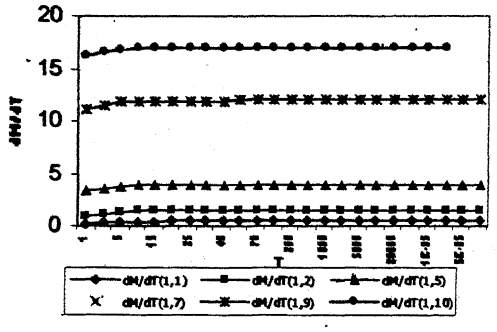


Fig. 3a– *dM/dT vs. T* for different β and fixed α.

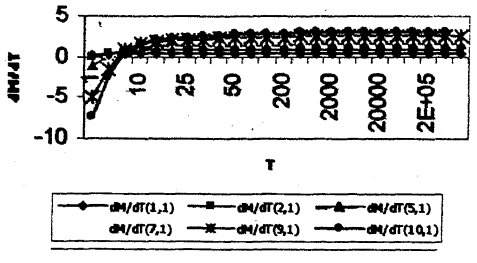


Fig. 3b– *dM/dT vs. T* for different α and fixed β.

3. Variation of mass flux is presented in Fig. 4(a) and 4(b) for similar variations in α, β. Results are similar and justify the results of release rates mentioned above. In fact, this presents a control problem which can fix up the parametric values for a pre-assigned value of release rate.

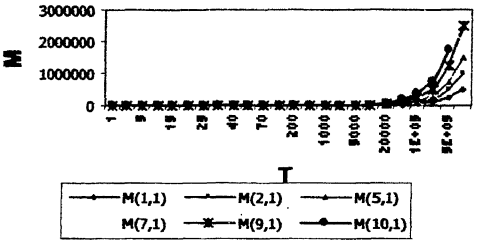


Fig. 4a– *M* vs. *T* for fixed β and different α.

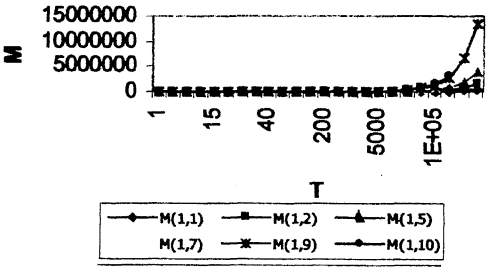


Fig. 4b– *M* vs. *T* for fixed α and different β.

4. Variations of $\frac{dV}{dT}$ with diffusion front velocity $\frac{dU}{dT}$ for different sets of values of α, β have been presented in Fig. 5(a) and Fig. 5(b). $\frac{dV}{dT}$ increases with increasing diffusion front velocity. For initial values of $\frac{dU}{dT}$, $\frac{dV}{dT}$ is almost constant. It starts increasing further with the diffusion front velocity. We have also presented diffusion front velocity

independent of $U$ with time in Fig. 2(a) and Fig. 2(b).

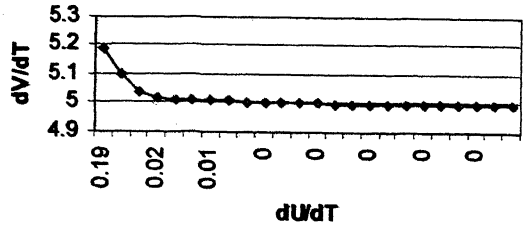


Fig. 5a– *dV/dT* vs. *dU/dT* for $\alpha$=1, $\beta$=5

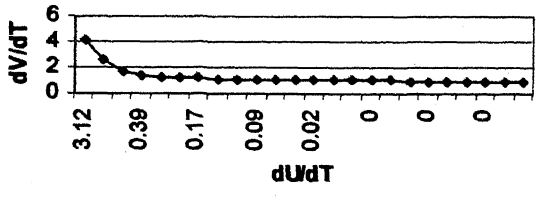


Fig. 5b– *dV/dT* vs. *dU/dT* for $\alpha$=5, $\beta$=1

## Acknowledgement

One of the author (P.N.T) thanks Professor R. Collins, Department of Biomedical Engineering, Wright University, Dqayton, Ohio, (USA) for long discussions on the subject.

## References

1. Carslaw, H. S. & Jaegar, J. S. (1959) *Conduction of Heat in Solids*, 2nd Ed, Oxford University Press, Oxford, p 282
2. Crank, J. (1975) *Mathematics of Diffusion*, Oxford University Press, p. 286.
3. Reiss, H., Patel, J.R. & Jackson, K.A.(1977) *J. Appl. Physics* **48**(12) : 5274.
4. Highuchi, T. (1963) *J. Pharm. Sci.* **52** : 1145.
5. Lee, P. (1980) *J. Membrane Sci.* **7** : 255.
6. Abdekhodaie, M. J. & Cheng, Y. I. (1996) *J. Membrane Sci.* 115 : 171.
7. Cohen, D. S. & Erneuxi, T. (1998) *SIAM J. Appl. Math* **54** : 483.
8. Cohen, D. S. & Erneuxi, T. (1998) *SIAM J. Appl. Math* **55** : 145l.
9. Cohen, D. S. & Erneuxi, T. (1998) *SIAM J. Appl. Math* **55** : 1466.
10. Peppas, N. A. (1998) "*Medical applications of controlled release*" Ed. H. R S. Langer & W. L. Wise, C.RC. Press 1984.
11. Shargel, I. & Yu, A.B.C. (1993) *Applied Pharmaceutics and Pharmacokinetics*, 3rd Ed. Norwalk, Connecticut, Appleton & Lange, Pub.

# Impact of bee pollination on amino acid and protein composition of mustard seed

**R. P. Singh**

*Apicultural Research Laboratory, Department of Entomology, Narendra Deva University of Agriculture & Technology, Kumarganj, Faizabad 224 229 U.P., India.*

Received January 13, 2004; Revised May 07, 2004; Accepted June 22, 2004

## Abstract

**The present paper is the first report for the effect of bee pollination on the amino acid and protein composition of mustard (*Brassica campestris* L. var. toria) seed. The self –pollinated plants (SP) consist of lowest concentration of free amino acids. In bee pollinated (BP) plants the free amino acids concentrations were low in comparison to naturally pollinated plants (NP) and hand pollinated plants (HP). However, the "total" amino acids concentrations varied in the ascending order as NP<HP<SP<BP. In the seeds of BP plants the "total amino acids and protein" concentration were about two times higher as compared to the seeds of NP plants. The concentration of protein was highest in the BP plants.**

**(Keyword: *Apis cerana* / pollination/ amino acid/ *Brassica campestris*/ seeds).**

Pollination is essential pre-requisite for major reproductive crop yield and perrenation of higher plant species. The bees visit the one flower to another flower. During this time, most probably, the highly positive charged pollen grains were attracted by the negatively charged stigma for pollination with most suitable pollen. The honeybees only provided this opportunity, because there is no other technique to provide the opportunity to the stigma for selection of desirous and suitable pollen grains to pollinate them. Since the pollination was performed by bees through highly suitable pollen, it increases the yield and improve the quality of mustard seed.

For collection of pollen, bees are known to sonicate the anthers. Consequent audible floral vibration has been investigated for many plants by many workers (approximately 31 families and over 500 genera of flowering plants)[1,2,3]. The entomophilic mustard pollen, because of its large number and greater amount of amino acids, is nutritionally superior than anemophillic[5] or non-mustard pollen. Bees, with their observed inclination to visit mustard flower (Boch *et al.*, 1978) may avail the advantage of superior nutritive value of mustard pollen to increase the brood area and larval weight[6]. This has also been found to enhance the yield of mustard seed[7]. Further, mustard is an important oil seed crop of India, whose yield enhances through bee pollination[7] which tempted us to investigate on these aspects. There is also worldwide interest in growing mustard for their seed oils. To our knowledge, no attempt has been made on the relationship between the pollination and maternal fitness, amino acid and protein composition of mustard seed (Brassica campestris L. var. toria).

The methods of pollination have a variable effect of the free amino acid

composition of the produced seeds. This paper studies the following different pollination methods: (i) *Self pollination* (SP); pollination was artificially performed in mature flower buds which were enclosed singly with perforated polyethylene paper bags; (ii) *natural pollination* (NP); plants were pollinated under natural conditions; (iii) *hand pollination;* fresh blooming flowers were emasculated and cross pollinated by hand and (iv) *honey bee pollination* (BP); pollination was accomplished by honeybees (*Apis cerana*). The nucleus beehive of *A. cerana* indica was kept within the caged plants for pollination. The cultural and treatment techniques have been published by us earlier.

Triplicate samples from each treatment were randomly collected, seventy days after sowing. Biochemical analysis was performed with dried ($70^0$C, 24h) and powdered (24 mesh) samples. Free amino acids and amides from hot ethanol (80% v/v) extracted dried samples and protein amino acids from 6 N HCI hydrolysates of the

Table 1– Effect of bee pollination on the amino acids composition of mustard (*Brassica campestris* var. toria) seeds (μg $100^{-1}$ mg dry wt.)

| Amino acids | POLLINATION TREATMENTS | | | | | | | |
|---|---|---|---|---|---|---|---|---|
| | Free amino acids | | | | Protein bound amino acids | | | |
| | SP | NP | HP | BP | SP | NP | HP | BP |
| Leucine + Isoleucine | 15.0 | 10.0 | 15.0 | 10.0 | 285.7 | 225.0 | 260.0 | 300.0 |
| Valine | 10.0 | 5.0 | 10.0 | 10.0 | 171.4 | 150.0 | 260.0 | 340.0 |
| γ amino butyric acid | 10.0 | 160.0 | 110.0 | - | - | - | - | - |
| Tyrosine | - | - | - | - | 142.8 | - | - | 160.0 |
| Glutamic acid | 80.0 | 40.0 | 80.0 | 100.0 | 440.0 | 125.0 | 200.0 | 480.0 |
| Threonine | 20.0 | - | - | 10.0 | 800.0 | - | - | 600.0 |
| Arginine | - | 10.0 | 10.0 | - | 457.0 | 150.0 | 220.0 | 260.0 |
| Aspartic acid | 20.0 | 20.0 | 60.0 | 40.0 | - | 84.0 | 260.0 | 20.0 |
| Glysine + Serine | 10.0 | 10.0 | 20.0 | 10.0 | 257.0 | 175.0 | 240.0 | 400.0 |
| Lysine + Histidine | 40.0 | 5.0 | 20.0 | 10.0 | 228.2 | 210.0 | 220.0 | 280.0 |
| Cystine | 2.5 | 10.0 | 10.0 | 5.0 | 85.7 | 300.0 | - | 220.0 |
| Proline | 73.0 | 20.0 | 76.6 | 146.6 | 300.0 | - | 380.0 | 530.0 |
| α alanine | - | 60.0 | 10.0 | - | - | - | - | - |
| Asparagine | 20.0 | - | 20.0 | 10.0 | - | 275.0 | - | - |
| β alanine | - | - | - | - | - | - | 300.0 | 380.0 |
| Total : | 300.5 | 350.0 | 441.6 | 351.0 | 3167.8 | 1694.0 | 2340.0 | 3970.0 |

ethanol extracted residue were resolved by two dimensional paper chromatography [8,9]. The 1st and 2nd dimensional runs of the chromatograms were performed in the solvent systems phenol: water: ammonia (80:20:3 v/v) and n-butanol : acetic acid : water (4:1:5 v/v), respectively. The different ninhydrin positive substances were detected by spraying the chromatograms with 0.1% ninhydrin in n-butanol and quantitatively measured spectrophotometrically against authentic (Sigma chemical) reference standards. Proline was estimated separately following the method outlined by Wren and Wiggal[10]. The fresh seed samples were deproteinized with trichloroacetic acid for protein estimation and quantified following the methods of Lowry *et al*[11].

Table 2 –Effect of bee (*Apis cerana*) pollination on the protein composition of mustard (*Brassica campestiris* var. toria) seed

| Pollination treatments | Protein (%) |
|---|---|
| SP | 1.65 |
| NP | 1.12 |
| HP | 1.99 |
| BP | 2.06 |

The concentration of free, protein bound amino acids and protein of mustard seed were influenced by the mode of transference of pollen grains for pollination and fertilization (Table 1 and 2). In the seeds of NP and BP the total concentration of amino acids and protein were about 2044 and 4321 μg $100^{-1}$ mg; 1.12 and 2.06 per cent respectively (Table 1 and 2). The concentration of total amino acids and protein of BP seeds were about 2 times and 1.8 times greater than the seeds of NP plants respectively. The free and protein bound amino acids namely leucine, isoleucine, valine, glutamic acid, glycine, serine, lysine and histidine were detected in the seeds of SP, NP, HP and BP plants respectively. The threonine was detected only in the seeds of SP and BP plants. The free proline concentration of BP seed was highest about 41 per cent and the protein bound was about 13 per cent. The tyrosine was detected in the protein bound amino acids of the SP and BP seeds.

Probably quality (maturity of pollen, time of pollination and highly fit) of pollen is responsible for higher yield, synthesis of amino acids and protein of the seeds. In the seeds of BP the concentration of protein and protein bound amino acids were highest. The insect or bee pollination of *Brassica rapa* and *Brassica napus* is essential[13] for higher yield, high seed meal lipid concentration [7], higher number of pods and seeds per pod [14]. Similarly, it also increases the total amino acids and protein concentration of seeds of bee pollinated plants (Table 1 and 2). Canola growers may be benefited to associate, co-operatively with beekeepers to enhance their seed yield [13]. On the one side honey bees increase the seed yield and improve the seed quality through pollination services, on the other side they collected the nectar from the flowers of mustard crops for production of honey i.e. about 70 kg per hectare.

## References


1. Buchmann, S. L. (1983) Buzz pollination in angiosperms. In Jones, C.E. and Little R.J. (eds.). Hand book of Experimental Pollination Biology, Van Nostrand Reinhold, New York.
2. Neff, J. L. & Simpson, B. B. (1988) *J Kans Entomol Soc.* **61:** 242.
3. Cane, J. H. & Buchman, S. L. (1989) *J. Insect Behavior*, **2:** 431.
4. Singh, R. P. & Singh, P. N. (1991) *Apiacta.* **26 :** 38.

5. Stanley, R. G. & Linskens, H. F. (1974) in *Pollen: biology, biochemistry, management*, Springer-Verlag, New York, 100.
6. Singh, R.P. & Singh, P.N. (1996) *Apidologie.* **27 :** 21.
7. Singh, R. P. & Singh, P. N. (1992) *J. apic. Res.* **31** : 128.
8. Consden, R., Gordon, A. M, & Martin, A. J. P. (1944) *Biochem. J* **38 :** 224.
9. Partridge, S. M. (1948) *Biochem. J.* **42 :** 238.
10. Wren, J. J. & Wiggal, P. H. (1965) *Biochem. J.* **57** : 508.
11. Lowry, O. H., Rosebrough, N. J., Farr, A. L. & Randall, R. J. (1951) *J Biol Chem.* **193 :** 265.
12. Boch, R., Shearer, D. A. & Shimanuki, H. (1978) *Environ Entomol.* **2 :** 237.
13. Westcott, L. & Nelson, D. (2001) *Bee World.* **82** : 115.
14. Williams, I. H. (1978) *J. Agri. Sci. Cambridge.* **91** : 343.

# Electrophoretic protein profiles of a few selected congenital cardiac tissues

**S.Krupanidhi, V.Venkata Arunachalam AND M. A. Chakravarthi***

*Department of Biosciences, Sri Sathya Sai Institute of Higher Learning, Prasanthinilayam–515 134, India.*

*e.mail: krupanidhi_srirama@yahoo.com*

* *Department of Cardiothoracic Surgery, Sri Sathya Sai Institute of Higher Medical Sciences, Prasanthinilayam- 515 134, India.*

Received May 19, 2004; Accepted June 30, 2004

## Abstract

**The SDS PAGE protein profiles of normal and congenital cardiac tissues reveal that TOF tissue protein retention is low. This situation may possibly be the reason for its spatial and temporal abnormalities. The molecular weights of protein profiles of cardiac tissues vary between 125 to 14 KDa with a prominent band in the range of 43 KDa. The variations in their spectral profiles, including profile heights and area under the peaks, have been analysed in the light of electrophoretic behaviour of proteins associated with cardiomyopathy.**

**(Keywords: TOF/DCRV/protein profiles).**

Cardiovascular diseases are the most important cause of death and hospitalisation in human population around the world. Among these, congenital cardiovascular malfunctions are the major cause of morbidity and mortality[1-3]. Tetralogy of Fallot (TOF) shows a prevalence of 10% and a double chambered right ventricle (DCRV) occurs in about 1%. During the past decade, it has become increasingly clear that genetic factors play a significant role in pathogenesis of many, if not most, cardiovascular disorders[4-7]. Several of these disorders have obvious genetic etiologies, such as long QT syndrome, familial hypertrophic cardiomyopathy or Marfan's syndrome[8]. In the present investigation, an attempt has been made to qualitatively evaluate the protein profiles of the resected muscle bundles from TOF & DCRV and papillary muscles around the mitral valve of normal human heart.

*Pathological symptoms* : The clinical and pathological features associated with cardiac hypertrophy have been described extensively[9]. Briefly, Fallot's tetralogy consists of four discrete anatomical lesions: namely, pulmonary infundibular stenosis; a ventricular septal defect; aorta overriding the ventricular septum; and right ventricular hypertrophy. Stenosis is the narrowing of valve opening due to inflammation and encrustation and consequently healing

by depositing fibrous tissue. Stenosis is accompanied by valvular incompetence allowing blood to flow back into ventricle when it relaxes.

The precise mechanism by which squatting relieves breathlessness and faintness after exercise in patients with TOF is complex. It is known that arterial saturation returns to its resting value more rapidly if the patient squats after exercise. In normal individuals, squatting produces an increase in systemic arterial pressure, venous return of the heart and systemic cardiac out put. In patients with tetralogy, the above mentioned changes appear along with a positive increase in peripheral resistance by compression and kinking of the femoral arteries. Growth is usually normal unless cyanosis is extreme. Clubbing occurs after 3 months of age and is proportional to the level of cyanosis. The radiological features of TOF patients reveal a boot-shaped heart (Fig. 1a), thus varying from that of normal individuals (Fig. 1b). The clinical and physiological picture in case of DCRV is similar to tetralogy of Fallot but differs in the site of lesion i.e., hypertrophic enlargement in the right ventricle makes it appear as double chambered. Cardiac hypertrophy may be reasonably categorised as either physiological or pathological. Physiological hypertrophy includes cardiogenesis during embryonic development, post natal cardiac growth and a modest additional increase in heart size. If the stimulus for pathological hypertrophy is sufficiently intense, decompensated hypertrophy and heart failure is ensured.

Tissue samples comprising normal, TOF & DCRV cardiac muscle bundles were obtained from Sri Sathya Sai Institute of Higher Medical Sciences, Prasanthinilaym. The normal tissue samples representing control constitutes papillary muscles around mitral valve obtained from the hospital after adult valve replacement surgical operations with no incidence of congenital heart disease. All these tissue samples were stored in saline and maintained at -80°C. As and when required they were thawed and 20% homogenate was made in physiological saline using acid-washed autoclaved sand and the same were used for immunisation of the mouse.

To obtain samples for electrophoresis the remaining portion of tissues were homogenised similarly to make a 20 % suspension in 0.01 M Tris HCl (pH 7.5) buffer. The homogenates were centrifuged at 5000 rpm for 15 min. The supernatants were further distributed in 1.5 ml eppendorf tubes and centrifuged at 16,000 rpm for 10 min. The clear supernatants were taken in small aliquots and stored at -20°C with a drop of glycerin, an anti-freeze compound.

SDS PAGE : The mini slab gel electrophoresis was carried out using 10 % homogeneous separation gel and 5 % stacking gel with 0.05 M Tris-glycine tank buffer, pH. 8.0 with 100 V, 50 mA applied for two hours. The protein sample solution and sample buffer (Tris-HCl 0.06 M , pH 6.8, 2 % SDS, 5 % Mercaptoethanol and 15 % glycerol and 0.001 % bromophenol blue) were mixed in a 1:1 ratio and incubated in boiling water bath for 5 min. Protein standard markers obtained from M/S Bangalore Genei Pvt. Ltd. were used. An equal amount of sample comprising 40 μg of protein was loaded in each lane. The coomassie brilliant blue stained gels were analysed through Syn. Gene tools Version 2.10.03.

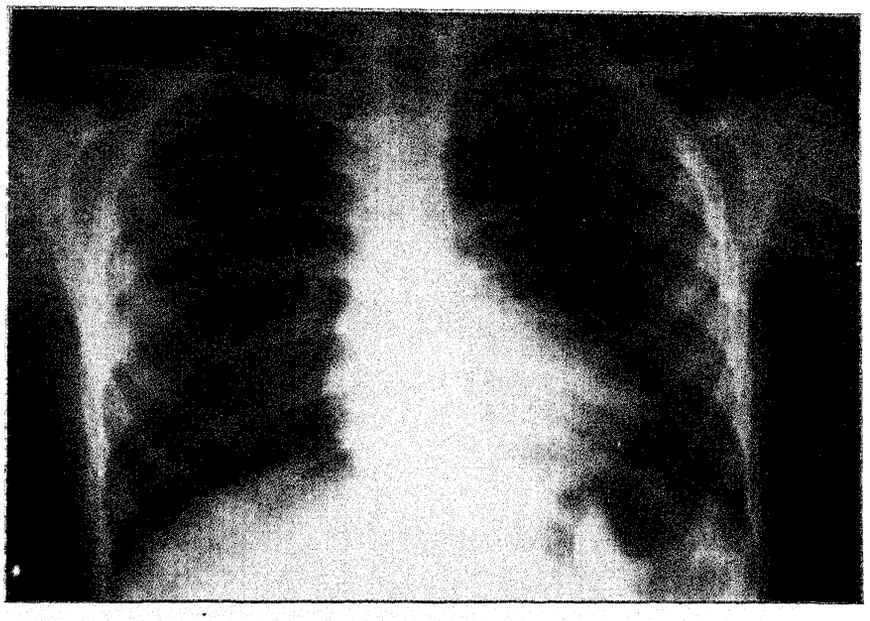

Fig. 1a- Chest X-Ray of TOF individual showing boot-shaped heart.

Fig. 1b- Chest X-Ray of normal individual showing the general appearance of heart.

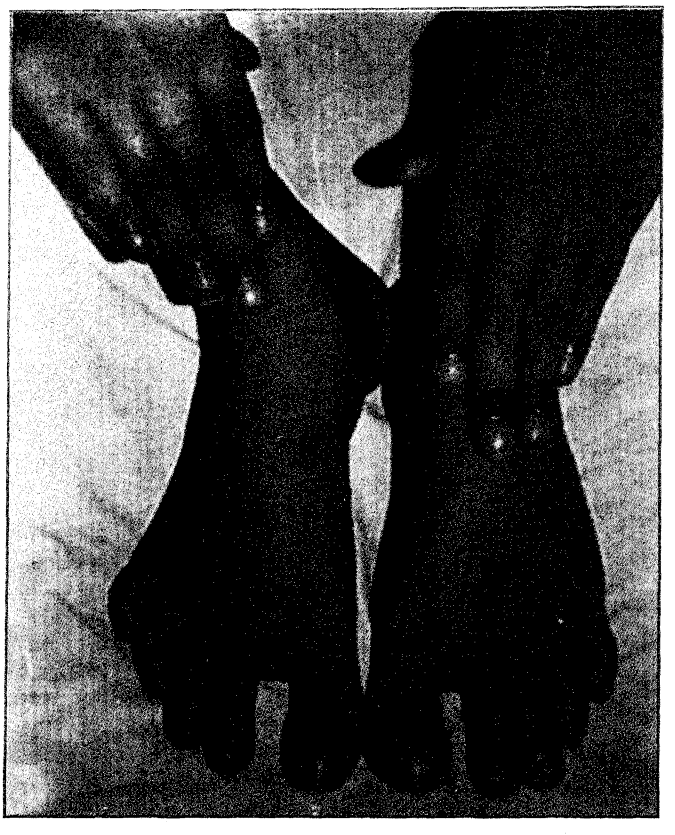

Fig. 2- A typical TOF individual exhibiting the symptoms of cyanosis and clubbing.

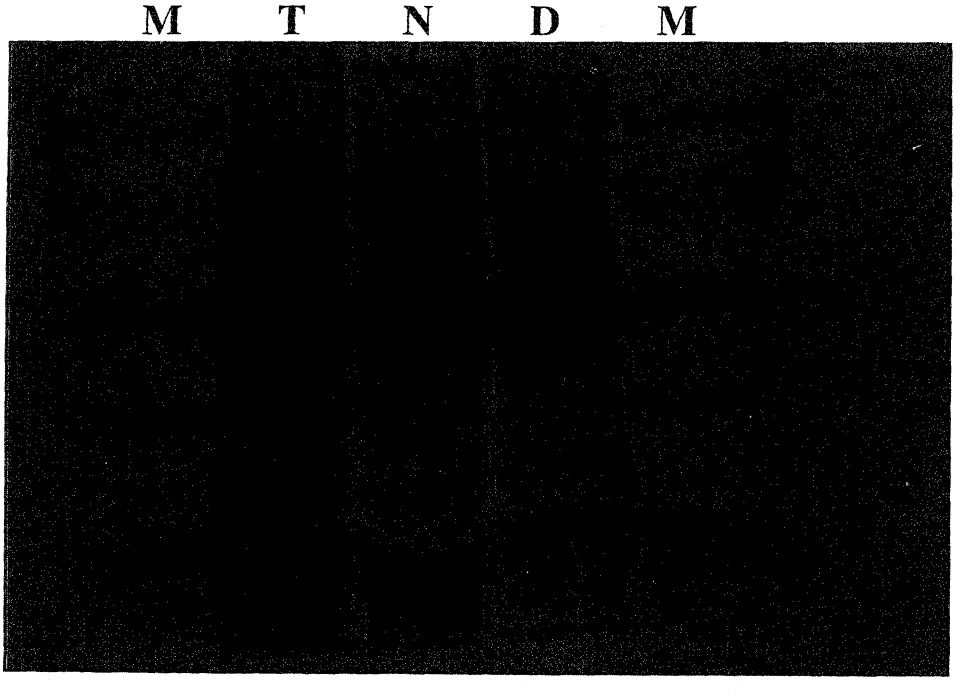


Fig. 3- SDF PAGE separation of myocardial proteins of TOF (T), normal (N) and DCRV (D) tissue samples with M.W. Markers (M) on either side ranging between 14.3, 29.0, 43.0, 68.0 and 97.4 K Da in the direction of anodal to cathodal.

The prominent physical symptoms of TOF and DCRV patients include blueness of the tips of toes, tongue and face (Fig. 2) and the chest X-ray revealing a prominent boot shaped heart in TOF patients (Fig. 1a) - all these attributes must have been due to the variation in their tissue protein profiles. Therefore, in the present investigation, SDS PAGE of cardiac protein profiles have been considered.

The pattern obtained in SDS PAGE (Fig. 3) was analysed through a software programme, Syn Gene tools (Version 2.10.03) for profile comparison (Fig. 4). The adopted software programme has identified only prominent dense fractions and they are 8, 10 and 9 protein fractions for normal ,DCRV and TOF tissue samples respectively. However, the total number of electrophoretic bands seen through normal eye varies between 22 to 24 protein fractions. The stained gel protein profile comparison revealed the variation in their relative mobility and molecular weights of the samples under study. The protein fractions were found to be about 125 KDa at the cathodal end; the prominent fractions in the range of 43 KDa through the middle region, possibly corresponding to actins and at the anodal end in the range of 29 to 14 KDa (Fig. 3).

The differences among the peak heights and the area under the peak for the scanned protein bands of standard protein markers and proteins of tissue samples of normal, DCRV and TOF are shown in tables 1, 2, 3, and 4 respectively. Out of all these fractions, the protein fraction nos. 5, 7 and 5 (Tables 2, 3 & 4) of normal, DCRV and TOF tissue samples respectively have shown the maximum profile height revealing the predominance of these particular fractions and the same must have been the muscular actins. Upon comparison among the areas under peak for these fractions 5, 7 and 5 of normal, DCRV, TOF samples respectively, the normal cardiac tissue sample represents the maximum revealing its high density, whereas, there is a decrease by 25% to 27% in both DCRV and TOF suggesting that the active contractile protein, actin must have been lowered as a proportion of the total protein profiles.

The $4^{th}$ fraction of the normal cardiac tissue represents the maximum area under peak namely 248180 $mm^2$ (Table 3) with a molecular weight 62.9 KDa and corresponding area under similar peak is totally missing in both DCRV and TOF and the same possibly be due to mal-expression of the corresponding gene. During cardiac hypertrophy certain genes are expressed and some are not. Also, certain proteins are over expressed as noticed in the anodal fractions of DCRV (Table 3). It has been reported that there is the re-expression of several foetal proteins, which are normally expressed only in the embryonic cells[10]. The rational basis for the re- expression of foetal proteins is not obvious except that the gene regulating mechanisms are misfunctioning at the promoter level in the adult cardiac cell since DCRV and TOF are inborn cardiac errors. It is reported that the atrial natriuretic factor gene expresses in the atria and ventricles in the embryonic state but not in the normal adult ventricle. However, it gets re-expressed in the ventricles during hypertrophy[10]. Also, the changes in the relative abundance of calcium cycling proteins in the altered cardiac function have been noticed in the hypertrophied and failing hearts[11]. The two protein fractions ($8^{th}$ and $9^{th}$) of low molecular weights, not represented in normal

cardiac tissue, show a greater profile height in the samples of DCRV (Table 3; indicated by arrows in Fig. 4) and this situation must have led to its altered cardiac function.

Table 1– Standard marker protein profiles

| S.No. | Molecular weight (KDa) | Profile Height (mm) | Area under peak ($mm^2$) |
|---|---|---|---|
| 1 | 97.4 | 48.74 | 31044 |
| 2 | 68.0 | 41.60 | 53736 |
| 3 | 43.0 | 87.22 | 71424 |
| 4 | 29.0 | 62.83 | 44474 |
| 5 | 14.3 | 76.83 | 62686 |

Table 2– Cardiac protein profiles of normal heart analysed through Syn Gene Tools-version 2.10.03- from the track 1 of figure 4.

| Protein Fraction Number | Molecular weight (KDa) | Profile Height (mm) | Area under peak ($mm^2$) |
|---|---|---|---|
| 1 | 126.59 | 69.81 | 21010 |
| 2 | 102.24 | 69.69 | 40418 |
| 3 | 89.24 | 83.36 | 47771 |
| 4 | 62.99 | 130.85 | 248180 |
| 5 | 41.01 | 156.30 | 226785 |
| 6 | 35.87 | 139.34 | 125776 |
| 7 | 16.92 | 46.79 | 40803 |
| 8 | 11.42 | 108.12 | 90945 |

Table 3– Cardiac protein profiles of DCRV heart analysed through Syn Gene Tools-version 2.10.03 from the track 2 of figure 4.

| S.No | Molecular weight (KD) | Profile Height (mm) | Area under peak ($mm^2$) |
|---|---|---|---|
| 1 | 124.16 | 47.82 | 24922 |
| 2 | 99.31 | 86.53 | 76791 |
| 3 | 86.68 | 77.68 | 40885 |
| 4 | 72.78 | 109.02 | 59562 |
| 5 | 57.38 | 103.38 | 40591 |
| 6 | 54.53 | 106.78 | 62566 |
| 7 | 43.36 | 133.57 | 167721 |
| 8 | 29.69 | 38.51 | 16262 |
| 9 | 21.18 | 54.70 | 47322 |
| 10 | 14.95 | 82.64 | 59693 |

Table 4– Cardiac protein profiles of TOF heart analysed through Syn Gene Tools-version 2.10.03- from the track 3 of figure 4.

| S. No | Molecular weight (KD) | Profile Height (mm) | Area under peak ($mm^2$) |
|---|---|---|---|
| 1 | 125.37 | 32.61 | 9249 |
| 2 | 86.68 | 43.21 | 28739 |
| 3 | 66.85 | 79.42 | 81047 |
| 4 | 55.46 | 88.76 | 99609 |
| 5 | 41.66 | 115.25 | 153016 |
| 6 | 27.41 | 35.50 | 22018 |
| 7 | 19.36 | 42.63 | 37422 |
| 8 | 12.08 | 52.93 | 35532 |
| 9 | 9.87 | 39.75 | 35489 |

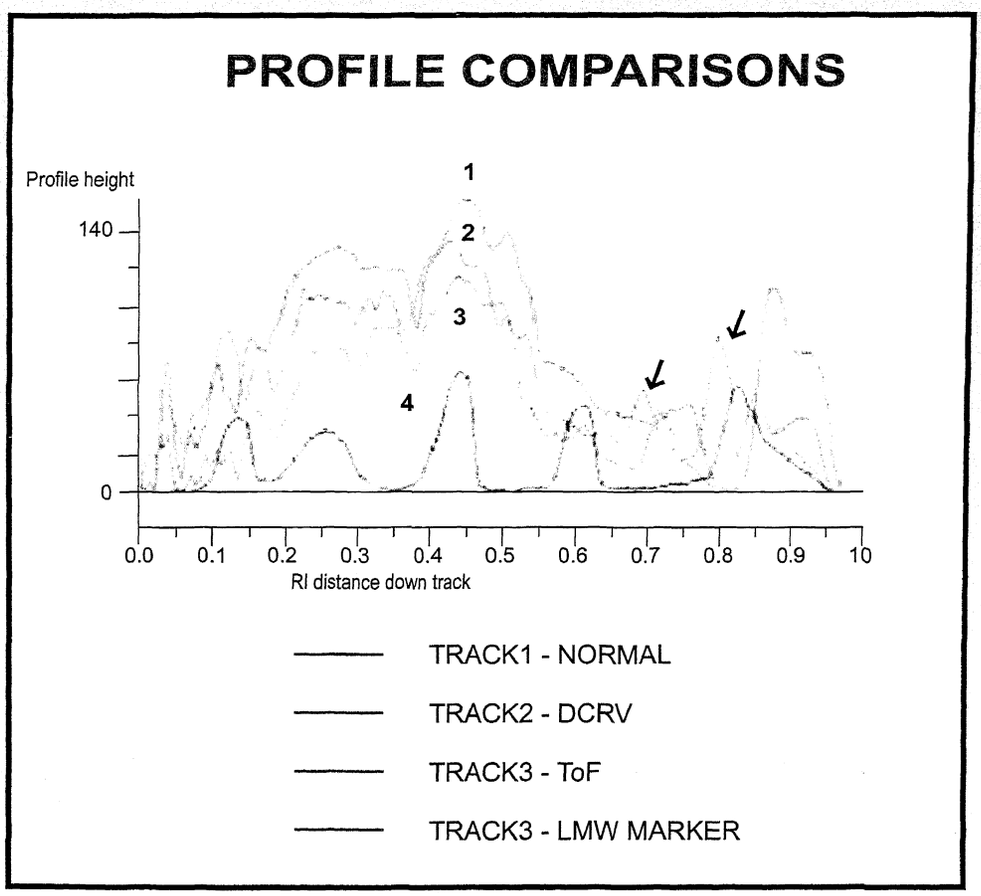


Fig. 4- Protein profile comparison of proteins separated in SDS PAGE (Fig. 3). The same evaluated through Syn Gene Tools version 2.10.03.

## References


1. Suresh, V., Rao, A.S. & Yavagal S.T. (1995) *Ind. Heart Journal*, **47**(2) : 125.
2. Mohanty, S.R., Airan, B., Bhan, A., Sharma, R., Kumar, A.S., Kothari, A.S., et al., (1999) *Ind. Heart Journal*, **51**(2) : 186.
3. Jacobs, E.G., Leung, M.P. & Karlberg J. (2000) *Pediatr.Cardiol.* **21**(2) : 148.
4. Gelb, B.D. (1997) *Curr. Opin. Cardiol.* **23**(3) : 321.
5. Tanner, F.C., Largiader, T., Yang, Z., & Luscher T.F. (1999) *Schweiz. Med. Wochenschrn.* **129**(46) : 1784.
6. Redwood, C.S., Moolman-Smook, J.C. & Watkins H. (1999) *Cardiovascular research* **44**(1) : 20.
7. Marian, A.J., Wu, Y., Lim, D.S., McCluggage, M., Youker, K. & Yu T. (1999) *J. Clin. Invest.* **104** (12) : 1683.
8. Shankar, K.R., Hultgren, M.K., Lauer, R.M. & Diehl A.M. (1967) *Am. J. Cardiol.* **20** : 122.
9. Marian, A.J., & Roberts, R.(1995) *Circulation.* **92** : 1336.
10. Parker, T.G., Packer S.E. & Schneider M.D. (1990) *J. Clin. Invest* **85:** 507.
11. Kadambi, V.J., Ponniah, S., Harrer, J.M., Hoit, B.D., Dorn, G.W II. & Walsh, R.A. (1996) *J. Clin. Invest.* **97**: 533.

# Unification of charge of the electron with proton and neutron through quantum Hall effect

**Keshav N. Shrivastava**

*School of Physics, University of Hyderabad, Hyderabad – 500046, India.*

Received July 2, 2004; Accepted July 20, 2004

**In the Dirac equation there are solutions such that one particle is negatively charged and the other is positively charged. A particle of zero charge can also be introduced. The sum of the three charges is zero. We report that it is possible to have the sum of the charges equal to zero by using fractions. Similarly, *l+s*, is conserved in the Dirac equation but *l-s*, is not. We use negative spin for the spin so that *l-s*, is conserved. We find that there is a contribution to the charge which is of the form $(2l+1)^{-1}\begin{pmatrix}1/2 & 0\\ 0 & -1/2\end{pmatrix}$ which for *l*=0 gives ±1/2 for the charge but for *l*=1, the charges of ±1/6 are generated. Combined with ½, the charges become (1/2)±(1/6) which for two particles adds to 1. In this way the charges become 1/3 and 2/3 instead of 0, ±1. This means that spin of the electron behaves like the charge. This phenomenon is well known for neutron and proton which have charges of 0 and +1, but it is new for the electron. Our representation of ±1/3 and ±2/3 still adds to zero as does the 0, ±1 except that now there are four particles where there were only 3.**

**(Keywords: quantum hall effect/unification of charge/proton/neutron)**

## Introduction

The energy of a particle is given by $\pm(c^2p^2+m^2c^4)^{1/2}$ where positive sign is associated with the electron and negative energy solution is interpreted to belong to positrons. The sum of the two charges, $\pm e$, is equal to zero. In the nonrelativistic theory, the lattice distortions are associated with soft modes which have zero frequency at the critical point. Therefore, motivated from the condensed matter physics[1], Jackiw has introduced a solution which has zero frequency in the Dirac equation[2]. Therefore, there are three solutions instead of the usual two solutions and the sum of the charges is equal to zero. In the usual Dirac Hamiltonian $L+S$ is conserved but $L-S$ is not. Jackiw has found that charge degrees of freedom are converted into spin degrees of freedom in the field of a magnetic monopole[3].

We make use of the theory of angular momentum to define an effective charge. In this case, the charge becomes dependent on $l$ and $s$ and for $l=0$, it can be zero or 1 but for $l$=1, the charges of 1/3 and 2/3 are found. The value of 1/3 requires the spin to be negative, i.e., -1/2 so that L-S is conserved instead of $L$+S. Similarly, the charge of 2/3 requires positive spin, $s$=1/2 and $L+S$ is conserved. The two values of the charge, i.e., 1/3 and 2/3 add up to 1 rather than zero. Therefore, our problem is similar to that of Jackiw and Schrieffer who consider fractional charge in the charge density waves.

## Electronic Isospin Type Quantity

In the case of relativistic energy $\pm(c^2p^2+m^2c^4)^{1/2}$ there are two solutions, one positive belongs to the electron and the

other negative belongs to the positron. Although Jackiw has found a zero-energy solution, there is no positive term in the energy. If the positive term is much larger than the negative term, the negative solution will become positive and instead of one negative and one positive, we will have both the solutions with positive energy. For example, the energy solution may be given by,

$$E = E_0 \pm (c^2p^2+m^2c^4)^{1/2} \qquad (1)$$

When $E_0$ is larger than the second term, both the solutions become positive. If $E_0$=0, we get Jackiw's solution, i.e., where $E_0$ belongs to charge-density waves. When $E_0=(c^2p^2+m^2c^4)^{1/2}$ one of the solutions of $E$ is zero and the other is positive. It was found by us[4] that in high magnetic field, the energy of the electron becomes,

$$E = [l+(1/2)\pm s](2l+1)^{-1}\hbar\omega_c \qquad (2)$$

which for $l$=0, s=1/2 gives $\hbar\omega_c$ and for $l$=0, $s$=-1/2 gives $E$=0. For $l$=1, more interesting values arise. For $l$=1, $s$=1/2, we get $(2/3)\hbar\omega_c$ and for $l$=1, s=-1/2, $(1/3)\hbar\omega_c$. When we look at the value of the Bohr magneton, $\mu_B=e\hbar/2mc$, the above value multiplies the charge so that it can be interpreted that the charge becomes $(1/3)e$ or $(2/3)e$. Although Jackiw's result of equivalence between charge and spin requires the presence of a magnetic monopole, our result occurs when the energy is $\mu_B.H$, where $H$ is the magnetic field and $\mu_B$ is replaced by an effective magnetic moment. Usually, there is only one solution for $\mu_B$ but in the present problem two solutions occur due to two signs of $s$. In the Hund's rule or in Lande's formula for $g$ value only positive sign of $s$ is used. We allow the $s$ to become negative so that there are two values. In the Dirac equation only $L+S$ is conserved but $L-S$ is not. However, in the case of negative $s$, $L-S$ conserves the angular momentum. Therefore, there is clearly an advantage to let s assume negative values. If s is considered as a matrix, we can write the above expression as an effective charge,

$$e_{eff}/e=(1/2)\begin{bmatrix}1 & 0\\ 0 & 1\end{bmatrix}+(1/\{2l+1\})\begin{bmatrix}1/2 & 0\\ 0 & -1/2\end{bmatrix} \qquad (3)$$

Here, the first term arises due to quantum mechanics and the second term for $l$=1 gives ±1/6. The effective charge then becomes, (1/2)±(1/6) or 1/3 and 2/3. This result is similar to Jackiw's result where isospin is determined by spin. The charges ±1/6 form a conjugate pair and the charge ½ is associated with quantum mechanical behavior of the angular momenta operators. We can define the charge as a quantity which operates like the angular momenta and hence is similar to isospin. In the present problem,

$$I = (e_{eff}/e)\begin{pmatrix}1 & 0\\ 0 & 1\end{pmatrix}. \qquad (4)$$

Hence the previous relation can be written as,

$$I = (1/2)\begin{pmatrix}1 & 0\\ 0 & 1\end{pmatrix}+(2l+1)^{-1}\begin{pmatrix}1/2 & 0\\ 0 & -1/2\end{pmatrix} \qquad (5)$$

For $l=0$, the isospin type quantity becomes, $I= (1/2)\pm s$. Therefore, for positive sign the charge is 1 and zero for the negative sign. For $l\neq 0$, taking integer values of $l$, we can obtain a whole series of charges. The spin need not be limited to ½. For example, it can be 0, 1 or 3/2, 5/2, etc. For $S$=0, the charge becomes ½. The energy of the electron in a magnetic field is $\mu_B.H$. When above value is used for the charge, this magnetic energy becomes,

$$\frac{e}{2mc}\hbar\sigma'.H = (\frac{1}{2} \pm s)\frac{e}{2mc} \hbar\begin{pmatrix}1 & 0\\ 0 & -1\end{pmatrix}H_z \qquad (6)$$

which has two terms. The first term gives half of the magnetic moment and the second term $\pm\mu_B HSS_z$ which has four solutions for $S$=1/2, $S_z$=±1/2. This provides an energy gap. The eigen function is of the form,

$$\psi_1 = b_{1/3}\psi_{1/3} + d_{2/3}^{\dagger}\psi_{2/3} \qquad (7)$$

where for $l$=1, the charges of 1/3 and 2/3 come from (1/2)±(1/6). Comparing this wave function with that of Dirac equation,

$$\psi = b_p\psi_{p+} + d_p^{\dagger}\psi_{p-} \qquad (8)$$

where $\psi_{p+}$ corresponds to positively charged particle and $\psi_{p-}$ to the negatively charged particle which is conjugate to the positively charged particle. It is found that the sum of the two charges is zero whereas in our case it is one. The Dirac equation conserves positive $S$ but not negative $S$. In our solution corresponding to the charge of 1/3, $S$ is negative and $L$-(-$S$) is conserved. So the conservation of angular momentum is favoured by both of our solutions. The positive $S$ is conserved. So we conserve $L$+$S$ as well as $L$-(-$S$) whereas the Dirac equation conserves only $L$+$S$.

## Angular Momentum and Isospin Type Quantity

We find that the sum of the angular momentum and the isospin type quantity is an angular momentum. We define the angular momentum as $j=l$+s. In order to make it dimensionless we measured it in units of $2(2l+1)$, so that the dimensionless $j$ becomes $j=(l+s)/[2(2l+1)]$. The charge is $(l+(1/2)\pm s)/(2l+1)$ which is already dimensionless. The sum of the two is given by,

$$[(l+s)/2(2l+1)]+(e_{eff}/e) =$$

$$[(l+s)/2(2l+1)]+\frac{1}{2}\pm s/(2l+1)=$$

$$3j+1/2(2l+1) \qquad (9)$$

## Application to Nuclear Physics

In the eq.(5) for $l=0$, s=1/2 gives a proton and $s$=-1/2 gives a neutron. The value $s$=0 gives neutral π-meson. In order to generate more particles, hypercharge, $Y$, is introduced, $I$= ½+$Y$/2 with $s$=1/2 and $Y$=1, and $l=0$, this equation becomes same as (5). On this basis, the quark model was developed by Gellman. Usually, the magnetic moments of proton and neutron are explained in terms of spin and orbital g-values. The magnetic moment of proton depends on the angular momenta, $j=l\pm$s, for which many states are possible. Similarly, the magnetic moment of the neutron depends on the angular momenta states. For the proton $g_l$=1 and $g_s$=5.585 so that by using the formula,

$g_j=g_l\pm(g_s-g_l)/(2l+1)$

and $\mu_P=g_j j$ the magnetic moment of the proton is correctly described. Similarly, for the neutron, $g_l=0$, $g_s=-3.826$ and the expression $\mu_n=g_j j$, gives the correct value of the magnetic moment of the neutron. However, the magnetic moment of the electron is determined by the Bohr magneton of which there is only one value. The Bohr magneton also uses the value of the electron charge of which there is only one value and fractional values do not arise too easily. We will show that there are many fractional values of the Bohr magneton and hence that of the electron charge and they do occur in condensed matter.

## Quantum Hall Effect and Electron Charge

We return to eq.(2) so that for $s$=-1/2, the charge of the electron becomes,

$$\nu_-= l/(2l+1) \qquad (10)$$

which gives 1/3 for $l$=1. For $s$=+1/2,

$$\nu_+= (l+1)/(2l+1) \qquad (11)$$

which is 2/3 for $l$=1. If we tabulate $\nu_-$ and $\nu_+$ for various values of $l$, the values obtained are exactly the same as those obtained experimentally by Stormer[5] from the measurements of plateaus in the quantum Hall effect in *GaAs*[See fig. 18]. Over the years, higher magnetic fields were achieved which gave rise to more values of the fractional charge[6]. These values have been explained by introducing the idea of clustering where the spin need not be ½, i.e., it can become 1 or 3/2 or some such value[7].

## The Agreement

As pointed out above, the values of the fractional charge predicted by our series (10) and (11) are exactly the same as those measured experimentally. The values obtained after 2003 also agree with those calculated with $s$>1/2. The only problem is that in Lande's formula only positive values of the spin were used whereas we use both the positive as well as the negative values[8]. It was pointed out by the experimentalists that some of the fractions were difficult to understand. We find that $j$=1/2 with spin appropriate to an electron cluster can explain all of the experimentally observed numbers.

When the field is varied, the orbital angular momentum changes so that spin of the electron flips to conserve the angular momentum. For $l$=0, $s$=+1/2, the value of $\nu_+$ is 1. Now, as the orbital changes to $l$=1, there is a need to conserve $L+S$ which can be done only by changing s to –1/2 so that $\nu_+$=1 changes to $\nu_-$=1/3. Here, $\nu_+$ =1, belongs to $l$=0, $s$=+1/2 and $l$+ s=1/2 whereas $\nu_-$=1/3 belongs to $l$=1, $s$=-1/2 so that $l+s$=1/2. Thus in going from $\nu_+$=1 to$\nu_-$ =1/3, $l+s$ is conserved. Similarly for $l$=1, $s$=+1/2, $l+s$=3/2 and for $l$=2, $s$=-1/2, $l+s$=3/2 and $\nu_-$=2/5 so that in going from $\nu_+$=2/3 to $\nu_-$=2/5, $l$+s is conserved. Similarly, there are pairs of $\nu_\pm$ for which $l+s$ is conserved. For $l$ =2, $s$=+1/2, $l+s$=5/2 and $\nu_+$ =3/5 and for $l$=3, $s$=-1/2, $l+s$=5/2 and $\nu_-$=3/7 so that in going from 3/5 to 3/7 the $l+s$ is again conserved. For $l$=0, $s$=-1/2, $l-s$=1/2 and $\nu_-$=0 and for $l$=1, $s$=1/2, $l-s$=1/2 and $\nu_+$=2/3 so that in going from 0 to 2/3, $l$-s is conserved, etc. We can go from $\nu_-$ =0 to $\nu_+$=1 or from 1/3 to 2/3 by conserving $l$. Considering the Dirac equation $l+s$ is conserved. If we allow "negative spin",

then $l$-$s$ is conserved. This is an important result from the view point of the Dirac equation. The value of $l$ is constant in going from 1/3 to 2/3. Therefore, this transition is "forbidden". In the case of the electron $g_l$ =1 and $g_s$=2 so that,

$$g_j = 1 \pm 1/(2l+1) \qquad (12)$$

Multiplying it by $s$=$j$=+1/2 so that,

$$g_j j = [\, l + (1/2) \pm s]/(2l+1) \qquad (13)$$

which is 0 for $s$=-1/2, $l$=0 and 1 for $s$=+1/2, $l$=0. For $l$=1, $s$=+1/2, it is 2/3 and for $l$=1, $s$=-1/2, it is 1/3, etc. When we compare the magnetic moment with the charge, these values imply a charge of 0, 1, 1/3, 2/3, etc. Here we have taken the value of $l$ while multiplying by $j$. If necessary, all of the components can be written down. For $l$=1, the charge is 2/3 for positive sign and 1/3 for the negative sign with $s$=1/2. Thus a charge of 1 splits into two particles of which one is (1/2)+(1/6) and the other is (1/2)-(1/6) and the sum of two is one. Alternatively, the charge of 1 splits into two particles of charges 1/3 and 2/3. Let us consider the negative sign of $j$=-1/2 so that 1/3 and 2/3 change into −1/3 and −2/3. Now there are four components ±1/3 and ±2/3 but the sum of these four charges is zero. This means that the charge of the electron behaves like the angular momentum which is another way of saying that at high magnetic fields the electron acquires an isospin type property. The quantity $\mu.H = g\mu_B H.S$ can be defined by aligning the field along the $z$ direction, so that H.S becomes $H_z S_z$ where $S_z$ = ±1/2. For the negative value, $S_z$=-1/2, the magnetic moment becomes, $\mu_{eff}$=(-1/2)[2$l$+1 ±1]/(2$l$+1) but $H_z S_z$ is invariant with respect to change in sign, i.e., $-H_z S_z$ is exactly the same as $+H_z S_z$. All that happens is that +1/2 and −1/2 get interchanged. Similarly, the energies of ±3/2 are the same as that of ∓3/2. So far we have discussed only the formula (13) with $j$=1/2. For $j$=3/2, the fractional charge is higher by a factor of 3 than those of $j$ = 1/2. The cyclotron frequency is multiplied by $\nu_\pm$ so that the Landau levels also get modified only by a factor $\nu_\pm$ and the levels continue to be determined by $\nu_\pm \hbar\omega_c(n+ ½)$.

## ESR and QHE

In the case of electron spin resonance (ESR), the transitions are obtained between various values of the angular momenta by means of a radio-frequency coil. Since the oscillating field is at an angle of 90°, it can be used to generate the spin raising and lowering operators. The resulting system absorbs microwaves so that the electron spin resonance line can be observed. On the other hand, the quantum Hall effect plateaus are produced without an rf coil. In quantum Hall effect, one goes from step to step because there is need to conserve $j$=$l$±$s$. For various values of $l$ one can go from one step to another such that there are more than 150 steps[7].

## Conclusions

The expression which gives the correct value for the magnetic moments of the neutron and proton also gives the correct charge for the electron except that two states of electron are produced. This new state is associated with negative spin. Upon considering various values of the orbital angular momenta, many new charged quasiparticles are predicted which also agree with the experimental data on the quantum Hall effect. The proton and

neutron are associated with charges 0 and ±1 but the angular momenta which describe the charges ±1/2 and ±3/2 are equally valid. The original Dirac equation did not conserve *L-S* but now for negative spin it does. Thus, there are many new quasiparticles which have fractional charge and satisfy the same theorems which the proton and neutron do except for the added advantage of negative spin in the Dirac equation. The approach used gives the proton and neutron magnetic moments correctly and in each of these particles there are solutions with positive as well as negative s. In the case of the electron there is only one particle then what are the solutions with negative *s*? Obviously, there is a need of a new particle. We have explained[9] the fractional charges using spin ½. After 2003, charges with spin > ½ were discovered[10]. We are now in a position to unify the electron with the proton and neutron.

## References


1. Jackiw, R. & Schrieffer, J. R. (1981) *Nuc. Phys. B* **190**: 253.
2. Jackiw R. & Rebbi, C. (1976) *Phys. Rev. D* **13**: 3398.
3. Jackiw, R. & Rebbi, C. (1976) *Phys. Rev. Lett.* **36**: 1116
4. Shrivastava, K. N. (1986) *Phys. Lett. A* **113**: 435.
5. Stormer, H. L. (1999) *Rev. Mod. Phys.* **71**: 875.
6. Pan, W., Stormer, H. L., Tsui. D. C. *et al.* (2003) *Phys. Rev. Lett.* **90** : 016801.
7. Shrivastava, K. N. (2003) cond-mat/0303621, 0302610.
8. Shrivastava, K. N. (2004) *Phys. Lett. A* **326**: 469.
9. Shrivastava, K. N. (1986) *Natl. Acad. Sci. Lett.* **9**: 145.
10. Shrivastava, K. N. (2003) *Natl. Acad. Sci. Lett.* **26**: 159.

# Celebration of the Scientific Awareness Year (2004)

The Govt. of India has declared the year 2004 as 'Scientific Awareness Year' to cultivate the scientific temperament among the students and general mass so that a rational approach towards life is developed.

The Academy has also decided to spread the horizon of its science communication programmes through-out the country starting from 2004. Several activities have been planned for communicating science specially among the students and rural mass through the twelve Chapters of the Academy. The Headquarter of Academy, has already started several programmes under the guidance of Prof. S.L. Srivastava, Co-ordinator, Science Communication Programme of the Academy.

**Science Extension Lectures at Allahabad**—On August 16, 2004 an informative and illustrative lecture was delivered by Dr. (Ms.) Sharda Sundaram on 'Atoms, Molecules and Bonds' in Golden Jubilee Jagat Taran Inter College, Allahabad, for the students of +2 level.

On August 21, two eminent scientists and Fellows of the Academy delivered two lectures. The first lecture was delivered by Prof. (Ms) D. Kaul in Gauri Pathshala Girls Inter College, Allahabad, on 'Basic and Advanced Concepts in Genetics' under which the structure of DNA, Genes, Recombinant DNA, replication, mechanism of genetic dogma, gene therapy, cloning and use of genetics in the development of mankind were illustrated. The second lecture was delivered by Prof. S.L. Srivastava on 'Advances in Certain Novel Materials and Devices' in Narayan Ashram Balika Inter College, Allahabad. He observed that such advancements may bring the health services directly in each home.

On August 23, Dr. Niraj Kumar, Assistant Executive Secretary of the Academy delivered an interesting lecture in M.L. Convent, Allahabad on the 'Basic Concepts in Life Sciences'. He explained the origin of life, evolution of man and preventive and promotive role of nutrition.

On August 24, Prof. U.C. Srivastava of the Zoology Department, Allahabad University, delivered an informative lecture on 'Endocrine and Diseases' in Govt. Girls Inter College, Allahabad for the students of class X to XII. He explained the role of endocrine glands in regulation of metabolic pathways and many diseases.

On September 2, another interesting and illustrative lecture was delivered by Prof. S.L. Srivastava in Hamidia Girls Inter College on "Several Aspects of Energy". He dealt in detail about the sources of energy: hydroelectric, thermal, wind, solar, nuclear, plasma and renewable sources of energy through coloured transparencies.

Dr. V.P. Kamboj, Formerly Director, Central Drug Research Institute, Lucknow and General Secretary of the Academy, spoke on "Intellectual Property Rights" in Ewing Christian College, Allahabad on September 4, 2004. He explained that in the era of globalization, Intellectual Property Management is extremely important, not only for Research Institutions but also for

the industries; and today in the global market place monopolies are built only on the basis of patents and other IPR's.

On September 6, Prof. U.C. Srivastava, delivered a lecture on 'Deficiency Diseases' in Umrao Singh Memorial Girls Inter College, Allahabad. The lecture was so interesting that the students kept on asking questions for more than an hour after the lecture.

On September 11, Prof. S.L. Srivastava delivered an interesting lecture on 'Smart Materials and Devices' in Maharishi Patanjali Vidyamandir, Allahabad. The lecture was appreciated by the students and teachers alike.

Prof. C.B.L. Srivastava, Formerly Head, Department of Zoology, Allahabad University dealt in detail on a complex topic on 'Brain and its Activities in Crosthwait Girls Inter College on October 5, 2004. He tried to make the students understand the mechanism of brain activities viz. conscious, unconscious and sleep states of brain and various parts responsible for such functions.

All these lectures were attended by a large number of students and teachers, who appreciated the efforts of the Academy to reach out to schools. There are several requests to organize such programmes time and again and also to cover other institutions in Allahabad.

**Outstation Science Extension Lectures** — A series of extension lectures was held at Satna (M.P.) from September 29 to October 1, 2004. A brief inauguration was held on September 29, 2004 at Govt. P.G. College, Satna where Prof. S.L. Srivastava, Coordinator of the Programme, delivered the Inaugural Address on Biometeorology.

The following lectures were delivered in different institutions of Satna by the speakers from Allahabad—

Prof. S.L. Srivastava gave an interesting talk on 'Smart Materials and Structures Mimicking the Living World' at Satna Institute of Information Technology on September 29, 2004. Prof. D.K. Chauhan, Botany Department, Allahabad University (AU.), explained the 'Role of biodiversity and its conservation', in Kendriya Vidyalaya and also delivered an illustrative lecture on Bioconservation in Govt. P.G. College on the same day.

Prof. P.W. Ramteke, Allahabad Agricultural Institute, Allahabad, delivered a talk on Biotechnology in Govt. P.G. College on 30th September and on the same day two lectures were also delivered by Prof. U.C. Srivastava, Department of Zoology, A.U., in Govt. P.G. College and Christukala Convent School. In Govt. P.G. College, he dealt in detail on Neurosecretion, endocrine and diseases, while in Christukala, his lecture was mainly focused on diseases.

Dr. (Mrs.) Sharda Sundaram, Chemistry Department, Ewing Christian College, Allahabad, delivered an illustrative lecture on Atoms and Molecules in the Govt. P.G. College and also in Bonanza School on October 1,2004. On the same day Dr. Pankaj Srivastava, Motilal Nehru National Institute of Technology, Allahabad delivered two lectures on Cryptography in Satna Institute of Information Technology and Govt. P.G. College. In the valedictory function, Prof. G.L. Tiwari delivered an

informative lecture on 'Algae and its Diversity'.

The next series of outstation science extension lectures was organized at Jaunpur (U.P.) from October 27-29,2004. Prof. C.B.L. Srivastava, formerly Head, Department of Zoology, AU. inaugurated the lecture series at B.R.P. Inter College, Jaunpur, on October 27, 2004. Members of the Management Committee of the College, Principal, Teachers and science students of +2 level attended the inaugural function. Dr. M.S. Sinha, Executive Secretary of the Academy, while briefing about the Science Communication Programmes of the Academy emphasized the importance of carrying out such programmes and stressed the need of cultivation of scientific temperament among the students and general mass. He also delivered a lecture on 'Computers and Internet'. On the same day Prof. C.B.L. Srivastava delivered an imformative lecture on 'Brain and Its Activities" in Shia Degree College. Dr. Pankaj Srivastava, Motilal Nehru National Institute of Technology, Allahabad, delivered a conceptual and interesting lecture on 'Security and Information Science' in Rizvi Learners.

On October 28, 2004, Prof. D.K. Chauhan, Botany Department, A.U. delivered illustrative lectures with the help of beautiful slides on Biodiversity in Rizvi Learners and B.R.P. Inter College. Dr. R.N. Seth, CIFRI, Allahabad also delivered informative talks on Fishes and Parental Care in Shia Degree College and B.R.P. Inter College.

On October 29, 2004, Prof. R.K. Srivastava, CAD-LAB, Motilal Nehru National Institute of Technology, Allahabad explained the mechanism of computer and its application in different fields of science in Rizvi Learners and B.R.P. Inter College. On the same day Dr. Abhai Pandey, Biochemistry Department, A.U. delivered conceptual lectures on 'Vaccination and Immunity' in B.R.P. Inter College and Shia Degree College.

All these lectures were well attended. The organizers, students and the teachers appreciated the efforts made by the Academy.

**Biological Sciences Workshop** — The Academy organized a one-day "Biological Sciences Workshop" in the Department of Zoology, University of Allahabad on Sunday, September 26, 2004 for the science students of +2 level of Allahabad Intermediate Colleges. Several teachers of the colleges also participated in the Workshop. Prof. U.C. Srivastava was the Convener of this workshop, Dr. V.S. Bhatnagar and Dr. R.R. Tiwari very kindly agreed to be the resource persons. The workshop was inaugurated by Prof. S.L. Srivastava. Prof. Pratima Gaur, Head of the Department of Zoology, AU. was the Chief Guest. While addressing the gathering of more than 80 students and teachers, Prof. S.L. Srivastava explained the importance of organizing such programmes and told that teachers should teach science by doing experiments and not only lecturing on the blackboard. Prof. U.C. Srivastava gave a brief account of the experiments and demonstrations to be done on that day and introduced the resource persons. Prof. Pratima Gaur welcomed the teachers and students in the department and assured that they will get full cooperation from the faculty and staff of the department to make the programme a success. After the inaugural session predemonstration lectures were given by Dr. V.S. Bhatnagar and Dr.

RR. Tiwari on basic concepts of cytogenetics, staining and preservation methods. Then, Prof. U.C. Srivastava, with the help of resource persons demonstrated the presence of Barr Body, Chromosome's slide preparation and preservation of laboratory animals for specimens. All the teachers and students found this programme very useful.

The Valedictory Function was organized on the same day in which certificates of participation were distributed to the teachers and students by Prof. U.C. Srivastava. Dr. Niraj Kumar, Assistant Executive Secretary of the Academy extended a vote of thanks.

# Obituary

## Prof. Ram Charan Mehrotra

Born on 16th, February, 1922 in Kanpur, Prof. R.C. Mehrotra, D.Phil (Alld.) Ph.D, D.Sc. (London), D.Sc. (h.c. : (Kanpur, Meerut, Jhansi and B.H.U.), F.N.A, F.N.A.Sc., F.F.A.C.S. was a unique combination of a gifted excellence, dedicated teacher and par excellence scientist. He was a Fellow of Royal Institution of Chemistry and Royal Society of Chemistry (London).

Prof. Mehrotra was honoured by fellowships of all three Academies : The National Academy of Sciences India, Allahabad, Indian National Science Academy, New Delhi and Indian Academy of Science, Bangalore as well as Fellow of Third World Academy of Sciences. Prof. R.C. Mehrotra was honoured and awarded several times for his excellent scientific achievements : E.G. Hill award (1949), Shanti Swaroop Bhatnagar Award (1965), Sheshadri Award (1976) of Indian National Science Academy, P.C. Ray Award (1977) of Indian Chemical Society, Platinum Jubilee Award (1980) of Indian Science Congress Association, P.C. Ray Award (1998) and Lifetime Achievement Award (1999-2000) by Chemical Research Society, Bangalore.

Prof. Mehrotra was elected General President (1978-79) of Indian Science Congress as well as President for Indian Chemical Society (1976-77) and Society for Peace, Security and Development (1993-2003). He was the Vice-President (1977-78) of Indian National Science Academy.

Prof. Mehrotra was solely responsible (giving directions) for reform in New Educational Policy in higher education through U.G.C. and he was appointed as Chairman, Policy Commission (U.G.C.) for College and University teachers (1984-86). Prof. Mehrotra had been rated as the foremost Inorganic Chemist in India and all over the chemical world by National Science Foundation (N.S.F.) America, American Chemical Society, UNESCO and inorganic chemistry section of IUPAC.

In his academic life, he worked as lecturer (1944-54), Allahabad University, Reader (1954-58) Lucknow University, Professor and Founder Head (1958-1962) Gorakhpur University. In 1968 he joined Rajasthan University, Jaipur. At all these places he established Excellent Education Centre for teaching and research. Prof. Mehrotra was Vice-Chancellor, Rajasthan University (1968-69 and 1972-73), Delhi University (1974-79) and Allahabah

University (1991-94). He was Emeritus Professor in Rajasthan University and Coordinator SAP, UGC till his death.

His life's favourite quotation was "Great Chemists never die. They just reach equilibrium."

The main research achievement of Prof. Mehrotra was the formation of "aluminium tri soap" which was known to be "non available."

He was known as the father of "Metal Alkoxide Chemistry", later he become dedicated for the preparation of new ceramic materials from alkoxide.

His extremely important books are: Metal Alkoxide (1978), Metal β-dliketonates (1978), Carboxyllates (1983), Organometallic (1999): Aryloxides and Alkoxides of Elements (2001).

In his passing away on July 11$^{th}$, 2004, at Mumbai after massive heart attack, the academic community has lost a great teacher, researcher, educationist, administrator and above all a remarkable great human being. He has left behind his loving wife Dr. (Mrs.) Suman, two daughters (Rashmi and Shalini) and one son (Piyush) as well as a large number of students, admirers, well wishers and friends to bemoan his death.

**R.K. Dubey**

Swedish Research Institute Fellowship Awardee, Stockholm (Sweden)

Reader, Department of Chemistry, University of Allahabad, Allahabad-211002 (U.P.)

# National Conference

# on

# Bioinformatics Computing NCBC'05

# to be held from March 18-19, 2005

## Contact

**Deepak Garg**

Convenor, NCBC'05

Computer Science & Engineering Department Thapar Institute of Engineering and Technology Patiala – 147 004

Email : deepakgarg@ieee.org

Tel : 0175-2393007

Mobile : 09815599654

## ADDENDUM

In Short Research Communication entitled 'Light induced transformation of quinine : Studies in the effect of pH', By Shubha Jain, Binita Kheradia and Amitbodh Upadhyay published in National Academy Science Letters, Vol. 27, No. 7 & 8, 2004, p. 273-274, the Schemes (I and II) were not printed inadvertently. The same are given below:

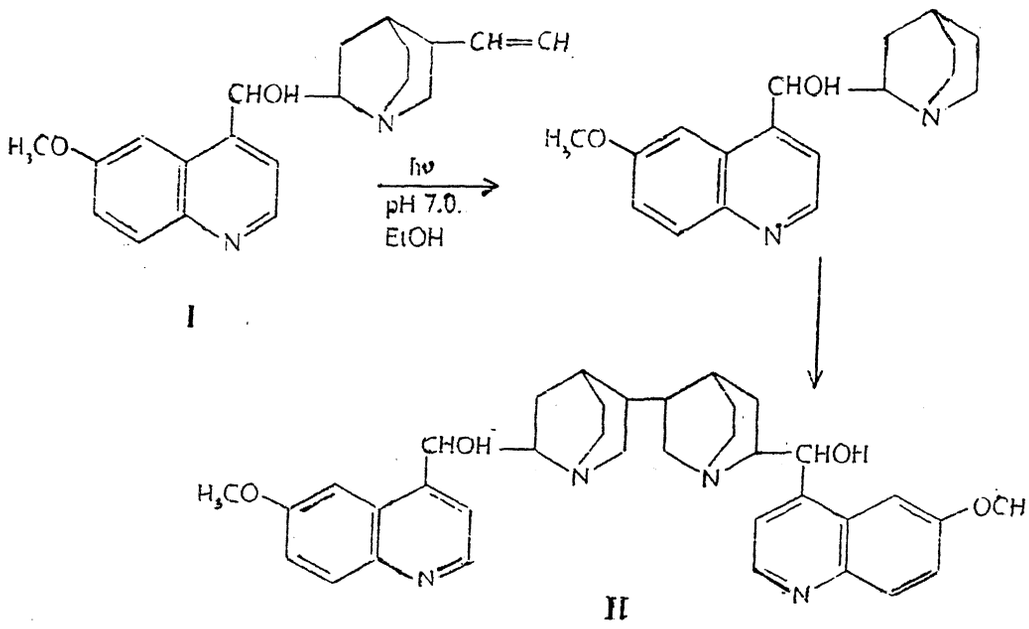


**Scheme – I**

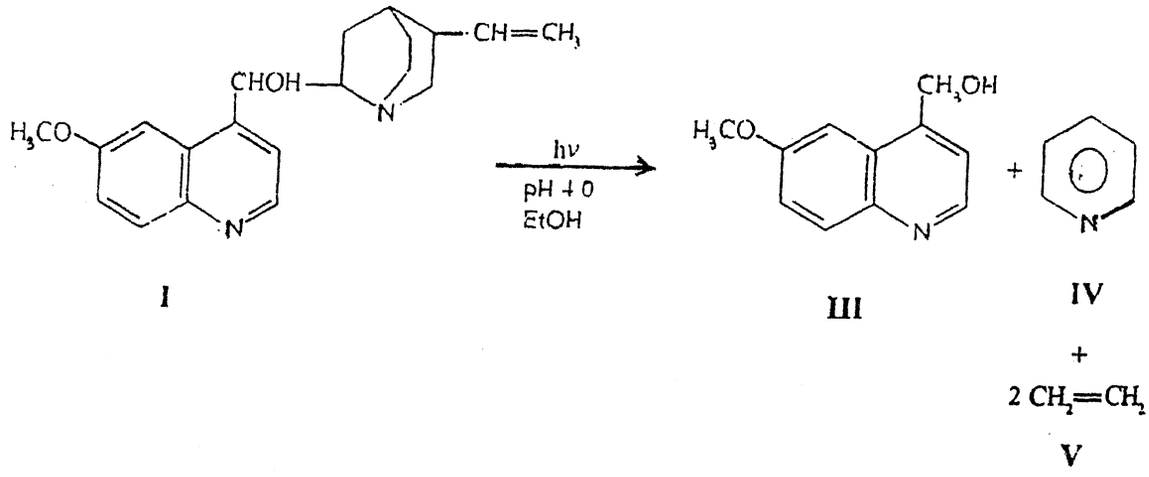


**Scheme – II**

# Author Index

# Subject Index

## JOURNAL FORMAT AND GUIDELINES FOR THE AUTHORS/CONTRIBUTORS

### [A] WHAT TO SUBMIT

All papers would pass through a strict "Peer review" to ensure high quality.

The National Academy Science Letters publishes articles under the following categories :

(i) ***Lead Articles/Overviews of new developments in Science and Technology*** from "recognized experts" to educate, initiate and provocate young scientists for undertaking research in innovative, challenging and cross – disciplinary new research areas. ALL EXPERTS ARE WELCOME TO CONTRIBUTE. These articles are not meant to be Bibliographic or complete literature reviews but are expected to give selected references and future/past trends. Articles may be of 3000 to 5000 words. Special "Academy Award Lectures" and "Presidential Addresses" etc. may occasionally be published under this category.

(ii) ***News/Views/Comments*** with an aim to bring out recent national/international scientific developments and controversial viewpoints. The number of words in such article should be less than 3000. Short Comments and author's rebuttal on articles published in this category are also welcome (max 500 words).

(iii) ***Science & Technology Development and Policy Issues*** with an aim to serve as Science-Society interface. Articles should be less than 2000 words.

(iv) ***Short Research Communications*** with an aim to publish *high quality* and break through *investigations*, which need immediate and rapid attention. Routine research work or data shall not be acceptable which may be submitted to the regular *Proceedings of the National Academy of Sciences, India* for consideration. The maximum number of words for these articles is 2000.

(v) ***Academy News/Announcements***

(vi) ***Forthcoming Meetings/Seminars/Conferences*** will serve as an avenue for informing a wide audience of professional scientists about the Meetings/Seminars etc. being organized by different organizations. This would include title and scope of the conference/organizer's address/important dates or deadlines. The maximum number of words is 100. All scientists/recognized professional organizations can submit such notifications.

(vii) ***Miscellaneous Special Issues.***

### [B] HOW TO SUBMIT

(a) Manuscripts may be submitted to either of the following :-

(i) **Prof. Girjesh Govil** (Member, Board of Editors), Formerly Senior Professor, Tata Institute of Fundamental Research, Colaba, Mumbai – 400 005, **E-mail : govil@tifr.res.in;** Fax No. (022) 22804610, 22804611.

(ii) **Prof. Jai Pal Mittal** (Member, Board of Editors), Director, Chemistry and Isotope Group, Bhabha Atomic Research Centre, Trombay, Mumbai – 400 085, E-mail : mittaljp@magnum.barc.ernet.in; Fax No. (022) 25505151, 25519613

(iii) **Prof. Suresh Chandra** (Member, Board of Editors) Emeritus Scientist, Department of Physics, Banaras Hindu University, Varanasi – 221 005, E-mail : schandra@banaras.ernet.in.; Fax No. (0542) 2317040.

(iv) **Dr. M.S. Sinha**, Executive Secretary, The National Academy of Sciences, India, 5, Lajpatrai Road, Allahabad – 211 002, E-mail : **nasi@sancharnet.in;** Fax No. (0532) 2641183.

(v) **Dr. Niraj Kumar**, Assistant Executive Secretary, The National Academy of Sciences, India, 5, Lajpatrai Road, Allahabad – 211002, E-mail : **nasi@sancharnet.in**; Fax No. (0532) 2641183.

(b) Manuscripts should be typewritten in English, double-spaced and should be submitted in triplicate. All mathematical expressions should be typed or written clearly in black ink. For speedy publication, an electronic version in a "Floopy (3.5", IBM PC format only, not Macintosh)" is desirable. The text of the manuscript as per format of the Journal, and preferably with scanned figures, should be supplied as a plain ASC II file (WordStar 5.5 or 7.0 and Microsoft Word for Windows 6.0 are acceptable, but ASC II is preferred).

(c) The communication should contain a minimum number of tables, figures and photographs. Figures must be drawn in such a way that they can be reduced to one column width (7.5 c.m.). Figures must be original drawings or exceptionally sharp glossy prints of about manuscript size. The space occupied by the figures/tables/photographs will be at the expense of text "word-length" as specified above in [A]. Each Figure will be counted as 200 words, each short table as 150 words and full-page table as 300 words.

(d) All references should be indicated in the text by superscript Arabic numerals, e.g. 'Mirri[2] while working on .....' The list of references should be arranged in order of their occurrence in the text. Reference should be given in the following style :

2. Mirri, M.A. (1982) J. Chem. Phys, 58 : 282 (for articles in Journals).
Author Year Journal Vol. I beginning page
White, M.J.D. (1973) Animal Cytology and Evolution, 3rd Ed., Cambridge University Press, London, p. 320 (for Books)
Osgood, C.F. (1977) in Number Theory and Algebra, ed., Zassenhaus, H., Academic Press, New York, p. 321 (for edited Books).
Abbreviations of the names of periodicals should conform to those given in the World list of Scientific Periodicals.

(e) Keywords : A maximum of 5 keywords should be supplied. Each of these words will be separated by a slash ( / ) and printed just below the title of the research paper, e.g. (steroid receptors/protein-DNA interaction/gene regulation).

(f) Acknowledgements, if any, should appear at the end of the letter but just before the references.

(g) Proofs will not ordinarily be sent to authors, unless desired.

[C] **REPRINTS : 25 free reprints will be given for each paper.**

[D] **SUBSCRIPTION RATE :**

| | | |
|---|---|---|
| (1) | Annual Subscription for non-members | |
| | Inland (by Book-Post) | Rs. 300.00 |
| | Foreign | U.S. $ 125.00 |
| (2) | Single issue for non-members | |
| | Inland (by Book-Post) | Rs. 40.00 |
| | Foreign | U.S. $ 20.00 |

**Note : Registration and Air Mail Charges Extra**